Far-Field Propagation of Airburst Events Using a Cartesian Method

Michael J. Aftosmis

Applied Modeling and Simulation Branch

NASA Advanced Supercomputing Division

NASA Ames Research Center

7-9 July, 2015

1st International Workshop on Potentially Hazardous Asteroids Characterization, Atmospheric Entry and Risk Assessment

Acknowledgements

- NASA Advanced Supercomputing Division – Task 3 & 4 teams

  Marian Nemec, Jonathan Chiew, Chris Mattenberger, Lorien Wheeler, Donovan Mathias, George Anderson, Darrel Robertson

- Entry Systems Division – Task 2 team

  Dinesh Prabhu, Ethiraj Venkatapathy

- New York University

  Marsha Berger

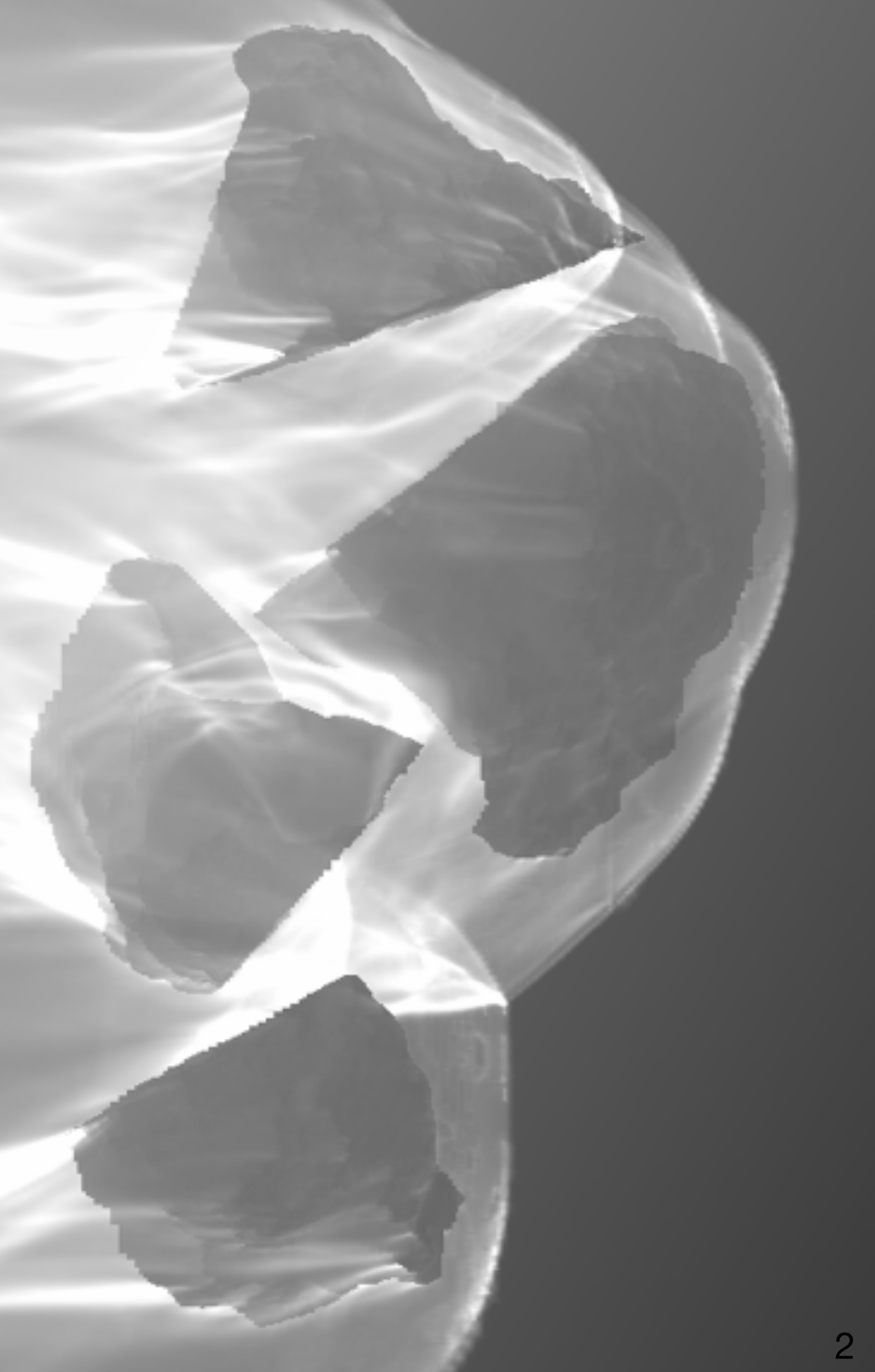

ARC Planetary Defense IPT

Ground & Water Effects

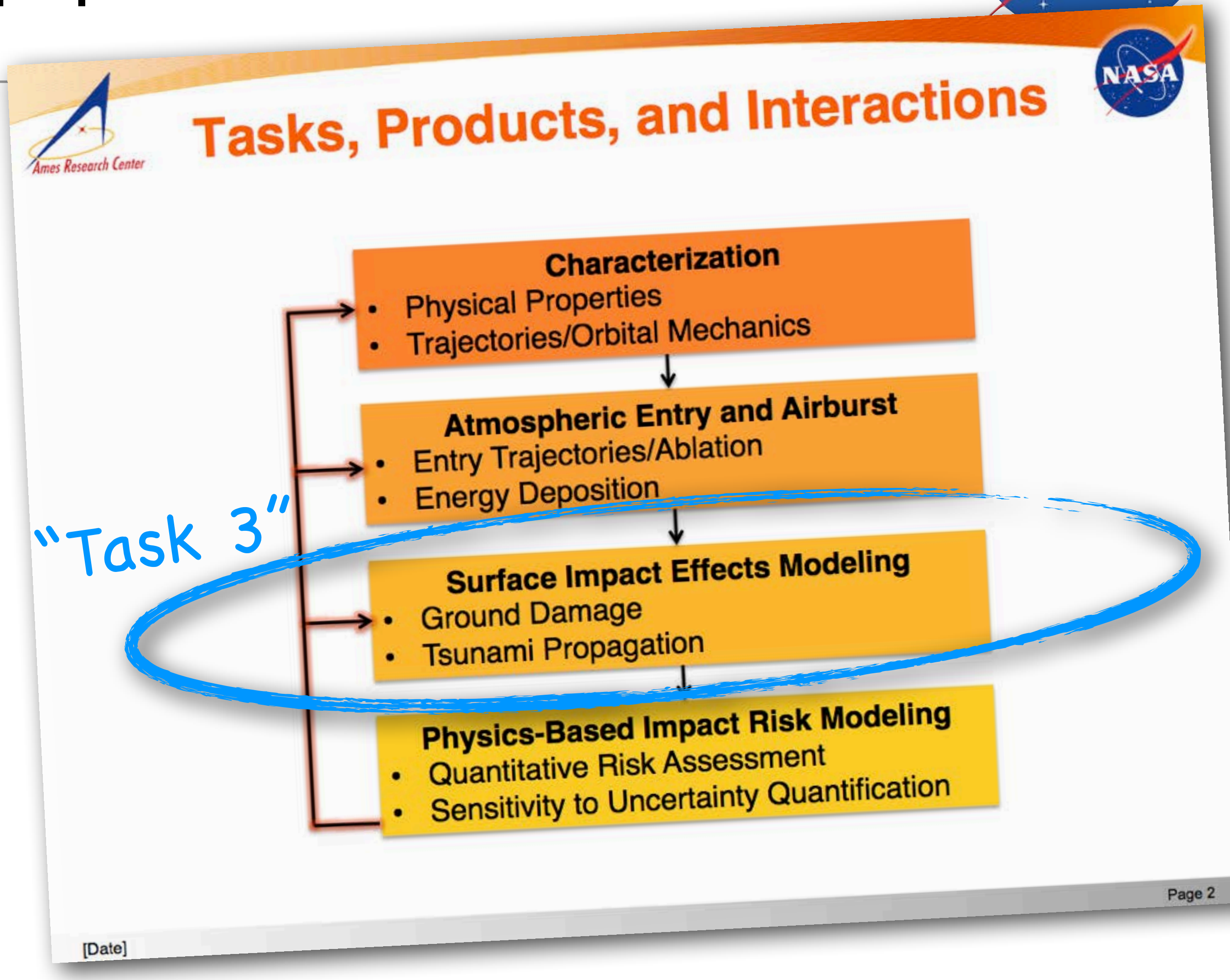

- "Task 3" of the PD IPT
- Focus on ground effects modeling
  - Airburst & atmospheric propagation
  - Surface overpressure & wind prediction
  - Ground damage
  - Tsunami propagation
- Inputs come from entry and airburst modeling in Task 2
- Outputs of atmospheric propagation feed tsunami modeling
- Outputs of atmospheric & tsunami modeling feed physics-based risk models in Task 4

ARC Planetary Defense IPT

Goal of atmospheric propagation is prediction of surface footprint

- Far-field atmospheric propagation drives
  - Ground footprint and land damage prediction
  - Atmospheric forcing for tsunami modeling
- Focus
  - Perform detailed reconstruction of specific events
  - Perform parametric studies to develop surface footprint models for PRA
  - Goal is to do thousands of such simulations – need to control computational expense

> Current work focuses on airburst only, no ground impact

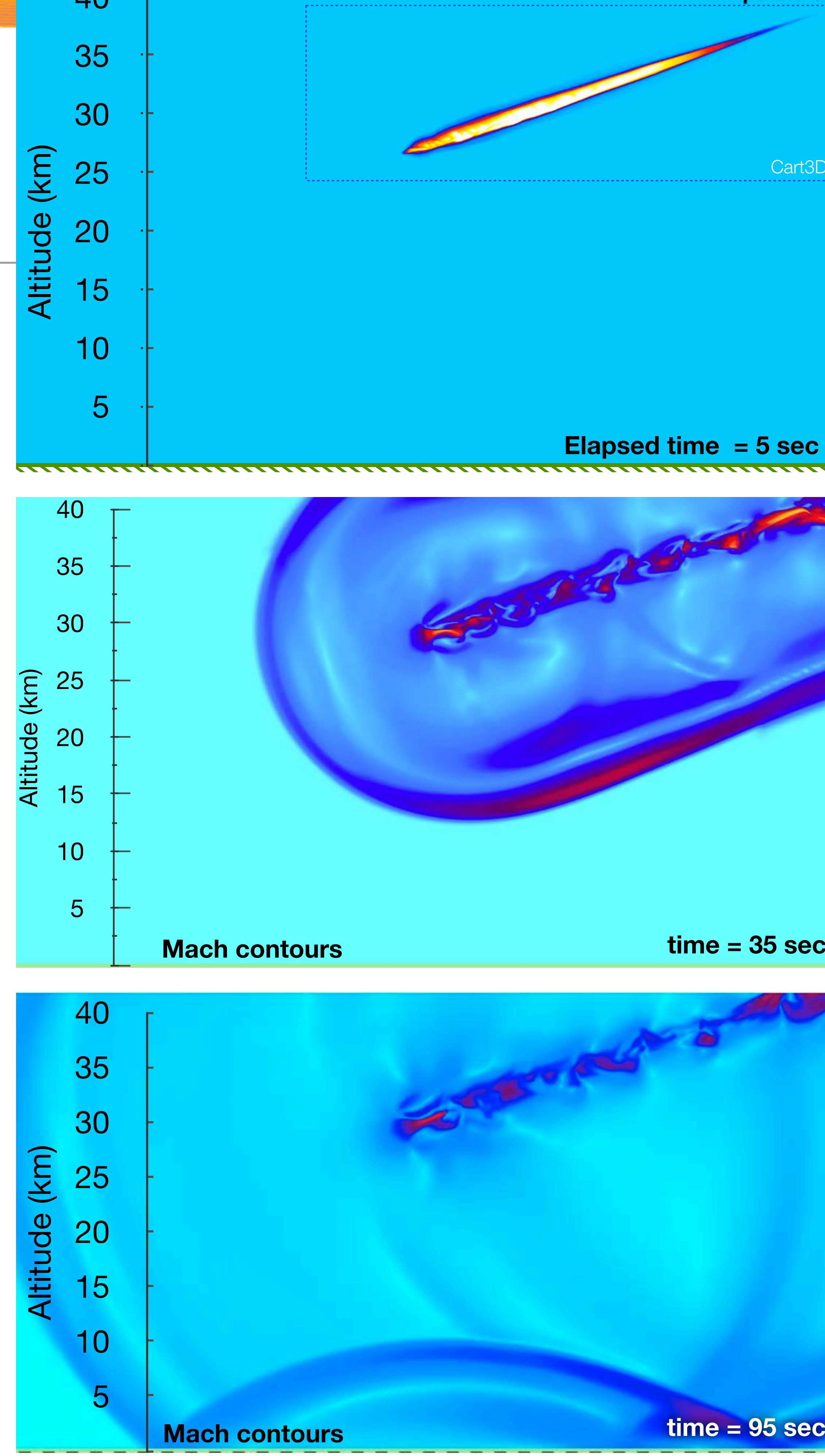

Overview

Report current status of effort and connection with PRA and tsunami

- Modeling tools & solver
- Verification & Validation
  - Basic
  - Chelyabinsk Case Study
- Investigations of ground-footprint sensitivity
  - Line-source vs time-dependent entry
  - Entry Angle
- Upcoming Efforts

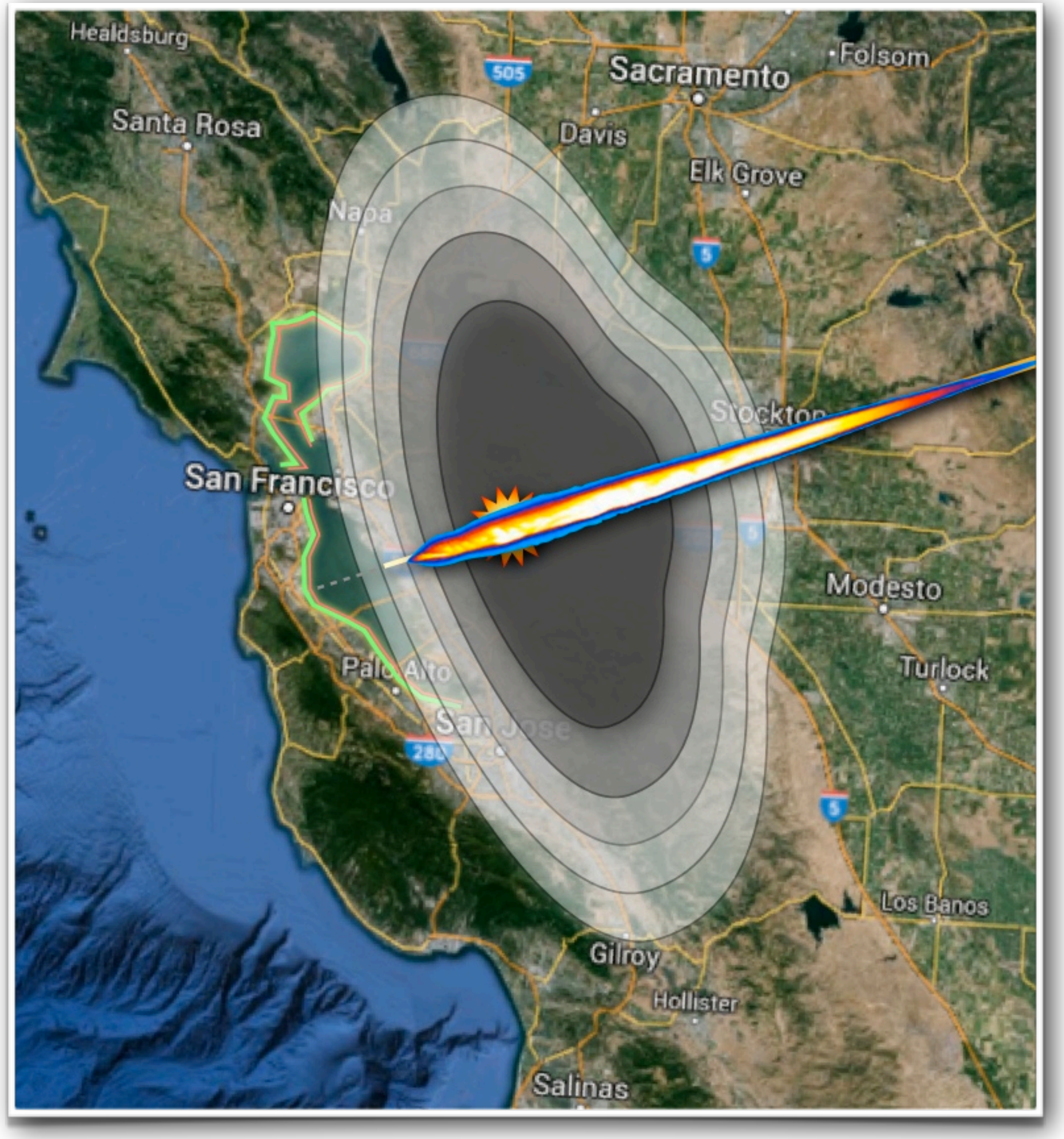

Overview

Report current status of effort and connection with PRA and tsunami

- Modeling tools & solver
  - Atmosphere model
  - Governing equations
  - Solver and simulation methodology
  - Model for deposition of mass, momentum & energy
- Veri
- Inve
- Upcoming Efforts

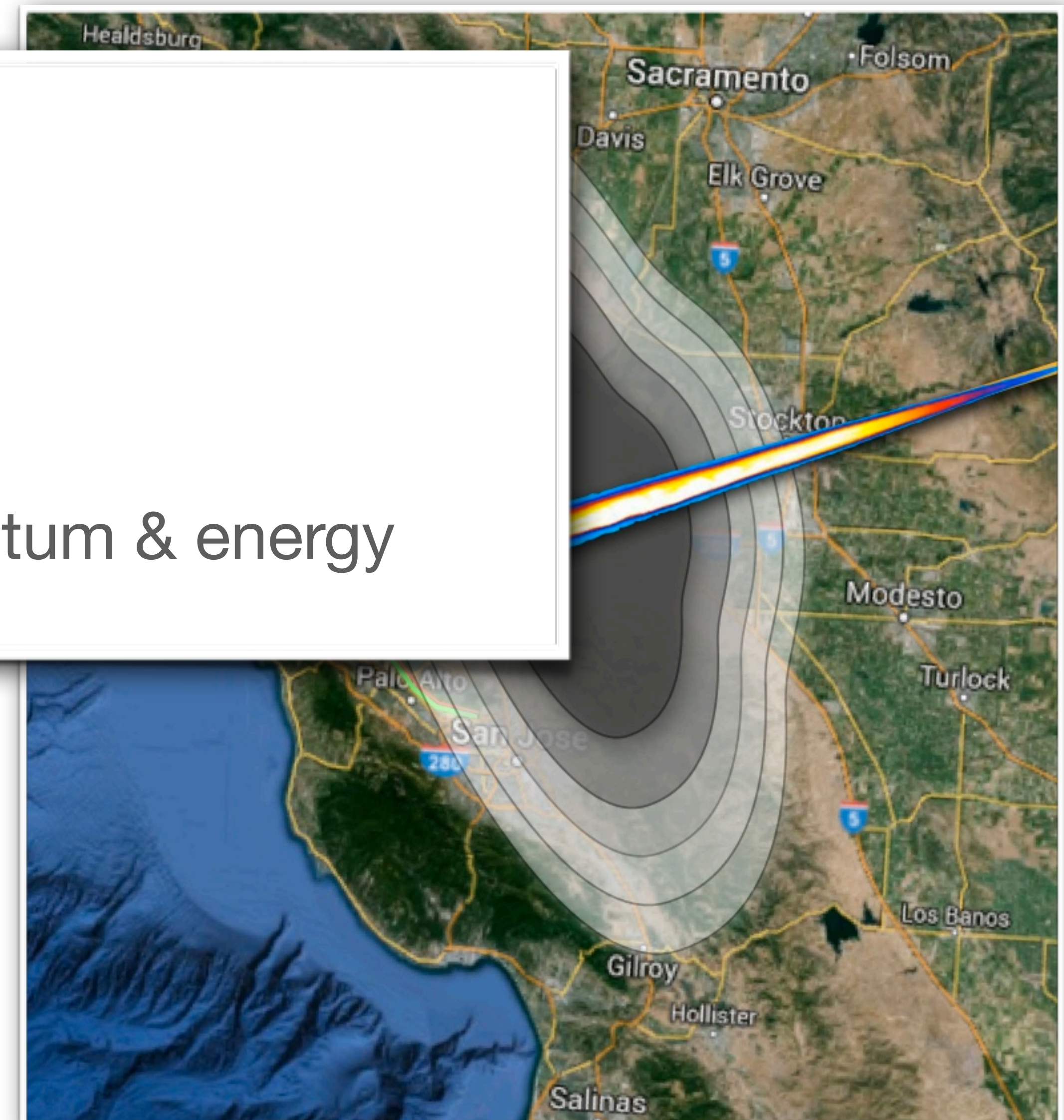

Modeling

Inviscid scale-height atmosphere model

- Atmosphere model based on 1976 Standard Atmosphere (ISO 2533:1975)
- Isothermal approximation for scale-height description

$$P(z) = P_\circ e^{-z/H}$$

$$\rho(z) = \frac{P(z)}{RT}$$

- Use $H = 8$, and initialize simulations with atmosphere in hydrostatic equilibrium

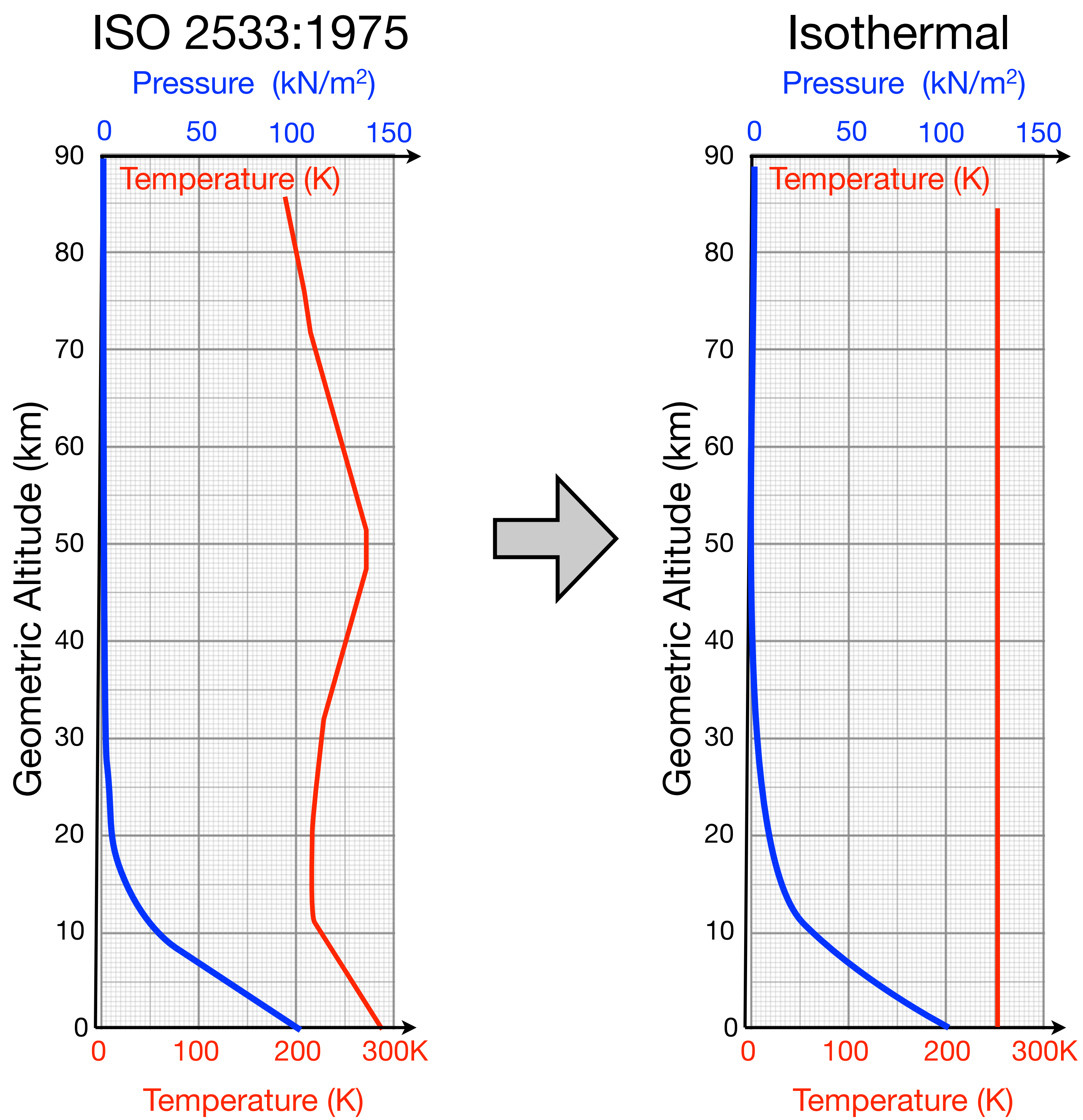

Modeling

Inviscid scale-height atmosphere model

- Atmosphere model based on 1976 Standard Atmosphere (ISO 2533:1975)
- Isothermal approximation for scale-height description

$$P(z) = P_{\circ} e^{-z/H}$$

$$\rho(z) = \frac{P(z)}{RT}$$

- Use $H = 8$, and initialize simulations with atmosphere in hydrostatic equilibrium

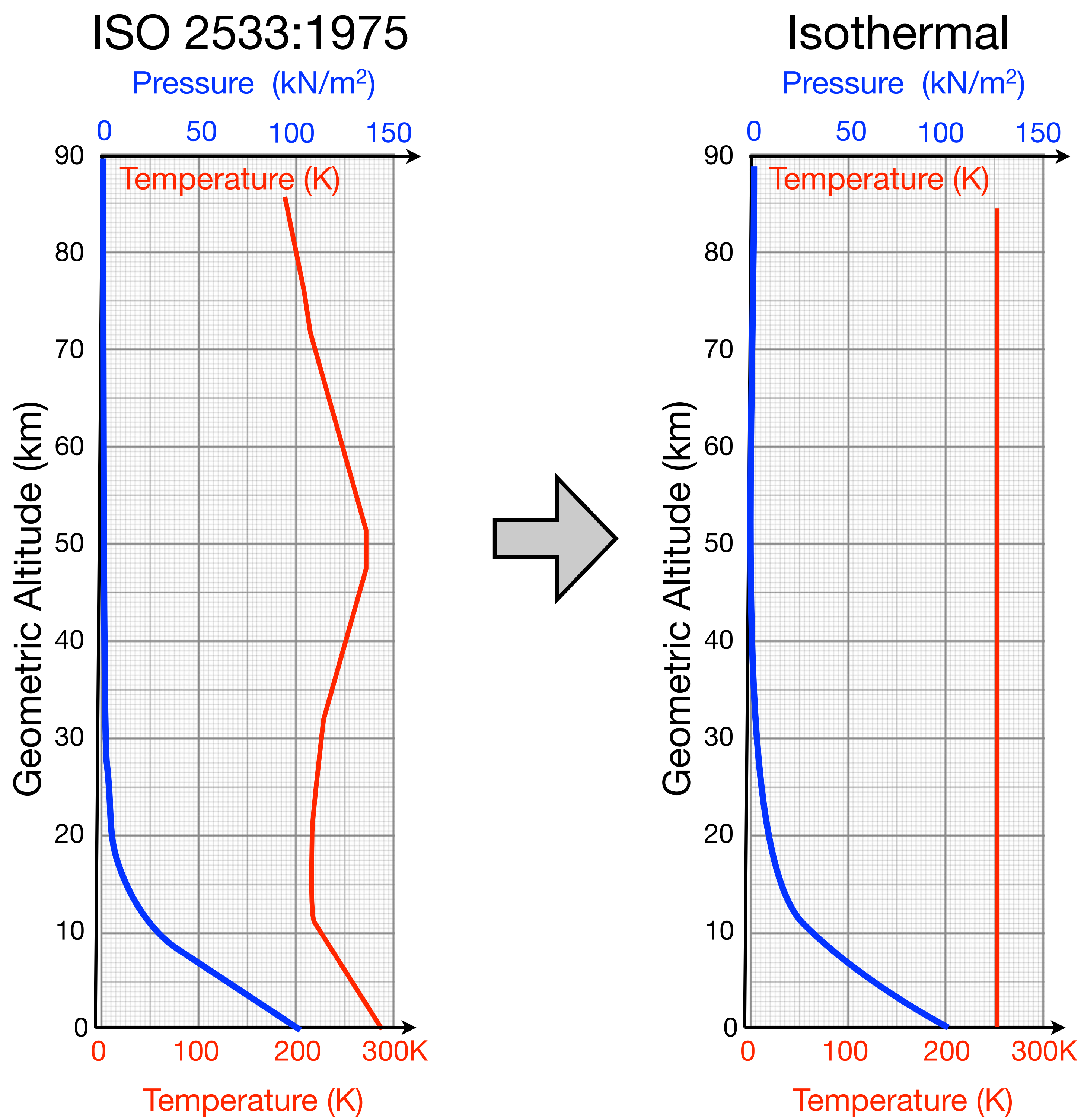

Modeling

Inviscid scale-height atmosphe

- Atmosphere model based on 1976 Standard Atmosphere (ISO 2533:1975)
- Isothermal approximation for scale-height description

$$P(z) = P_\circ e^{-z/H}$$

$$\rho(z) = \frac{P(z)}{RT}$$

- Use $H = 8$, and initialize simulations with atmosphere in hydrostatic equilibrium

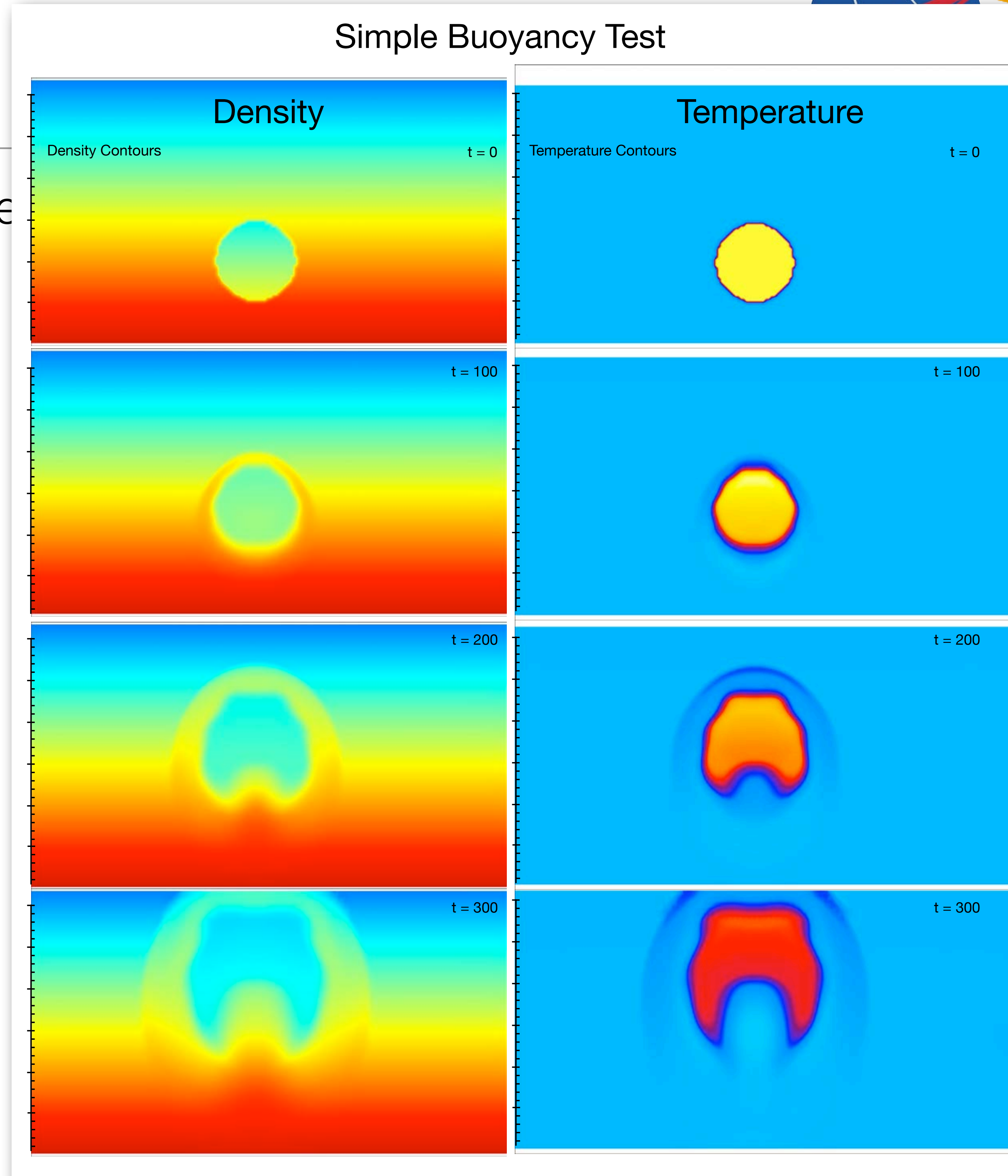

Modeling

Inviscid scale-height atmosphere model in hydrostatic equilibrium

- Use 3D Euler eqs. in strong conservation law form, including body force due to gravity

$$\frac{d}{dt}\int_{\Omega} U\,dV + \oint_{\partial\Omega} (\mathbf{F}\cdot\hat{n})\,dS = \int_{\Omega} S\,dV$$

- The state vector of conserved variables is

$$U = (\rho, \rho u, \rho v, \rho w, \rho E)^T$$

- Flux density tensor and gravitational body force term are

$$\mathbf{F} = \begin{pmatrix} \rho u & \rho v & \rho w \\ \rho u^2 + p & \rho uv & \rho uw \\ \rho uv & \rho v^2 + p & \rho vw \\ \rho uw & \rho vw & \rho w^2 + p \\ u(\rho E + p) & v(\rho E + p) & w(\rho E + p) \end{pmatrix} \qquad S = \begin{pmatrix} 0 \\ 0 \\ 0 \\ -\rho g \\ -\rho w g \end{pmatrix}$$

Solver: Cart3D Overview

Production solver based on cut-cell Cartesian mesh method

- Original development 1998-2002
- Fully-automated mesh generation for complex geometry
- Unstructured Cartesian cells
- Fully-conservative finite-volume method
- Multigrid accelerated 2nd-order upwind scheme
- Excellent scalability through domain decomposition
- Broad use throughout NASA, US Government and industry
  - Over 500 users in aerospace community
  - One of NASAs most heavily used production solvers, large validation database

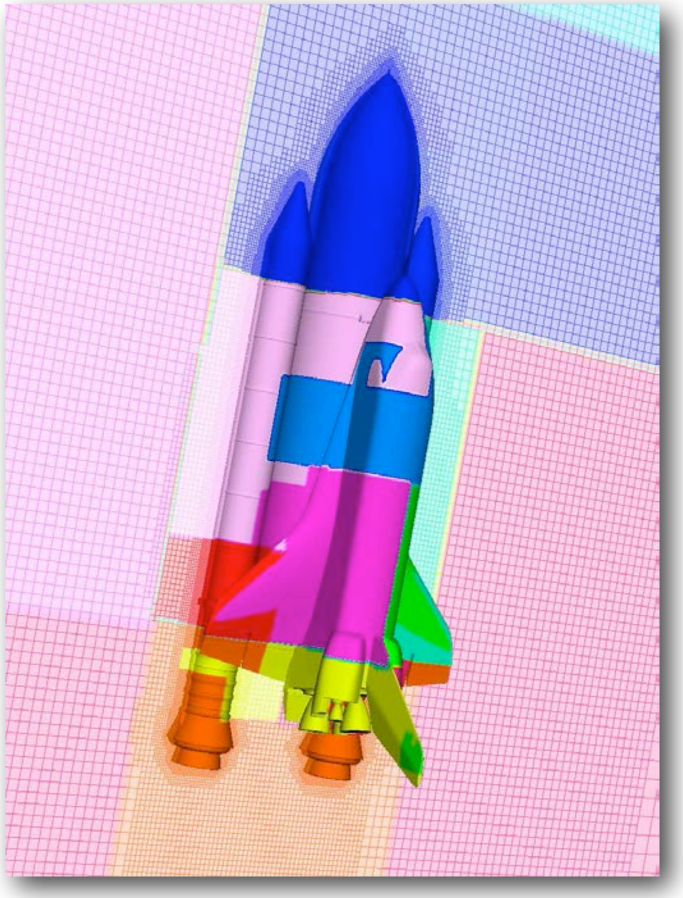

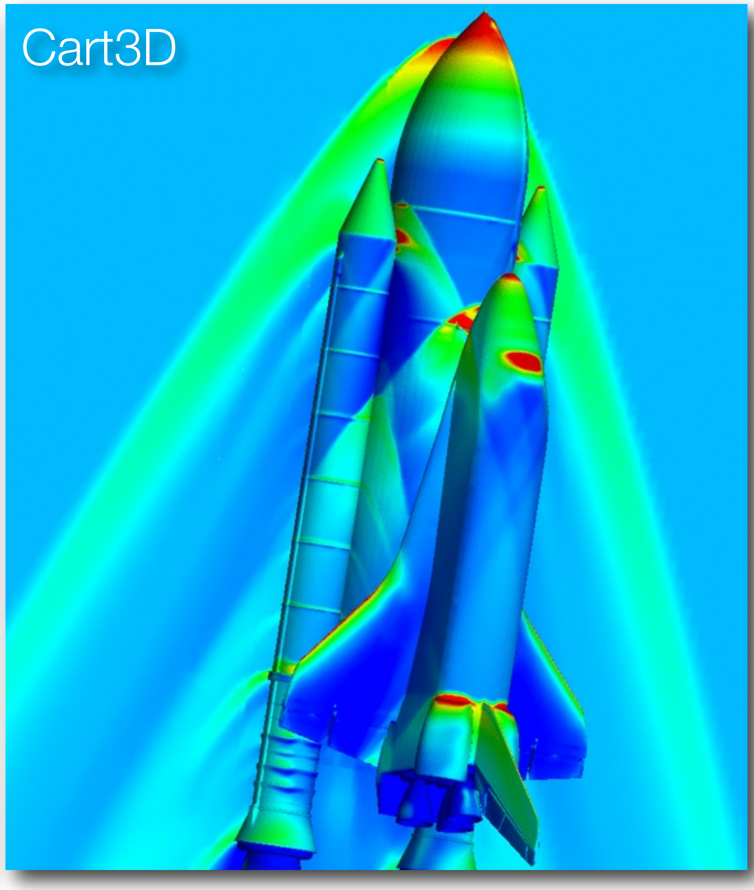

Solver: Cart3D Overview

Production solver based on cut-cell Carte

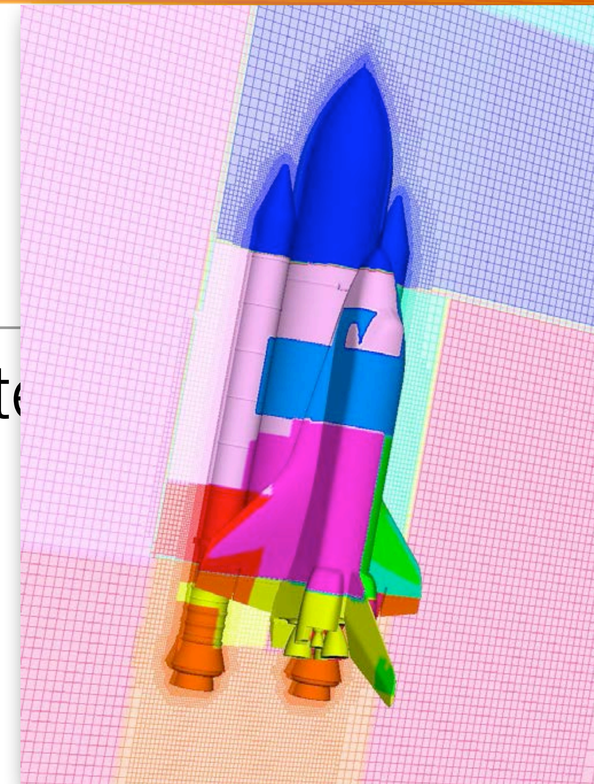

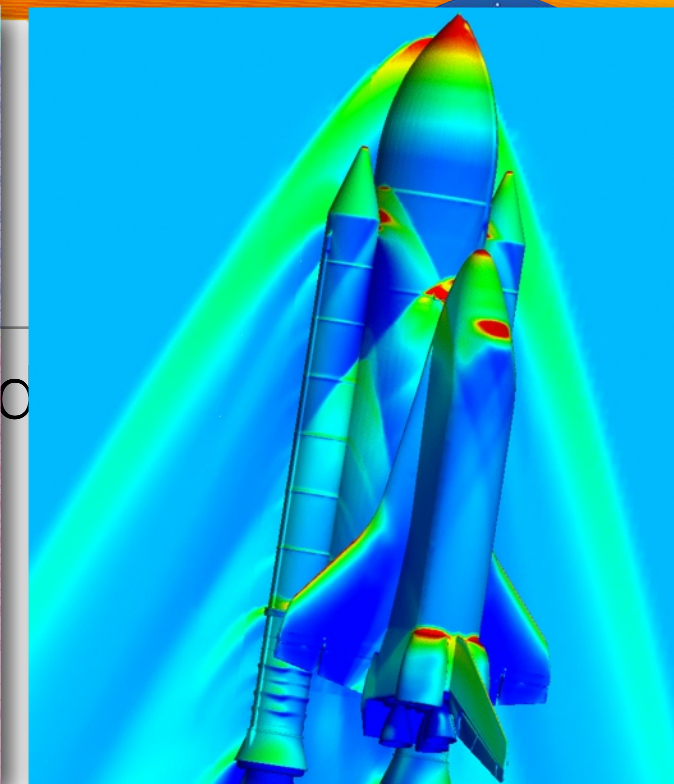

- Original development 1998-2002
- Fully-automated mesh generation from watertight geometry
- Unstructured Cartesian cells
- Fully-conservative finite-volume method
- Multigrid accelerated 2nd-order upwind scheme
- Excellent scalability through domain decomposition
- Broad use throughout NASA, US Government and industry
  - Over 500 users in aerospace community
  - One of NASAs most heavily used production solvers, large validation database

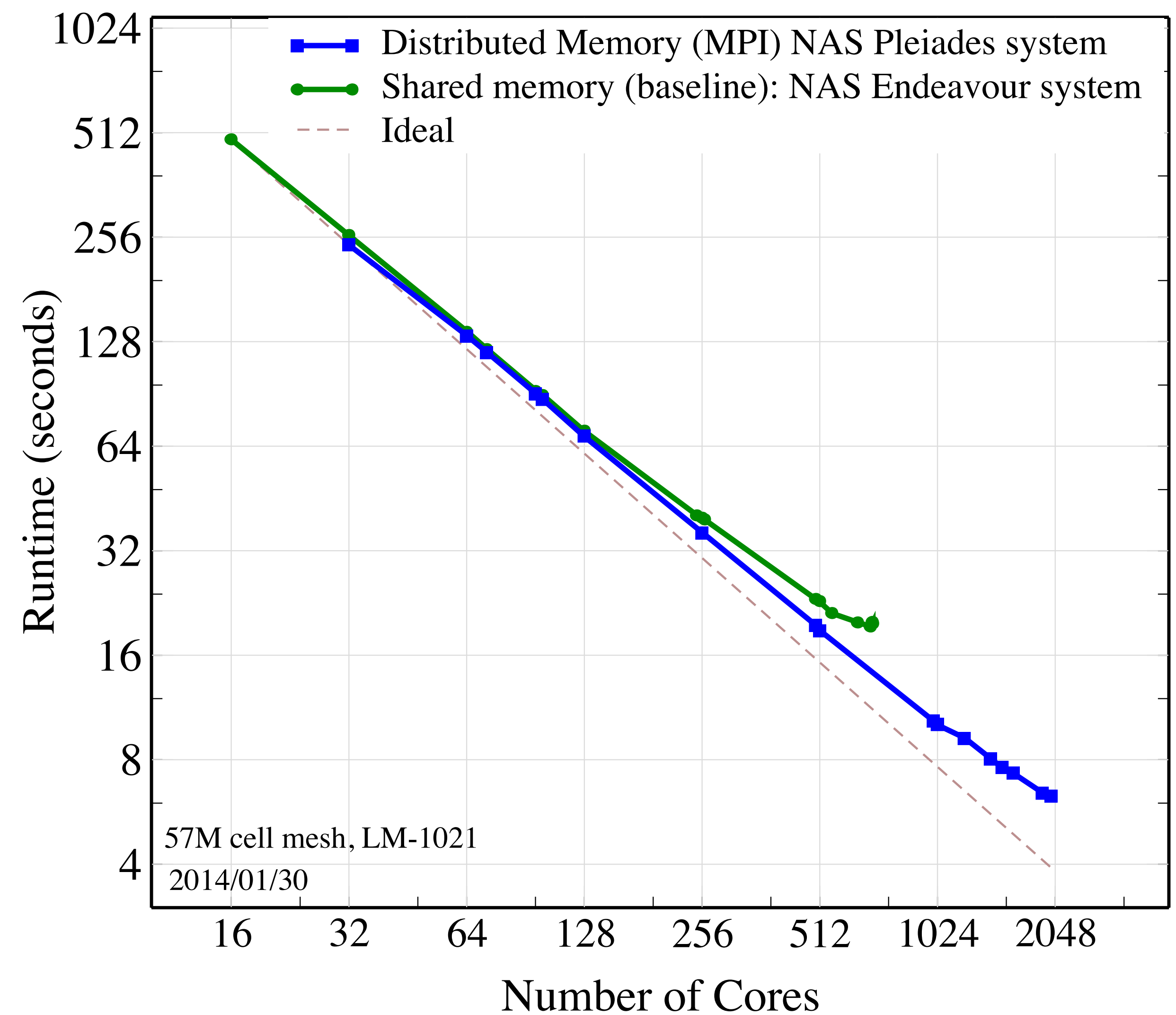

Deposition of Mass, Momentum & Energy

Goal is accurate prediction of surface effects from energy deposition inputs

- Focus on ground footprint, not near-field physics
- Abstract entry physics as simply sources of mass, momentum & energy
- Drive simulations via deposition profile taken from:
  - Models (e.g. ReVelle, Ceplecha, H&G, Shuvalov)
  - Simulations (Task 2, CTH, ALE3D, Shuvalov, Boslough)
  - Light-curve derived profiles (Jenniskins, Popova)
  - Infrasound based energy deposition (Brown, ReVelle)
- Need to derive source terms from deposition profiles

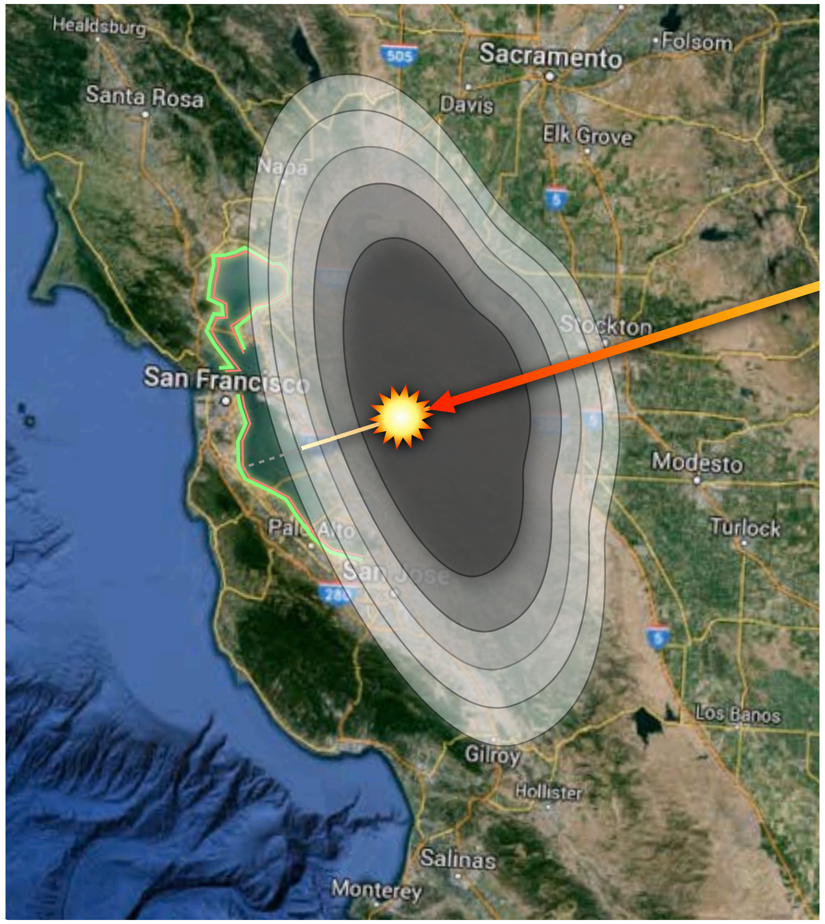

Deposition of Mass, Momentum & Energy

Derive source terms through conservation analysis

- Release energy, mass and momentum into a corridor of known radius, r
- Over each time step, Δt, the meteor travels a distance d
- Given: energy deposition profile as a function of altitude
  - From modeling
  - From simulation
  - From observational data

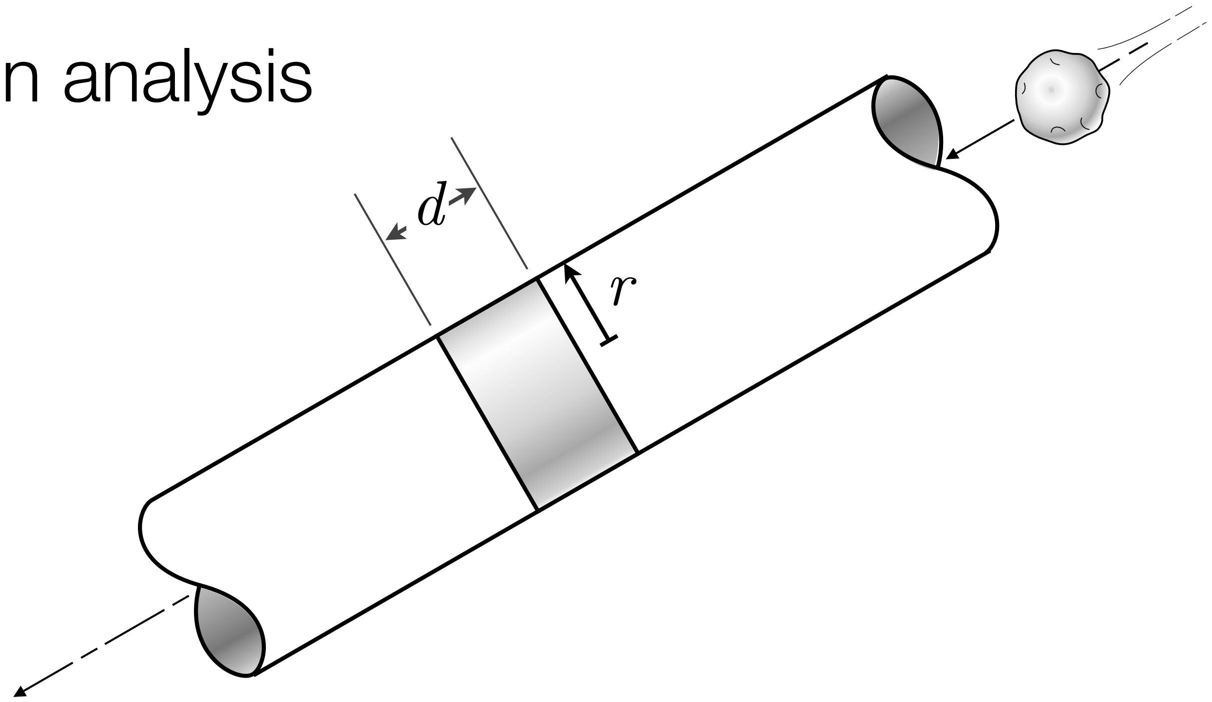

Brown *et al.*, Nature, November 2013

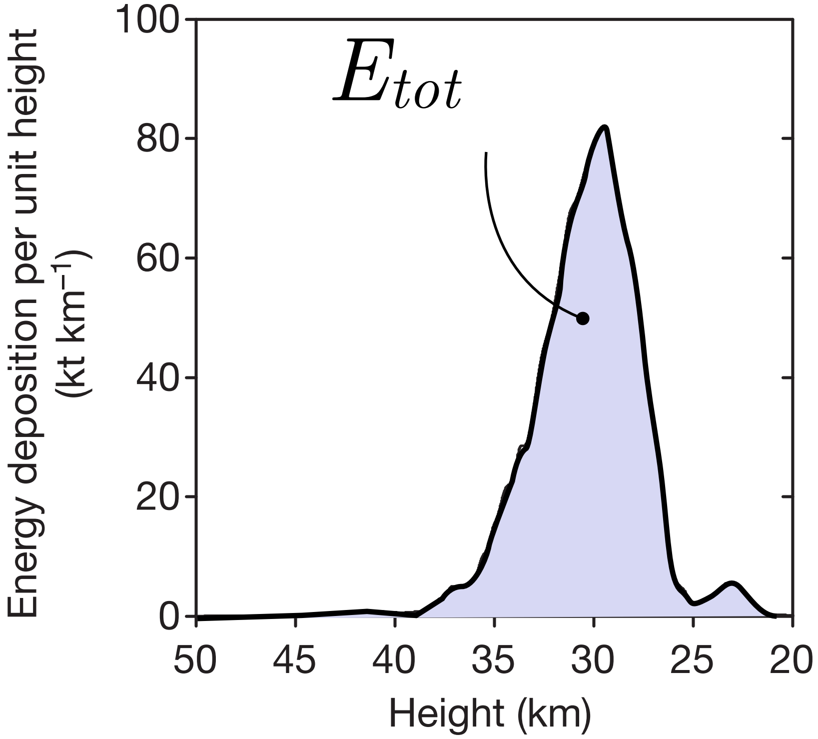

Deposition of Mass, Momentum & Energy

Conservation of energy

- Given energy deposition we know the total energy released is area under profile

$$E_{tot} = \int \frac{dE}{dh}\, dh \quad (\text{ + radiation })$$

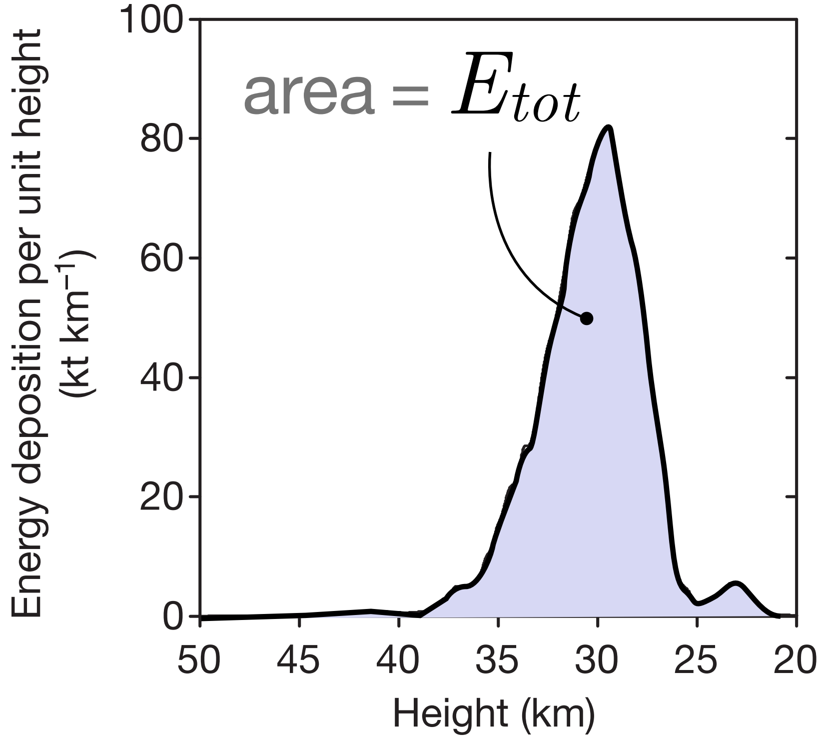

Deposition of Mass, Momentum & Energy

Conservation of energy

- Given energy deposition we know the total energy released is area under profile

$$E_{tot} = \int \frac{dE}{dh}\, dh \quad (\text{ + radiation })$$

- For known entry angle, can rescale profile to be energy released along trajectory, x

$$E_{tot} = \int \frac{dE}{dx}\, dx$$

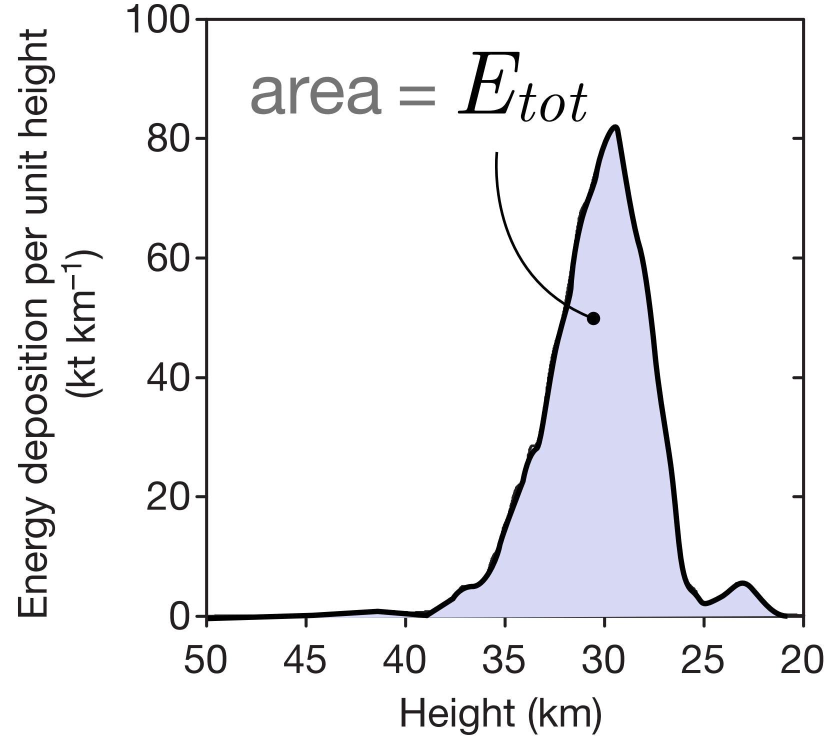

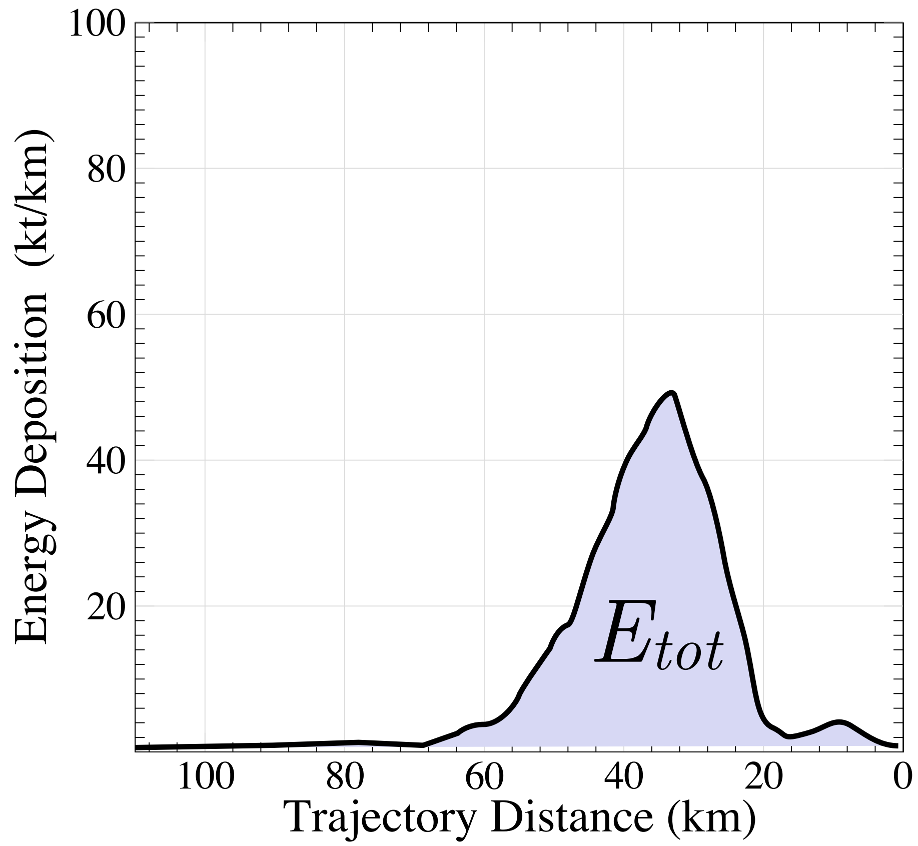

Deposition of Mass, Momentum & Energy

Conservation of energy

- Given energy deposition we know the total energy released is area under profile

$$E_{tot} = \int \frac{dE}{dh}\, dh \quad (\text{ + radiation })$$

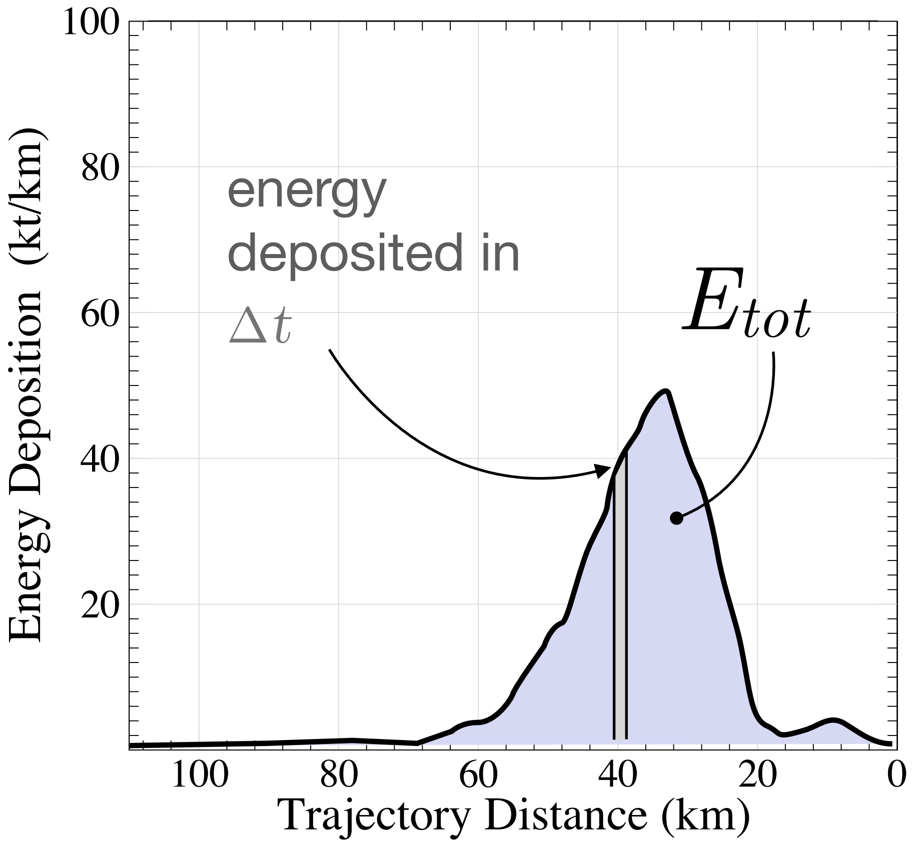

- For known entry angle, can rescale profile to be energy released along trajectory, x

$$E_{tot} = \int \frac{dE}{dx}\, dx$$

- This energy gets released into the mesh cells which intersect the tube surrounding the meteor at each time step, Δt

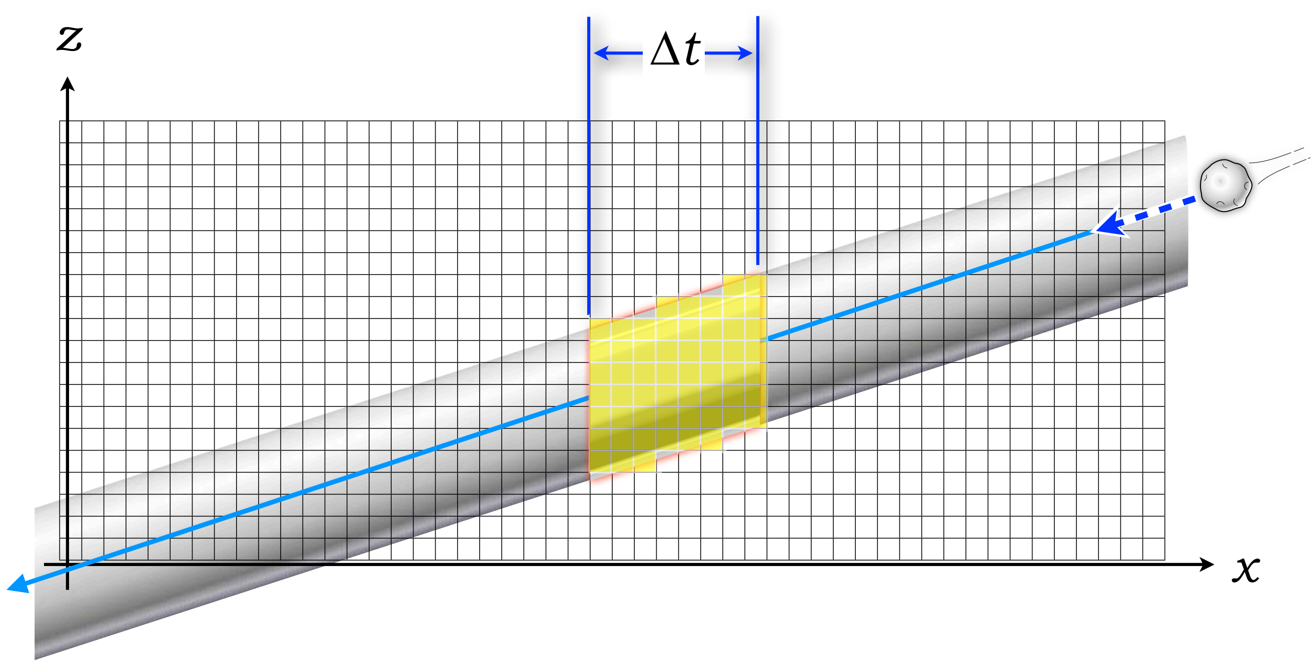

Deposition of Mass, Momentum & Energy

Conservation of energy

- Given energy deposition we know the total energy released is area under profile

$$E_{tot} = \int \frac{dE}{dh}\, dh \quad \text{(+ radiation)}$$

- For known entry angle, can rescale profile to be energy released along trajectory, x

$$E_{tot} = \int \frac{dE}{dx}\, dx$$

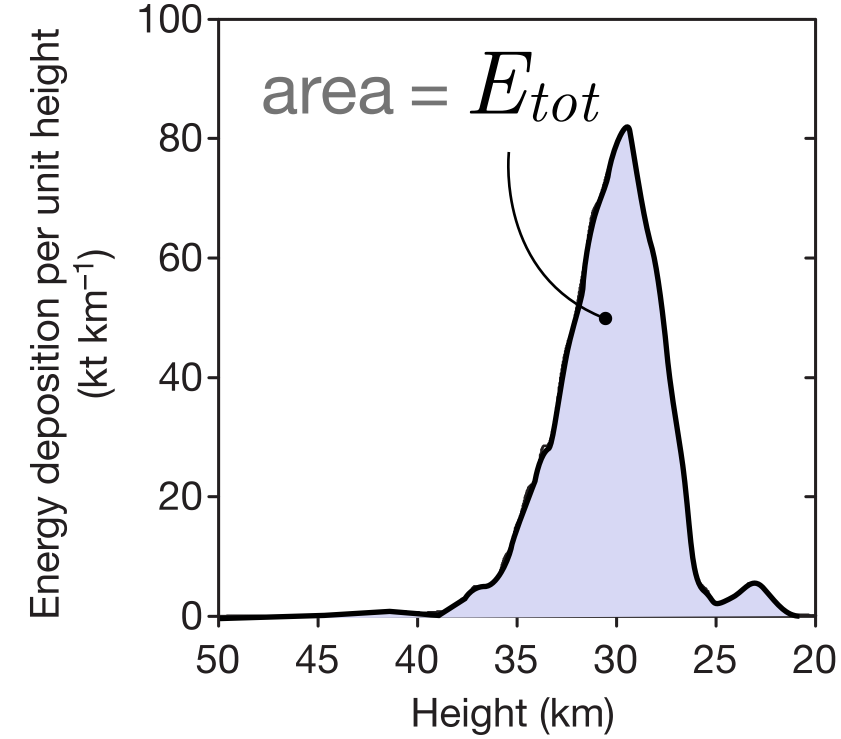

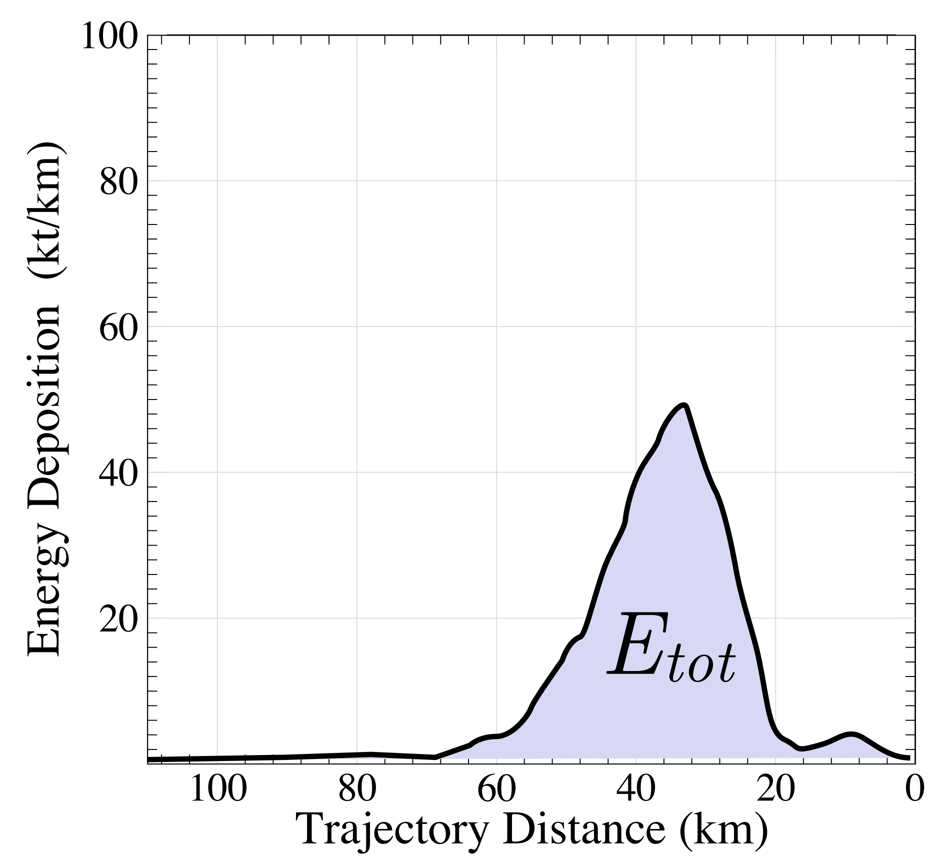

Deposition of Mass, Momentum & Energy

Conservation of energy

- Given energy deposition we know the total energy released is area under profile

$$E_{tot} = \int \frac{dE}{dh}\, dh \quad (+\text{ radiation })$$

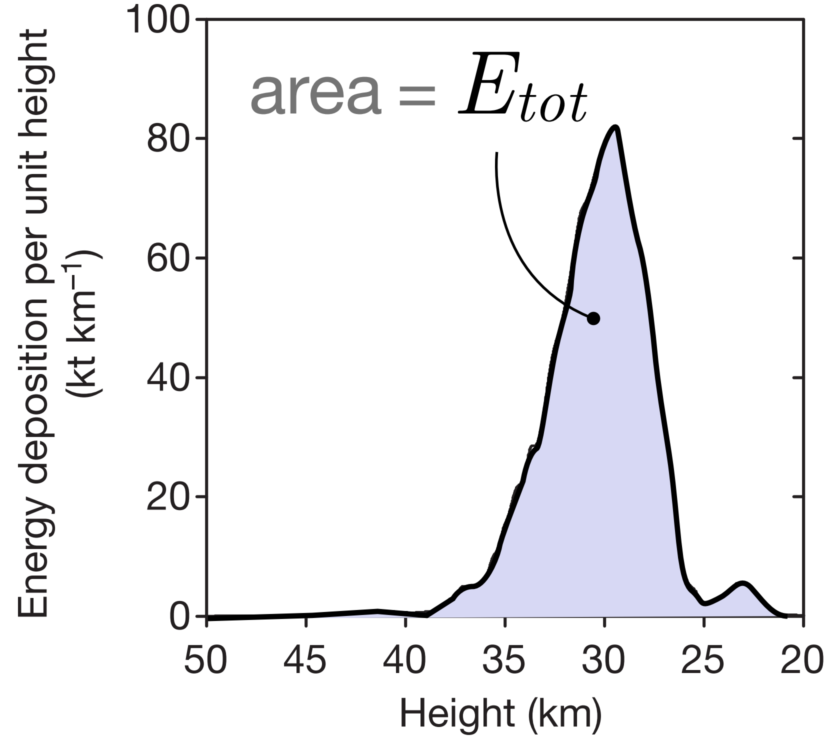

- For known entry angle, can rescale profile to be energy released along trajectory, x

$$E_{tot} = \int \frac{dE}{dx}\, dx$$

- Since work = (force x distance), and aerodynamic drag is doing all the work, this profile **is identically drag** along the trajectory

$$E_{tot} = \int \frac{dE}{dx}\, dx = \int D(x)\, dx$$

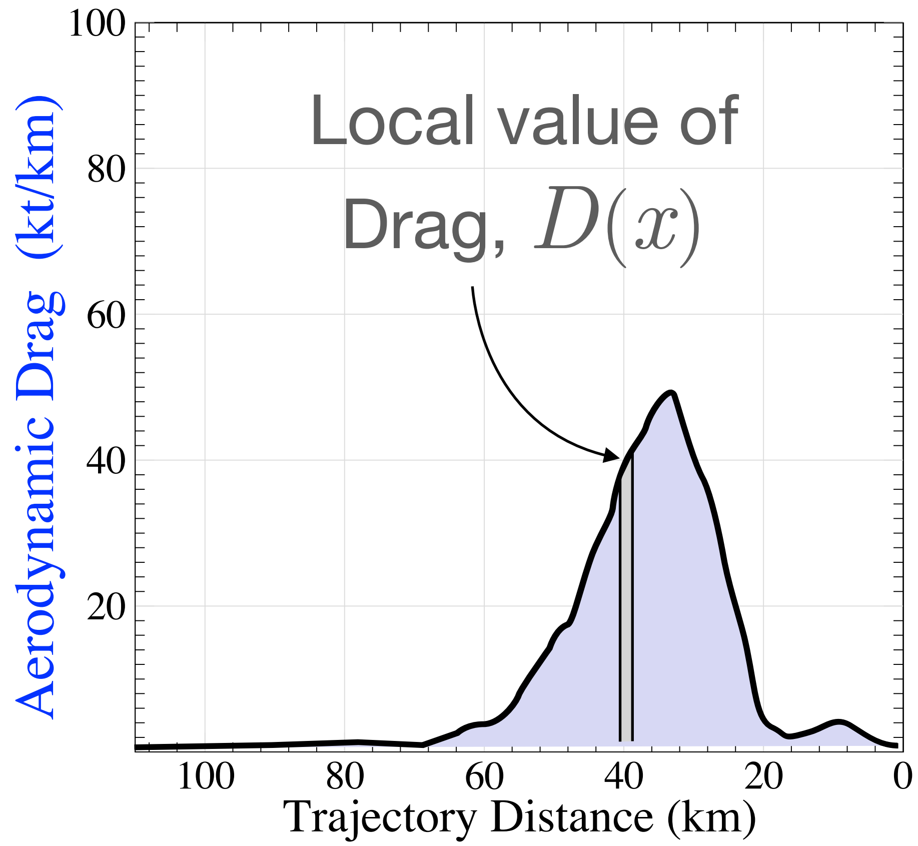

Deposition of Mass, Momentum & Energy

Conservation of mass & momentum

- Mass loss equation $$\frac{dM}{dt} = -\sigma C_D S_m \frac{1}{2}\rho_{\text{air}} U_m^3$$

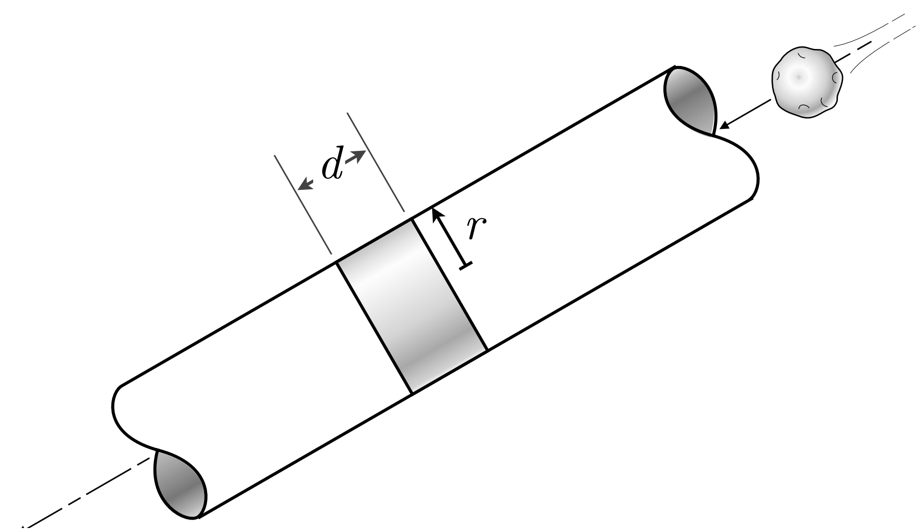

- Recall that aerodynamic drag is

$$D = C_D S_m q_\infty \quad \text{with} \quad q_\infty = \frac{1}{2}\rho_{\text{air}} U_m^2$$

- So mass loss is simply $$\frac{dM}{dt} = -\sigma D U_m$$

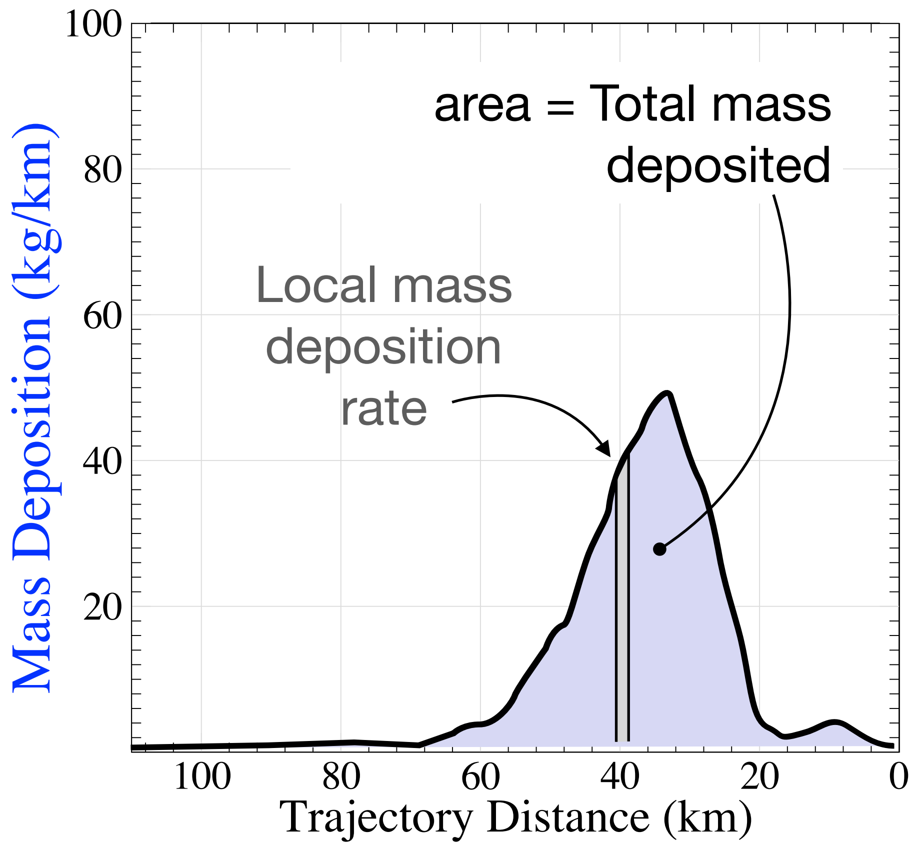

Deposition of Mass, Momentum & Energy

Conservation of mass & momentum

- Mass loss equation $$\frac{dM}{dt} = -\sigma C_D S_m \frac{1}{2}\rho_{\rm air} U_m^3$$

- Recall that aerodynamic drag is

$$D = C_D S_m q_\infty \quad \text{with} \quad q_\infty = \frac{1}{2}\rho_{\rm air} U_m^2$$

- So mass loss is simply $$\frac{dM}{dt} = -\sigma D U_m$$

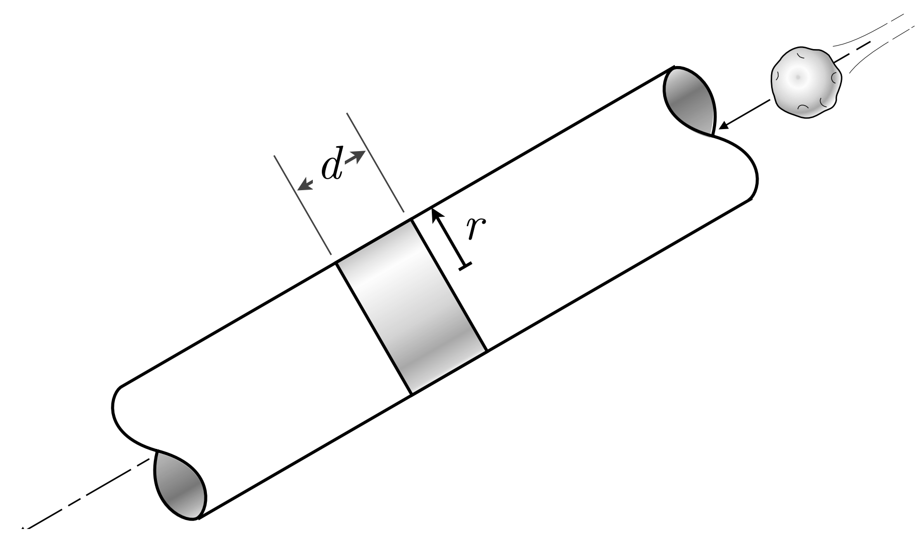

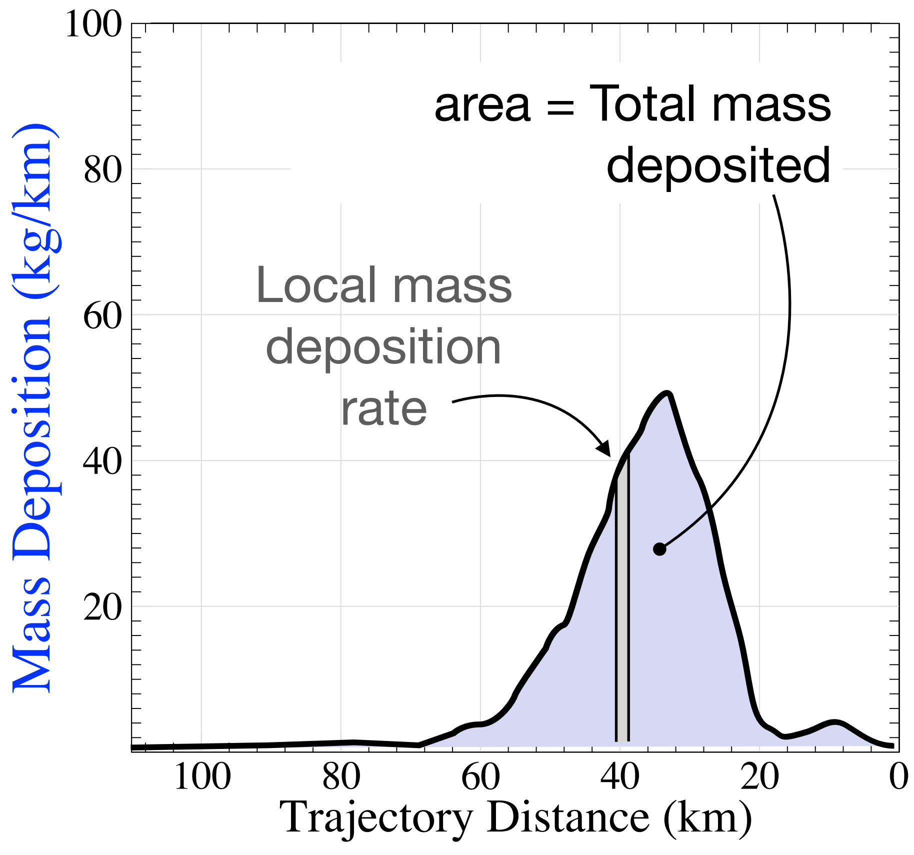

Deposition of Mass, Momentum & Energy

Conservation of mass & momentum

- Mass loss equation $$\frac{dM}{dt} = -\sigma C_D S_m \frac{1}{2}\rho_{\text{air}} U_m^3$$
- Recall that aerodynamic drag is

$$D = C_D S_m q_\infty \quad \text{with} \quad q_\infty = \frac{1}{2}\rho_{\text{air}} U_m^2$$

- So mass loss is simply $$\frac{dM}{dt} = -\sigma D U_m$$
- Assuming constant U_m and σ, local deposition of mass scales directly with Drag

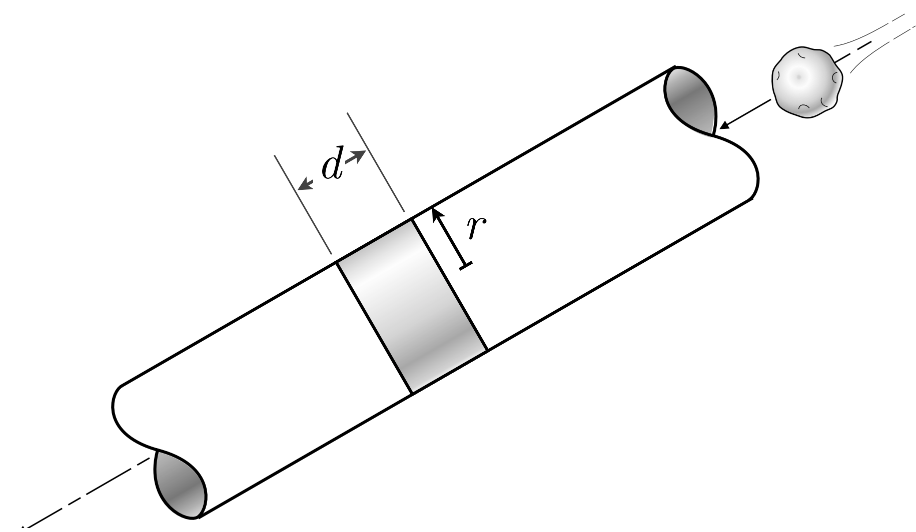

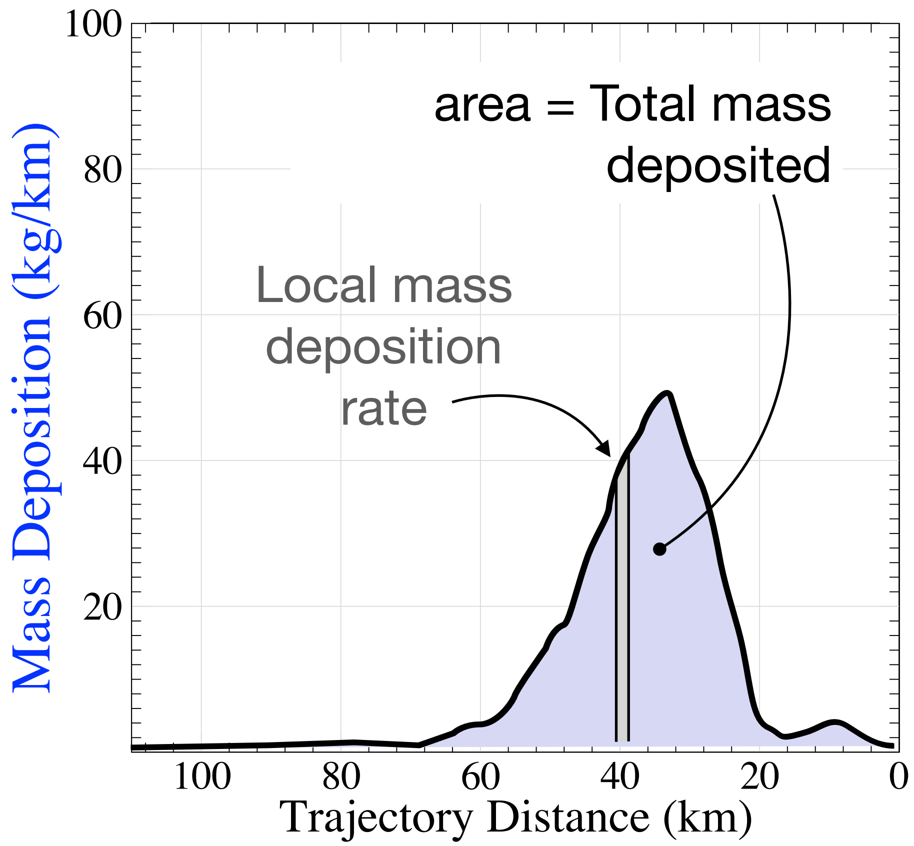

Deposition of Mass, Momentum & Energy

Conservation of mass & momentum

- Mass loss equation $$\frac{dM}{dt} = -\sigma C_D S_m \frac{1}{2}\rho_{\text{air}} U_m^3$$

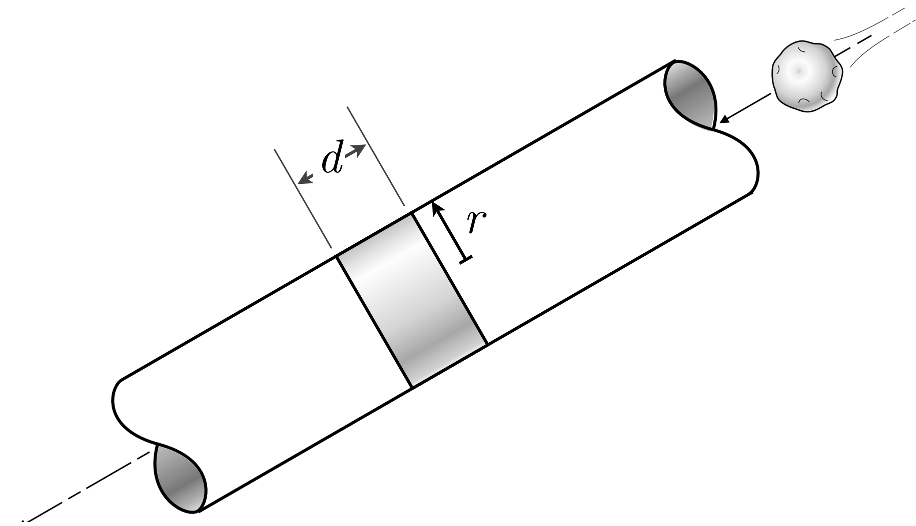

- Recall that aerodynamic drag is

$$D = C_D S_m q_\infty \quad \text{with} \quad q_\infty = \frac{1}{2}\rho_{\text{air}} U_m^2$$

- So mass loss is simply $$\frac{dM}{dt} = -\sigma D U_m$$
- Assuming constant U_m and σ, local deposition of mass scales directly with Drag
- Area under profile is total mass deposited ($M_{\text{entry}} - M_{\text{GroundFragments}}$)
- From mass deposition and velocity, we also know momentum deposition

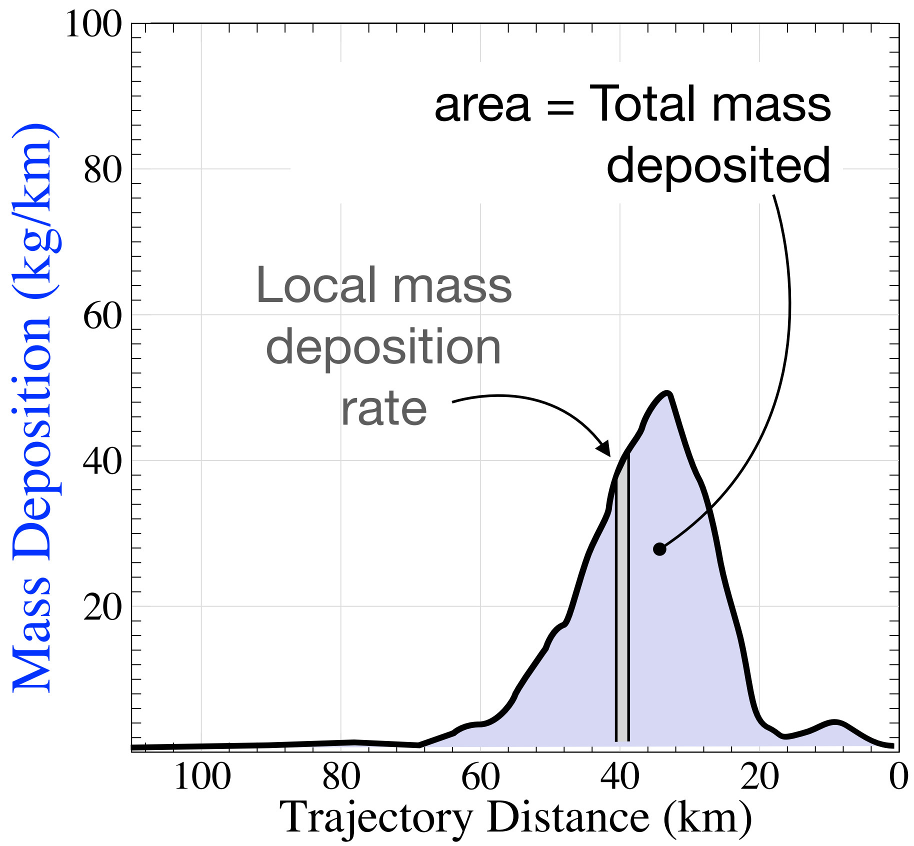

Overview

Report current status of effort and connection with PRA and tsunami

- Modeling tools & solver
- Verification & Validation
  - Basic – Spherical charge examples
  - Chelyabinsk Case Study
- Investigations of ground-footprint sensitivity
  - Line-source vs time-dependent entry
  - Entry Angle
- Upcoming Efforts

Basic Verification & Validation

Blast from a spherical charge

- Static spherical charge with
  - No buoyancy
  - E_{tot} = 520 kt,
  - Initial radius, r_i = 1km

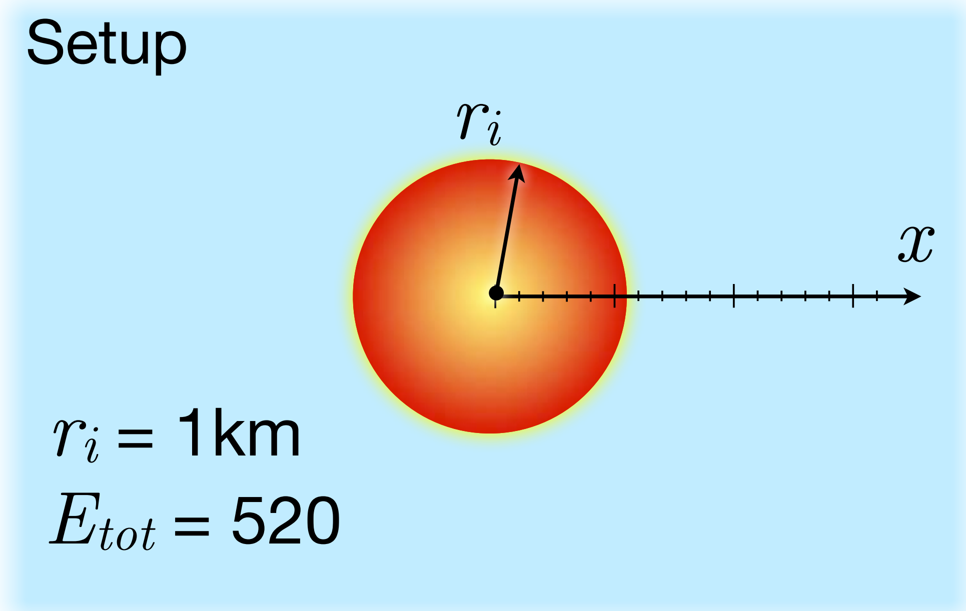

- Classical refs.
  - Brode, H. L.,Blast wave from a spherical charge, J. Phys. Fluids. (1959)
  - D. L. Jones. Intermediate strength blast wave. Physics of Fluids (1968)

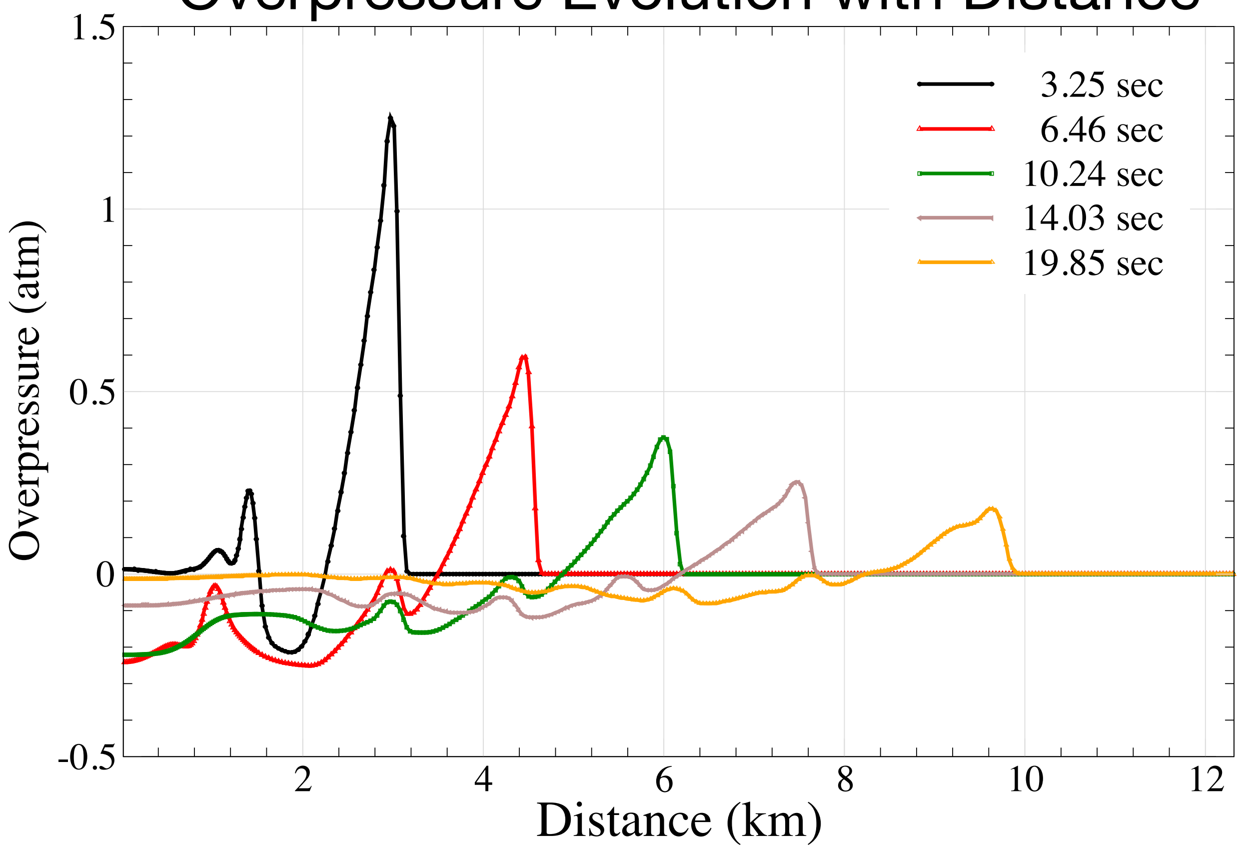

Basic Verification & Validation

Blast from a spherical charge

- E_{tot} = 520 kt, Initial radius, r_i = 1km, no buoyancy

Space-time overpressure evolution

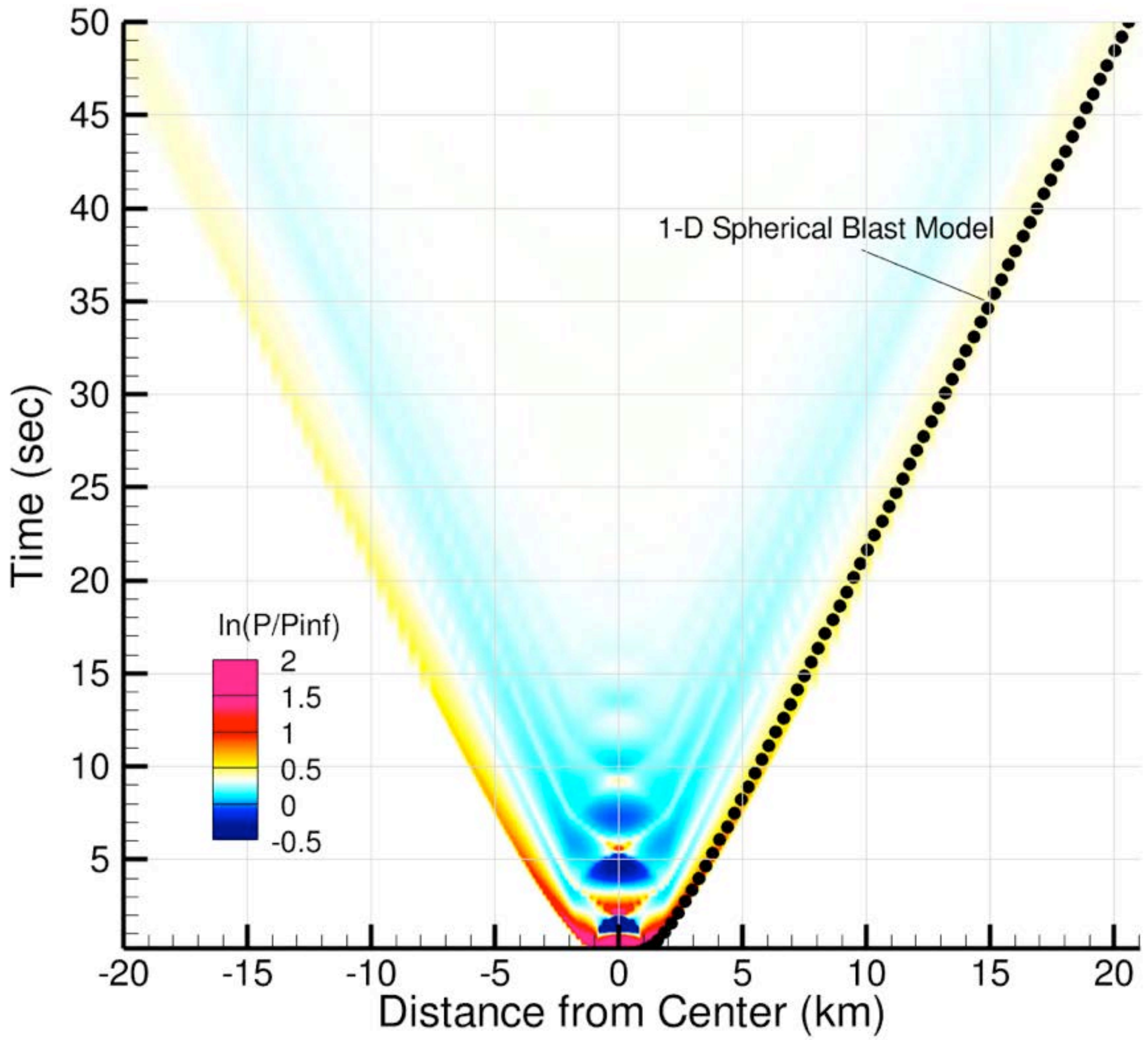

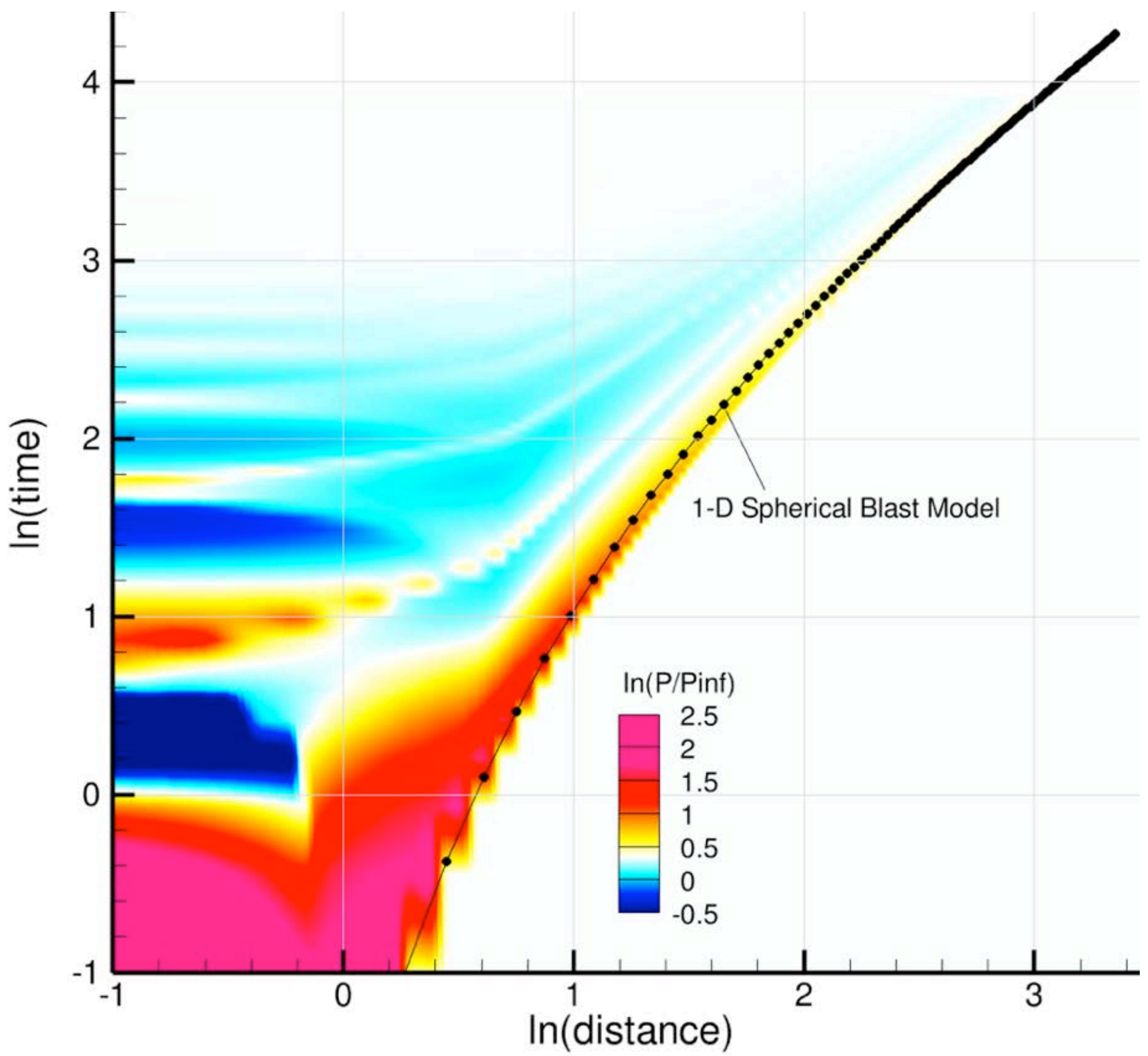

Basic Verification & Validation

Blasts over ground plane

- Numerous examples static and moving blasts over ground plane with buoyancy
  - Static airburst with buoyancy

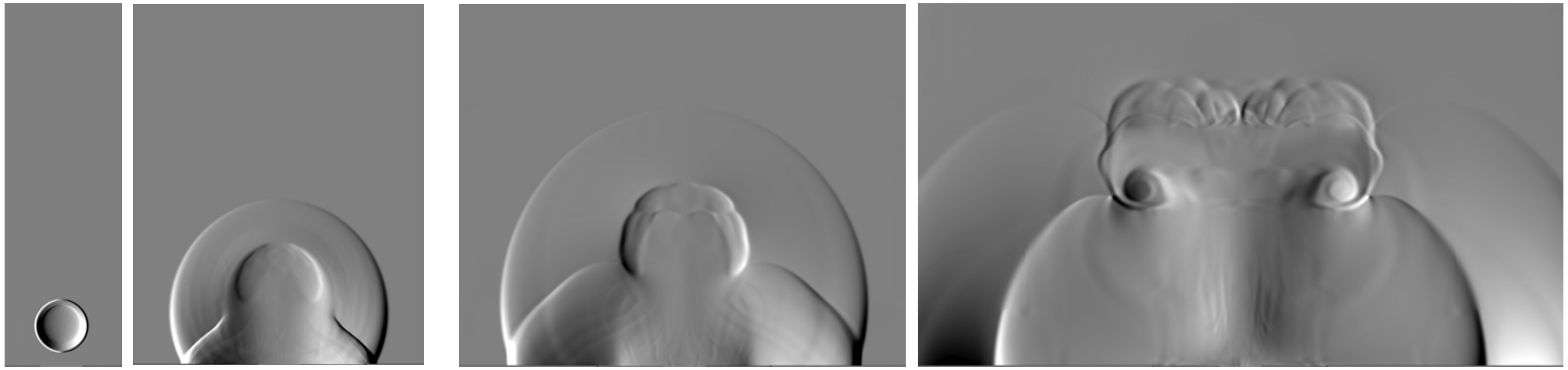

  - Moving airburst

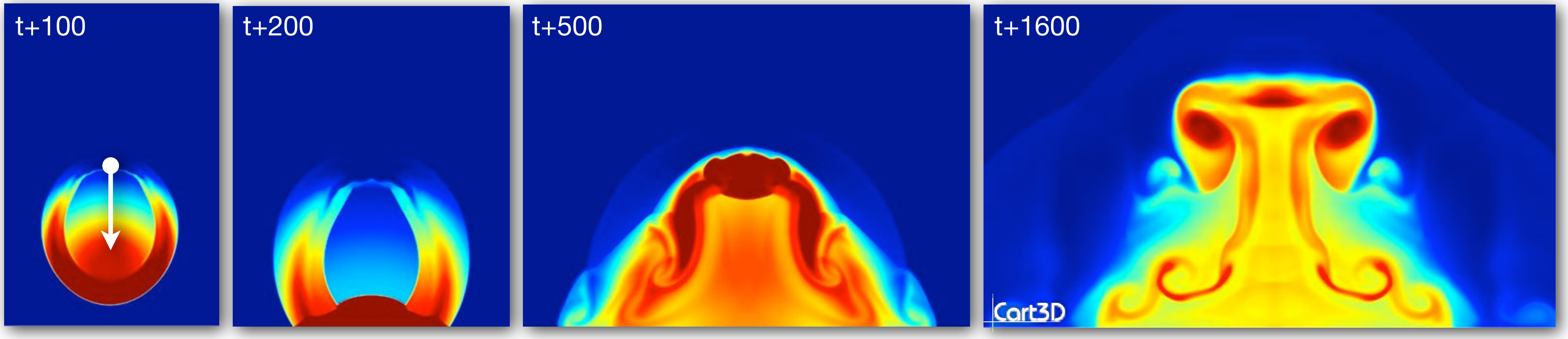

Basic Verification & Validation

Blasts over ground plane

- Numerous examples static and moving blasts over ground plane with buoyancy

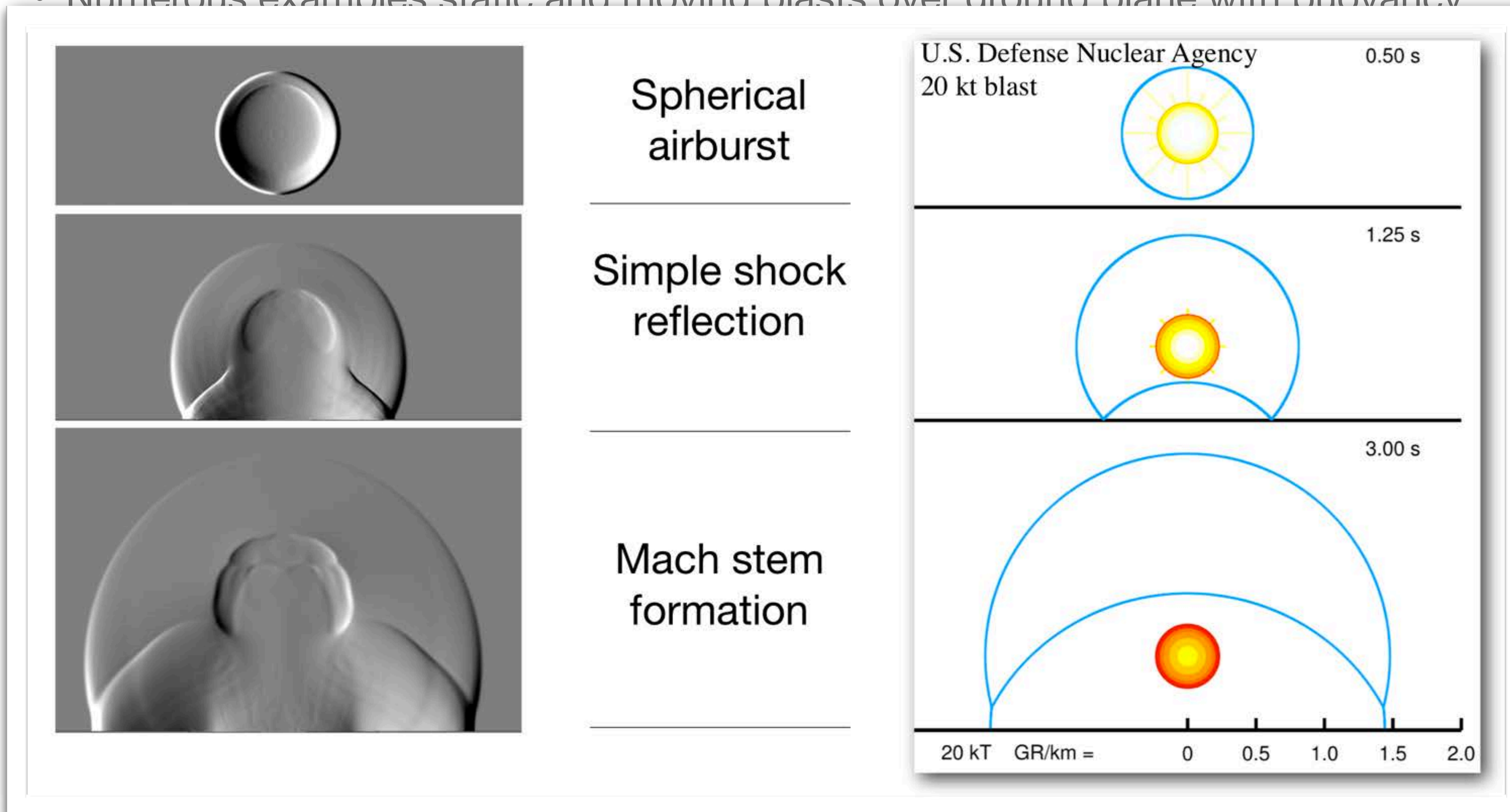

Basic Verification & Validation

Blasts over ground plane

- Numerous examples static and moving blasts over ground plane with buoyancy
  - Static airburst with buoyancy

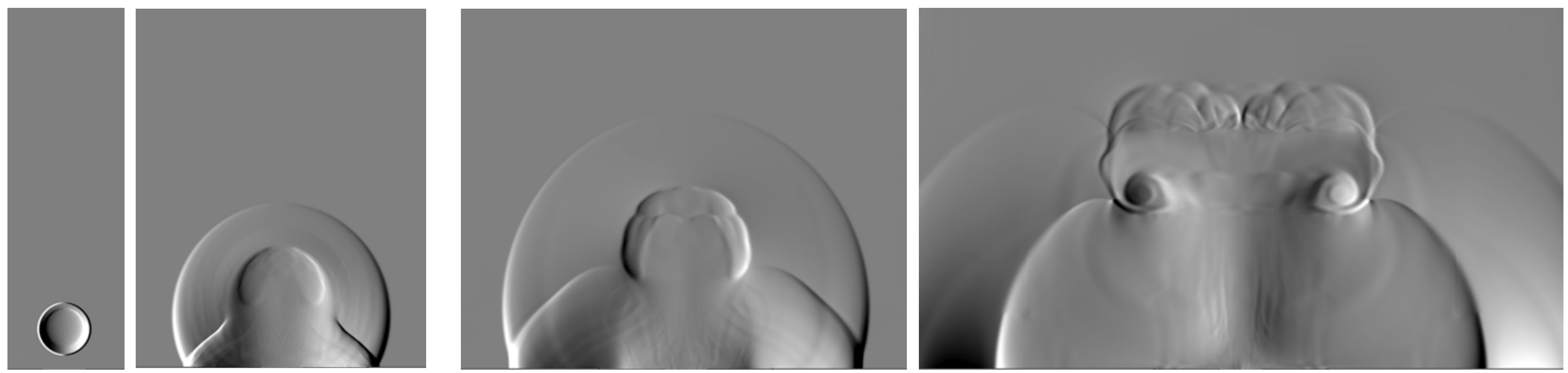

  - Moving airburst

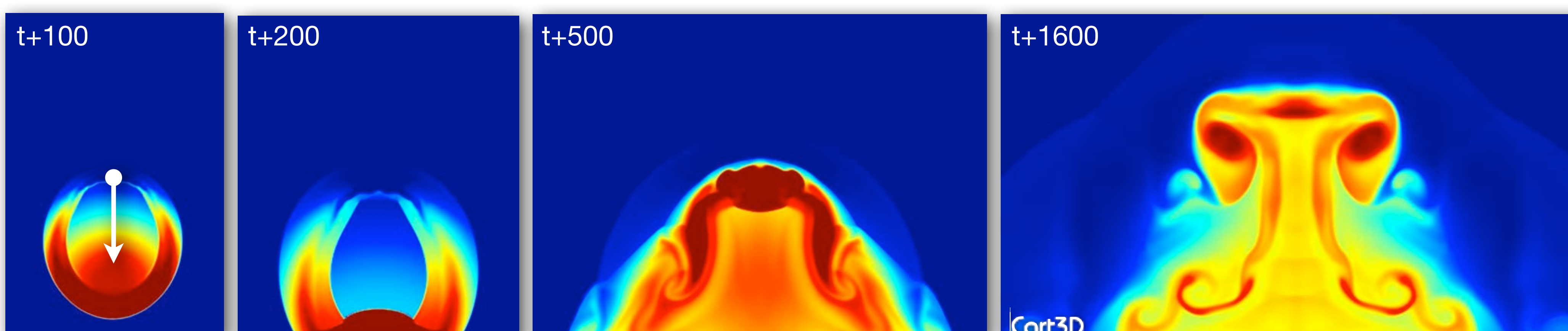

Basic Verification & Validation

Blasts over ground plane

- Numerous examples static and moving blasts over ground plane with buoyancy
  - Static airburs
  - Moving airbu

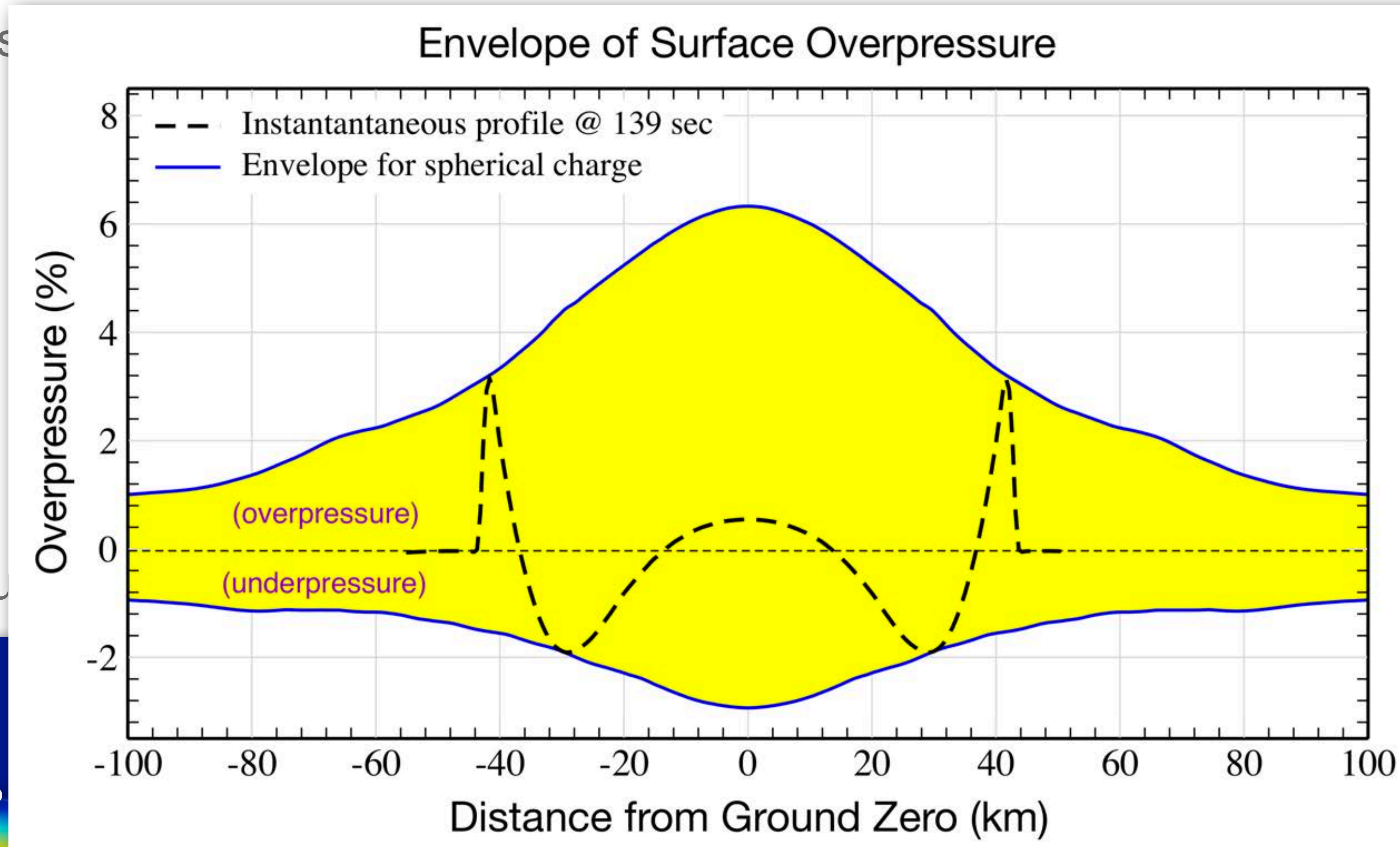

Basic Verification & Validation

Blasts over ground plane

- Numerous examples static and moving blasts over ground plane with buoyancy
  - Static airburst with

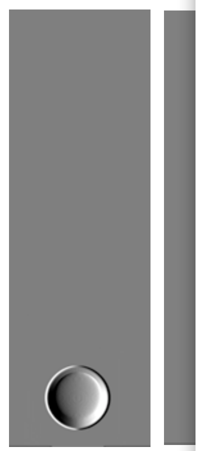

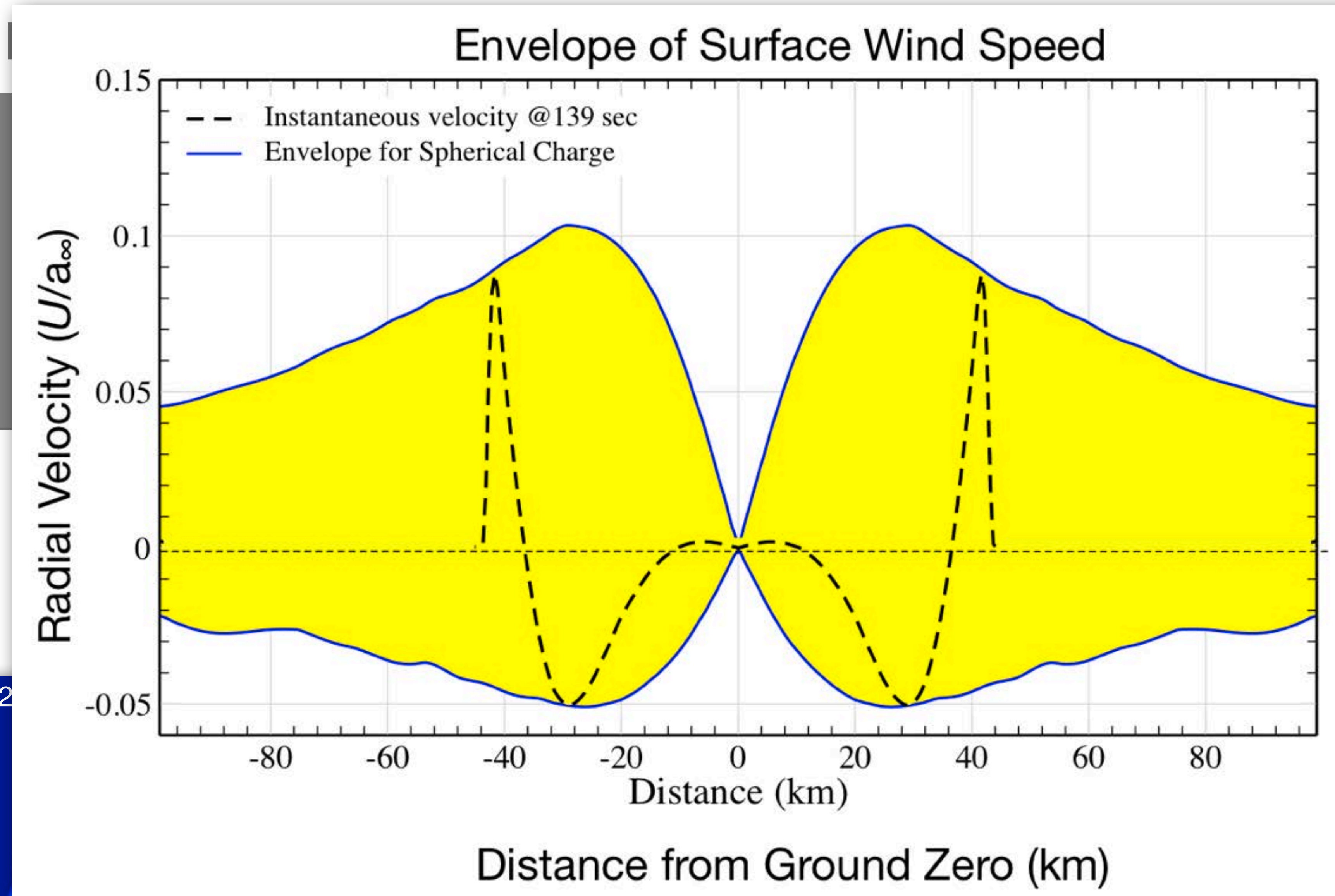

  - Moving airburst

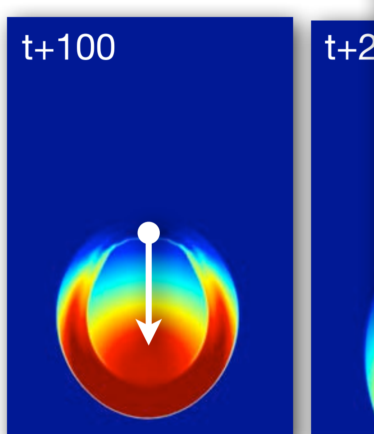

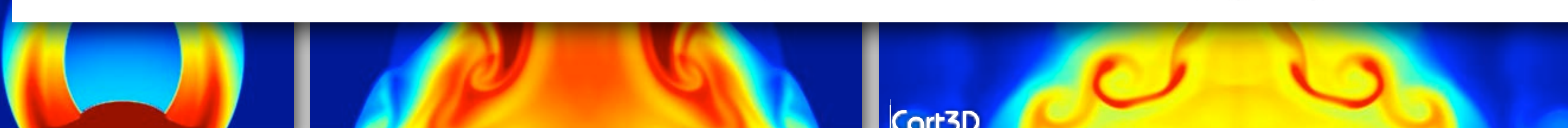

Basic Verification & Validation

Blasts over ground plane

- Numerous examples static and moving blasts over ground plane with buoyancy
  - Static airburst with buoyancy

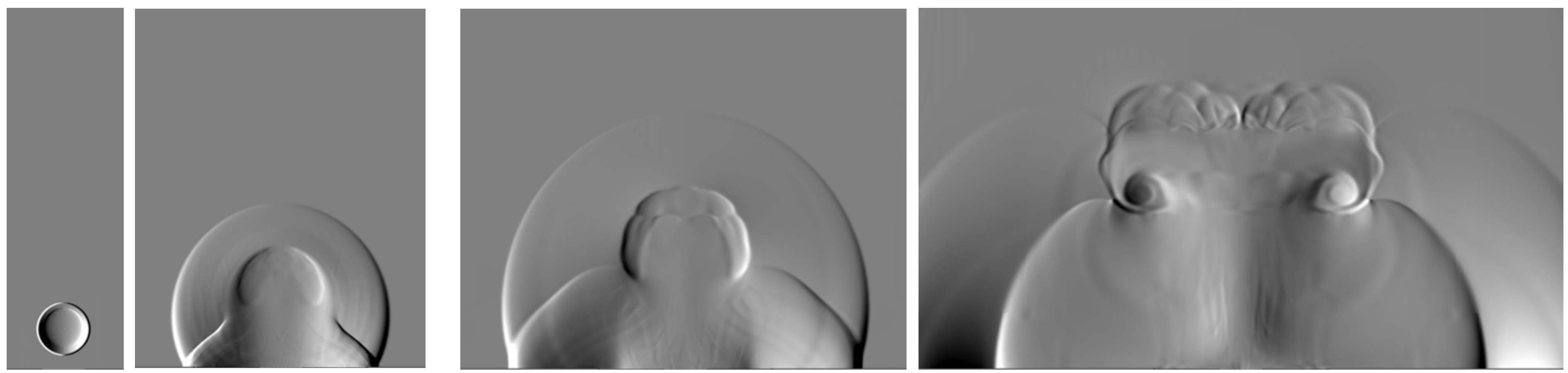

  - Moving airburst

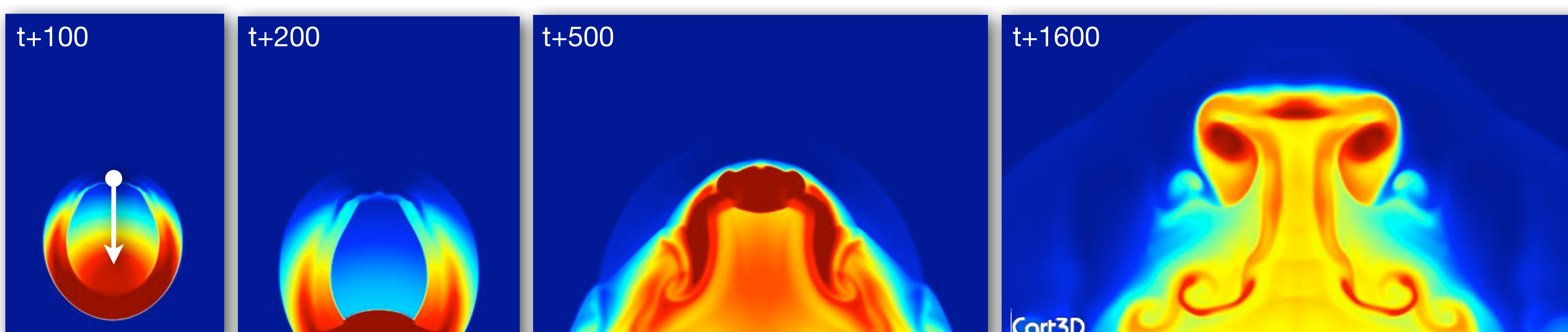

Basic Verification & Validation

Blasts over ground plane

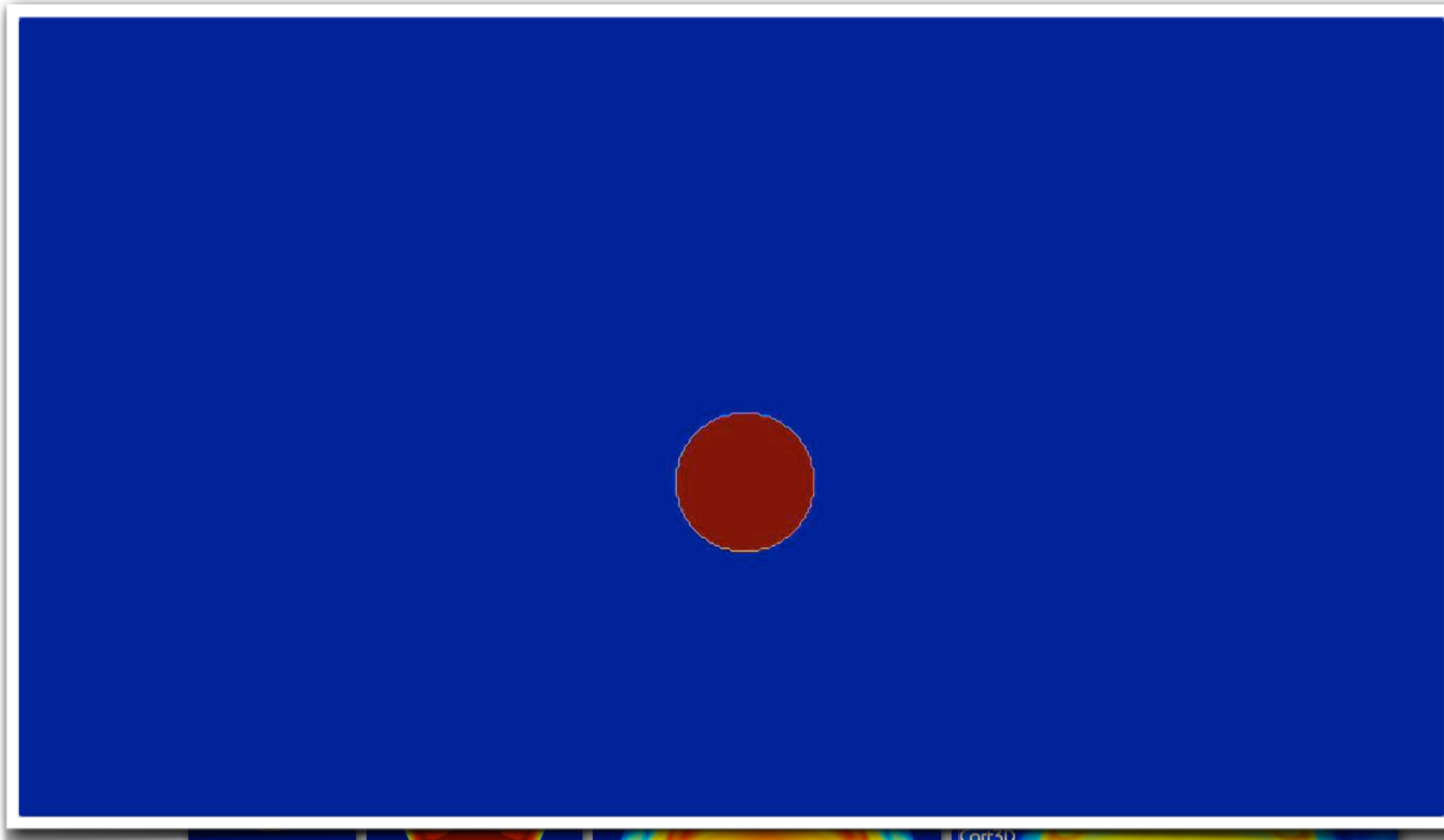

Validation: Chelyabinsk Meteor

February 15, 2013

- 12,500 metric tons, 19.8 m diameter
- Trajectory:
    - 18.6 km/sec, (~Mach 61.7)
    - 18° entry angle
- Data
    - Ground Damage (glass breakage data)
    - Shock arrival times
    - Light curve reconstruction
    - Energy deposition from infrasound measurements

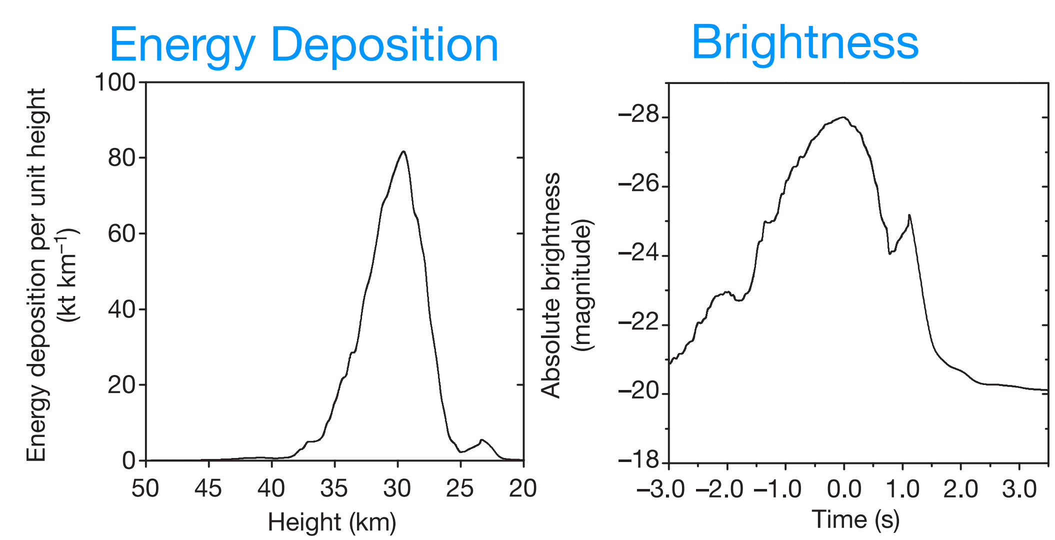

Brown et.al, Nature, 2013

Very well studied event, simulations of virtually all aspects of entry, breakup, analysis of composition, blast propagation, ground damage, etc.

Validation: Chelyabinsk Meteor

February 15, 2013

- 12,500 metric tons, 19.8 m diameter
- Trajectory:
  - 18.6 km/sec, (~Mach 61.7)
  - 18° entry angle
- Data
  - Ground Damage (glass breakage data)
  - Shock arrival times
  - Light curve reconstruction
  - Energy deposition from infrasound measurements

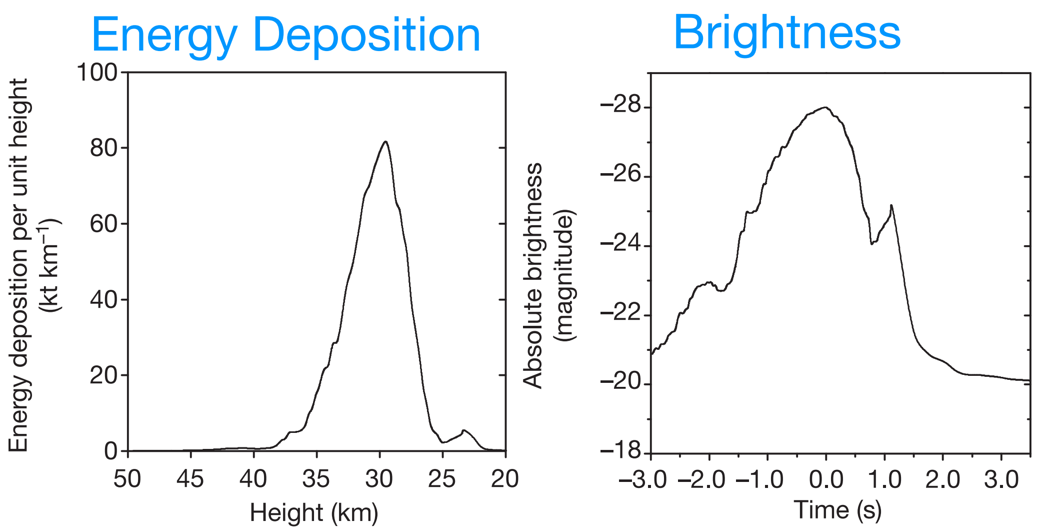

Brown et al, Nature, 2013

- Primary references used
  - Popova & Jenniskens *et al*., Science Express, November 2013
  - Brown *et al.*, Nature, November 2013
  - Chelyabinsk Airburst Consortium, + various other media

Validation: Chelyabinsk Meteor

Simulation Details

- Energy deposition:
  - E_{tot} = (520 kt – 5% radiation)
  - Profile from Brown et al. Nature 2013
- Net mass deposited:
  - m_{tot} = 12.5e6 kg
- Trajectory:
  - 18.6 km/sec, (~Mach 61.7) @ 18° angle
  - Peak brightness @ 29.5 km
  - ~110 km length, 60→24 km altitude
  - Assume constant velocity
- 3D simulation with ~90M cells
  - Resolution of ~20 m along trajectory & ~100 m resolution near ground
  - Simulation covers ~300 sec. of real time

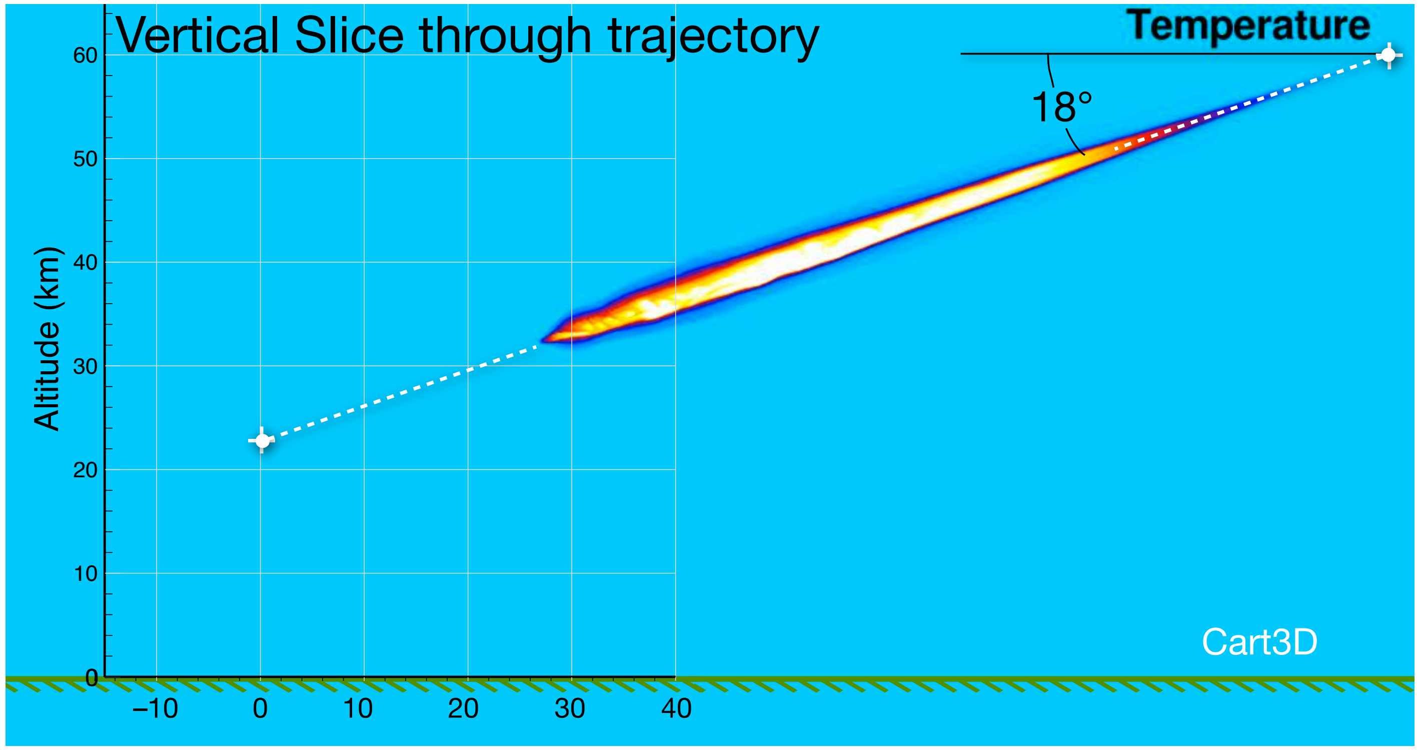

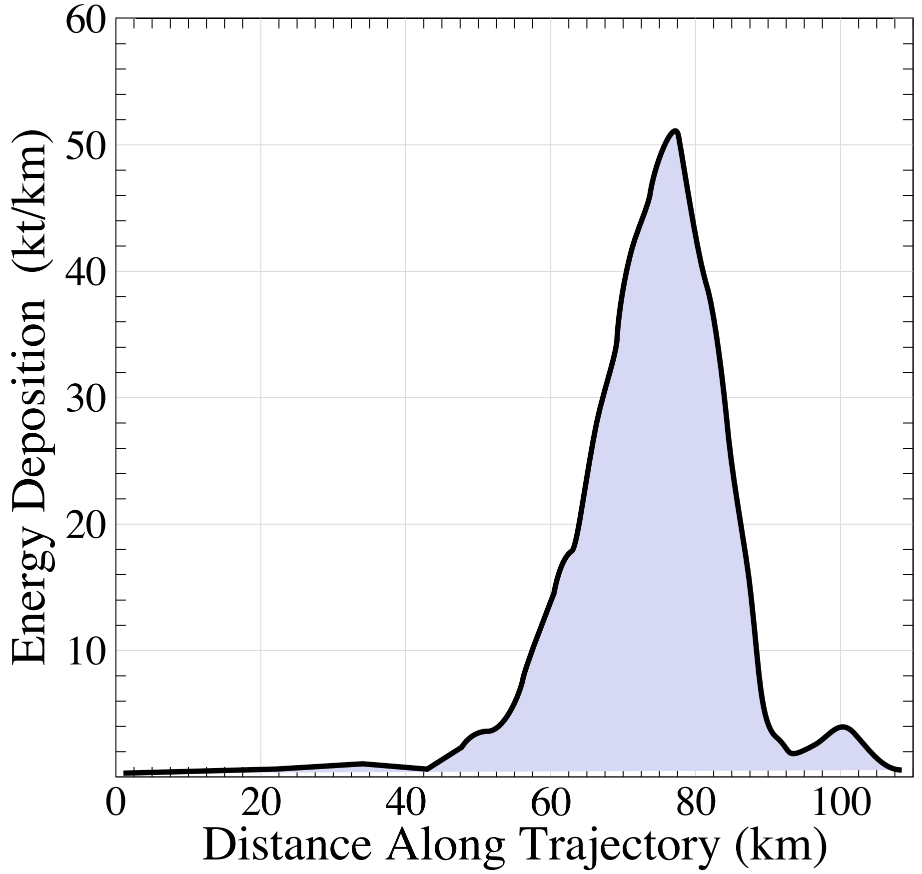

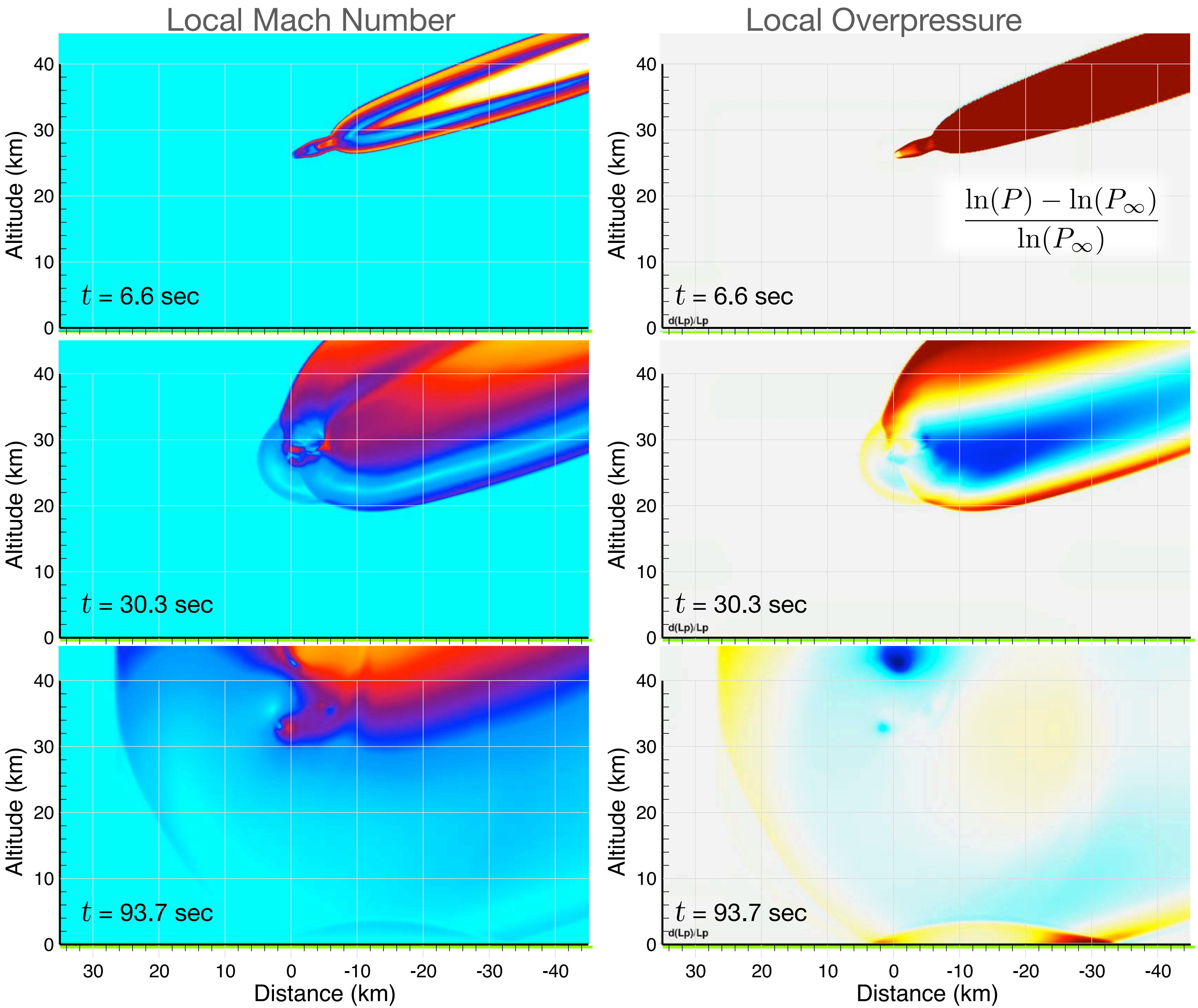

Local Mach Number
Local Overpressure
Altitude (km)
Distance (km)
t = 6.6 sec
t = 30.3 sec
t = 93.7 sec
$\dfrac{\ln(P) - \ln(P_\infty)}{\ln(P_\infty)}$
d(Lp)/Lp

Validation: Chelyabinsk Meteor

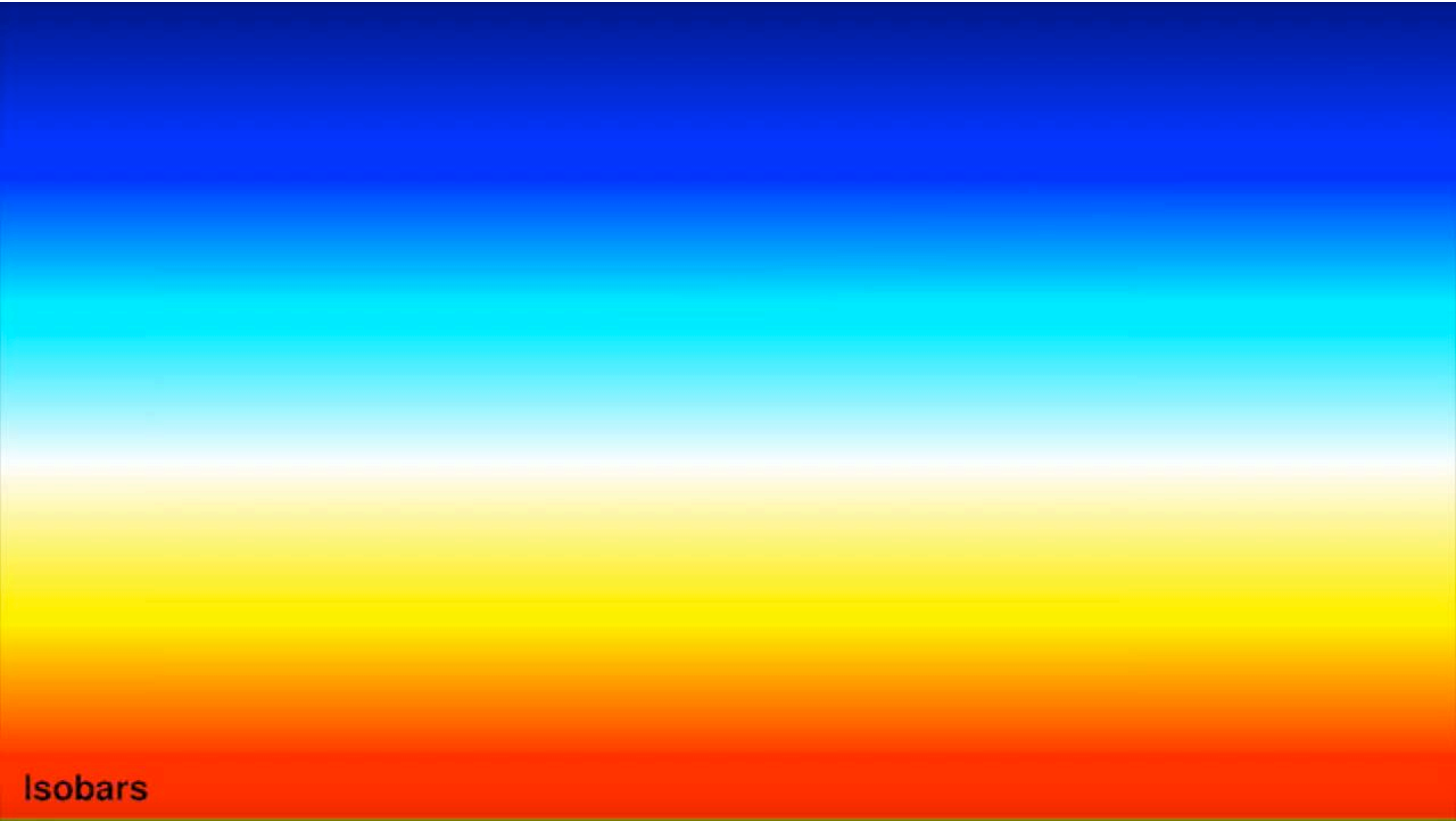

Validation: Chelyabinsk Meteor

Ground footprint

- Goal is prediction of pressure & velocity on the ground
- Blast first contacts ground at t = ~82.7 sec elapsed time (~78 sec. after peak brightness)
  - Excellent agreement with earliest data on blast arrival time data (76 – 90 sec) (Popova et al.)

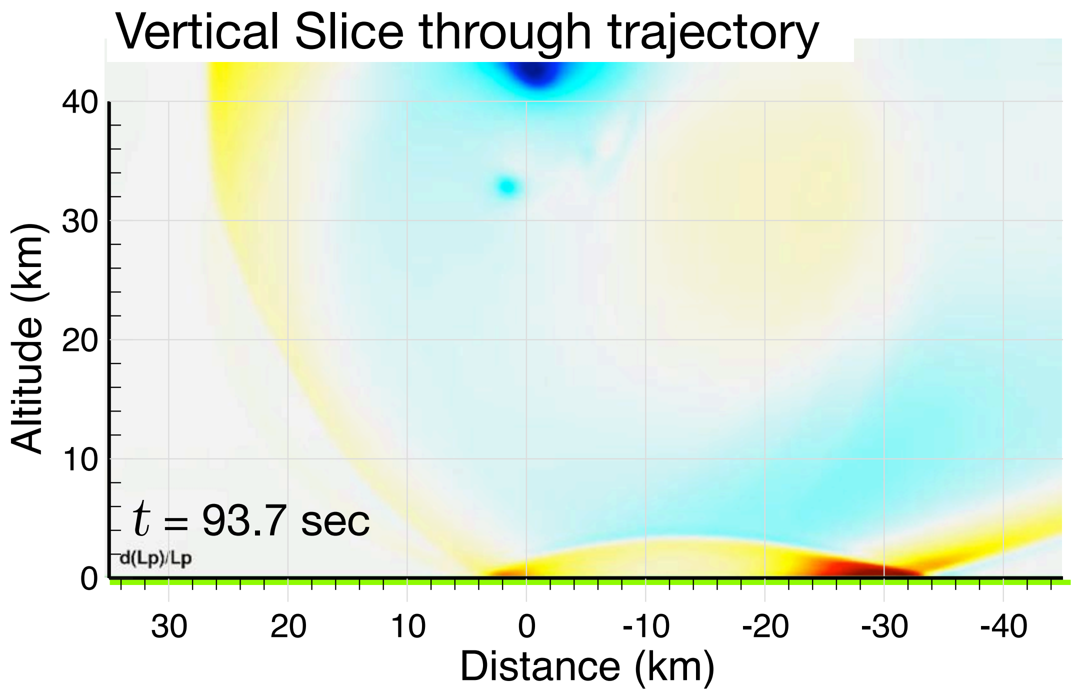

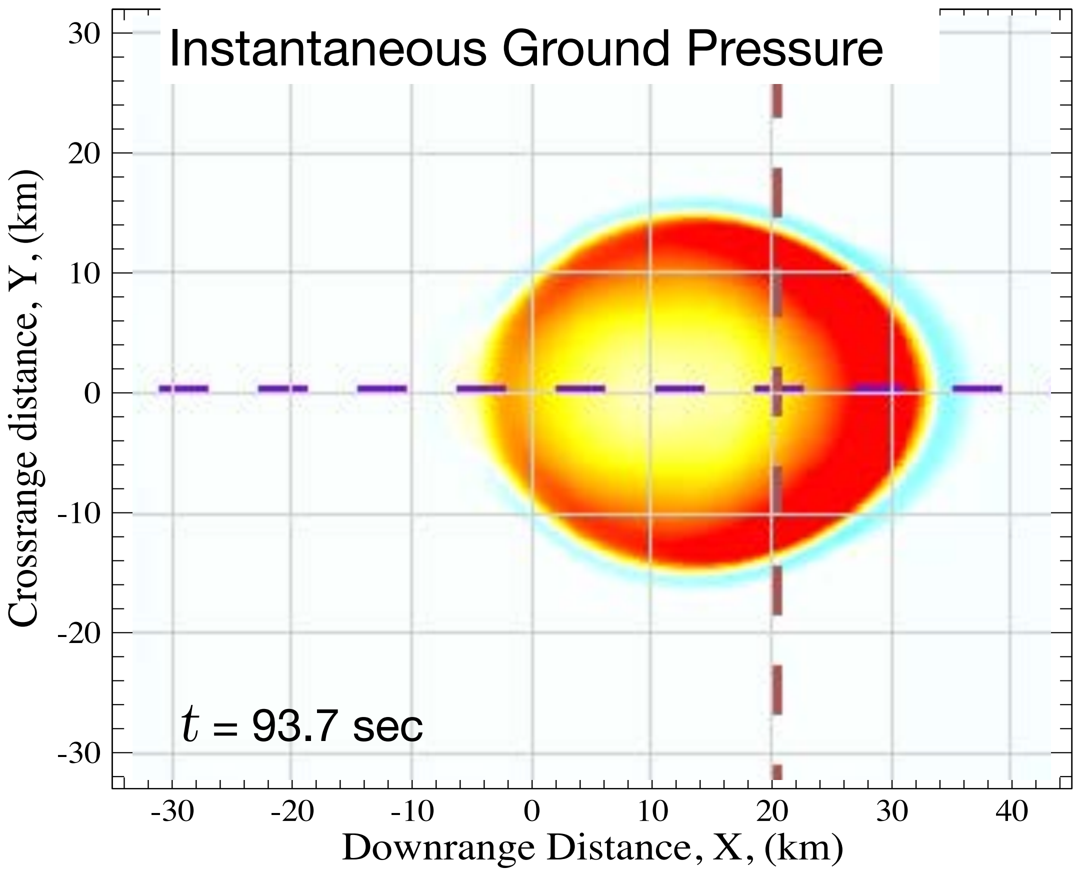

Validation: Chelyabinsk Meteor

Ground footprint evolution

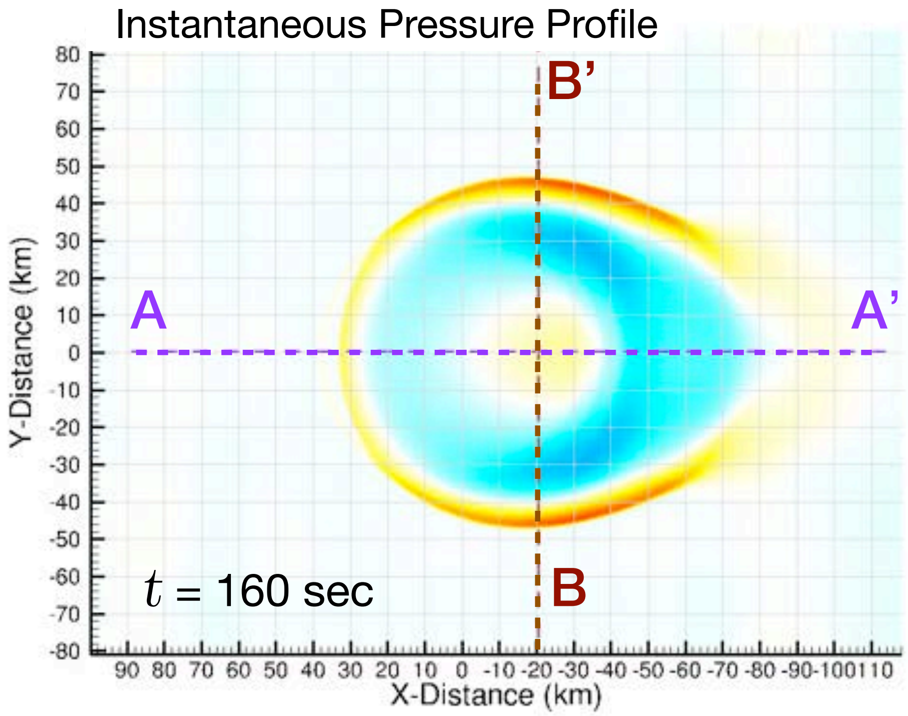

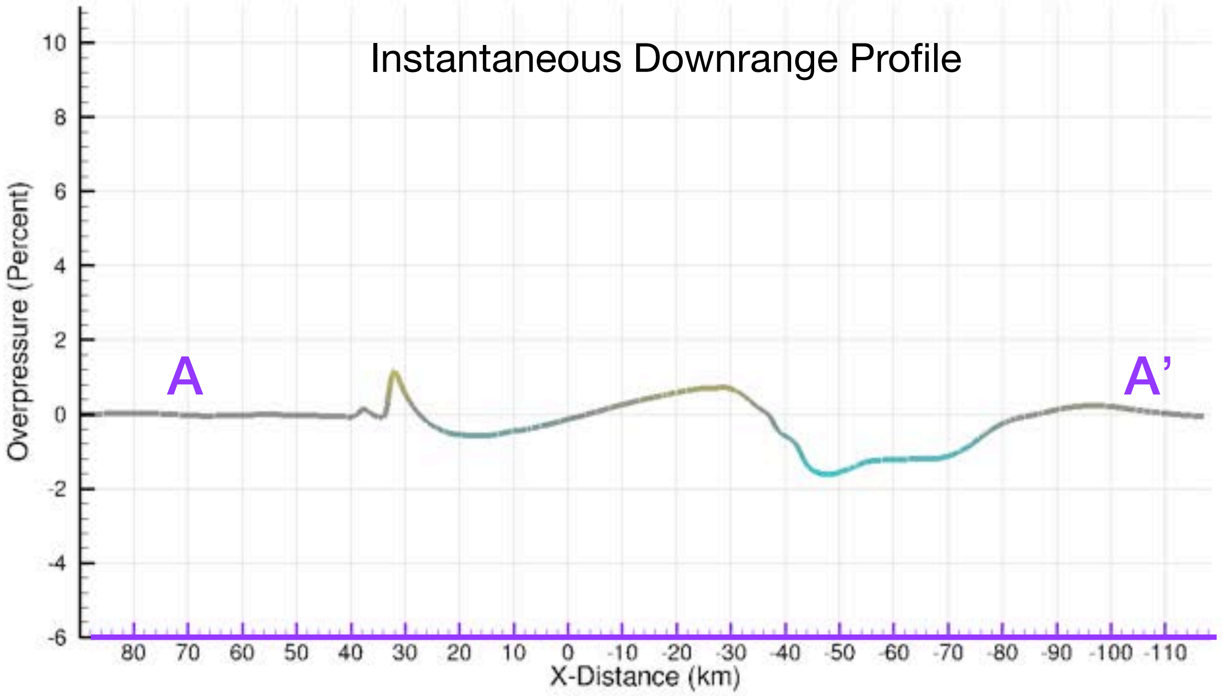

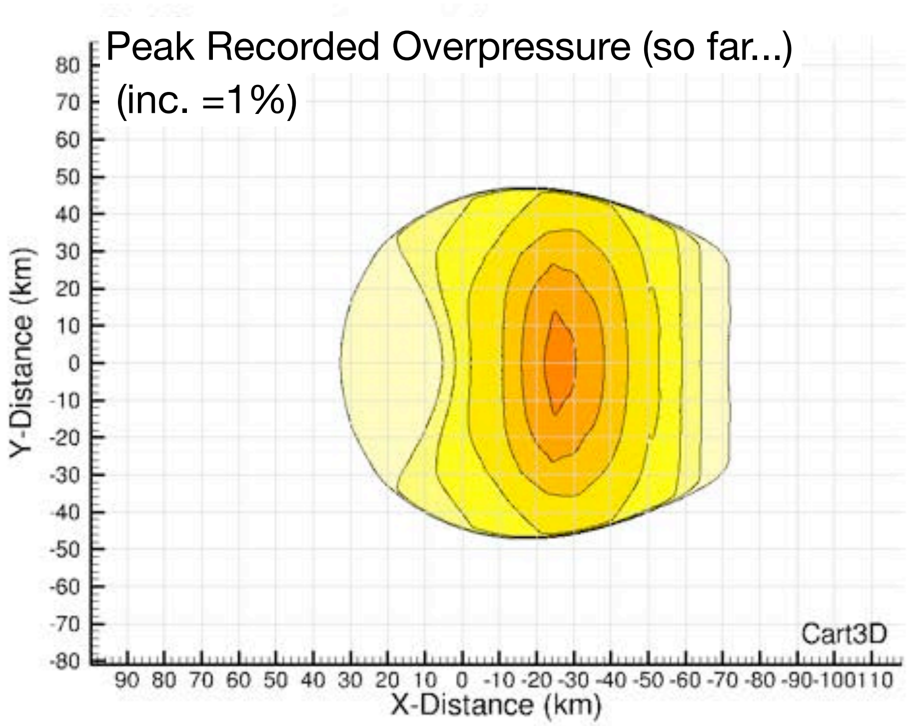

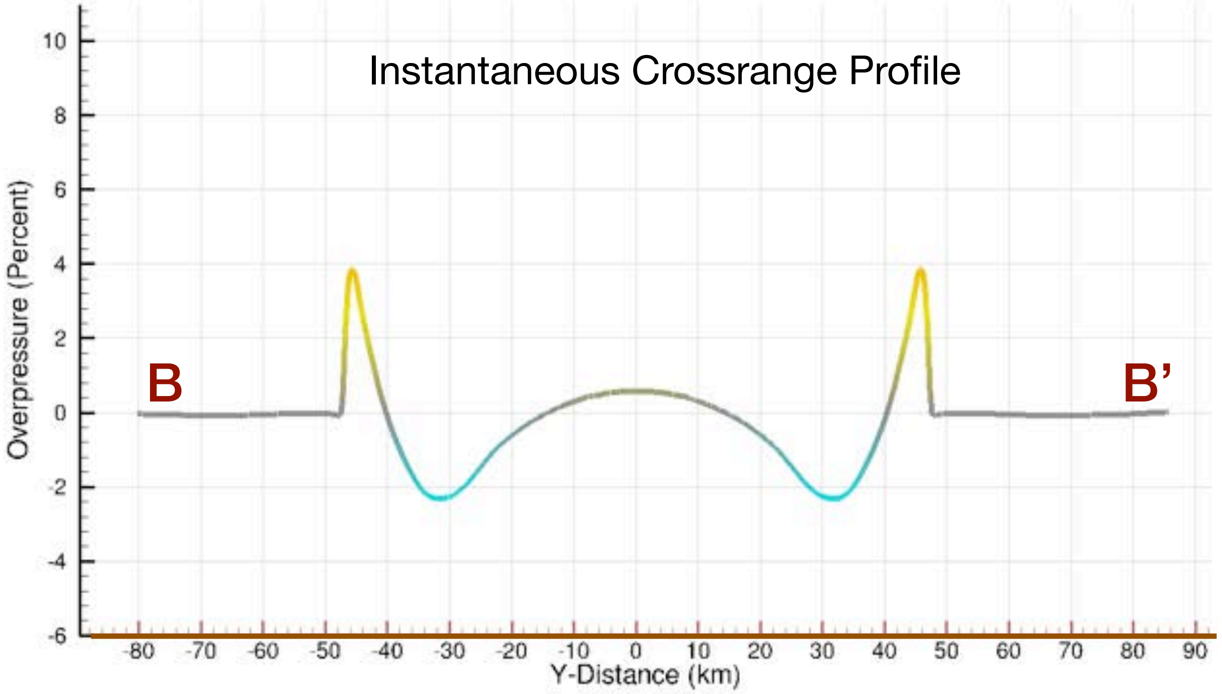

Validation: Chelyabinsk Meteor

Ground footprint evolution

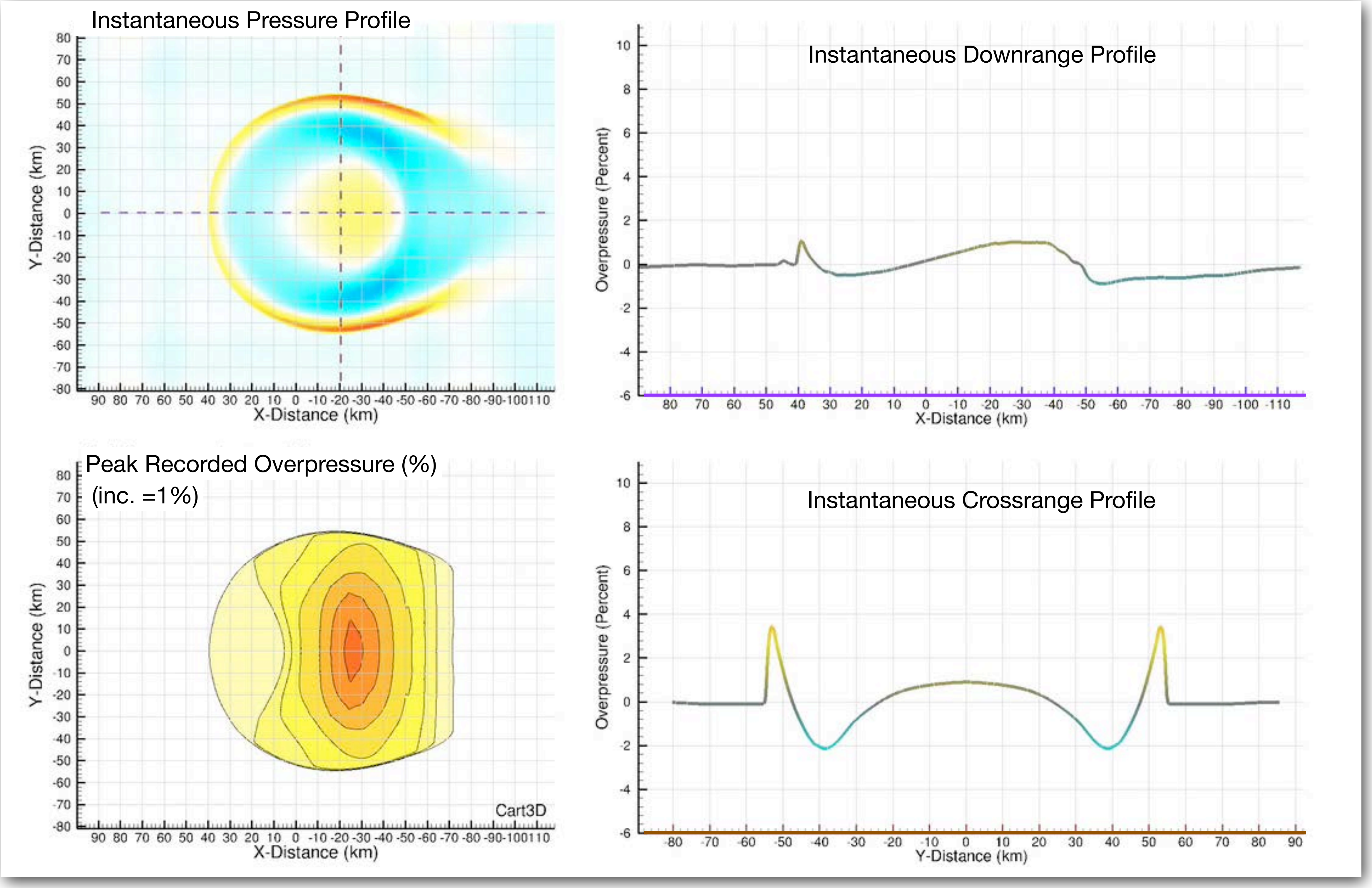

Validation: Chelyabinsk Meteor

Peak Ground Overpressures

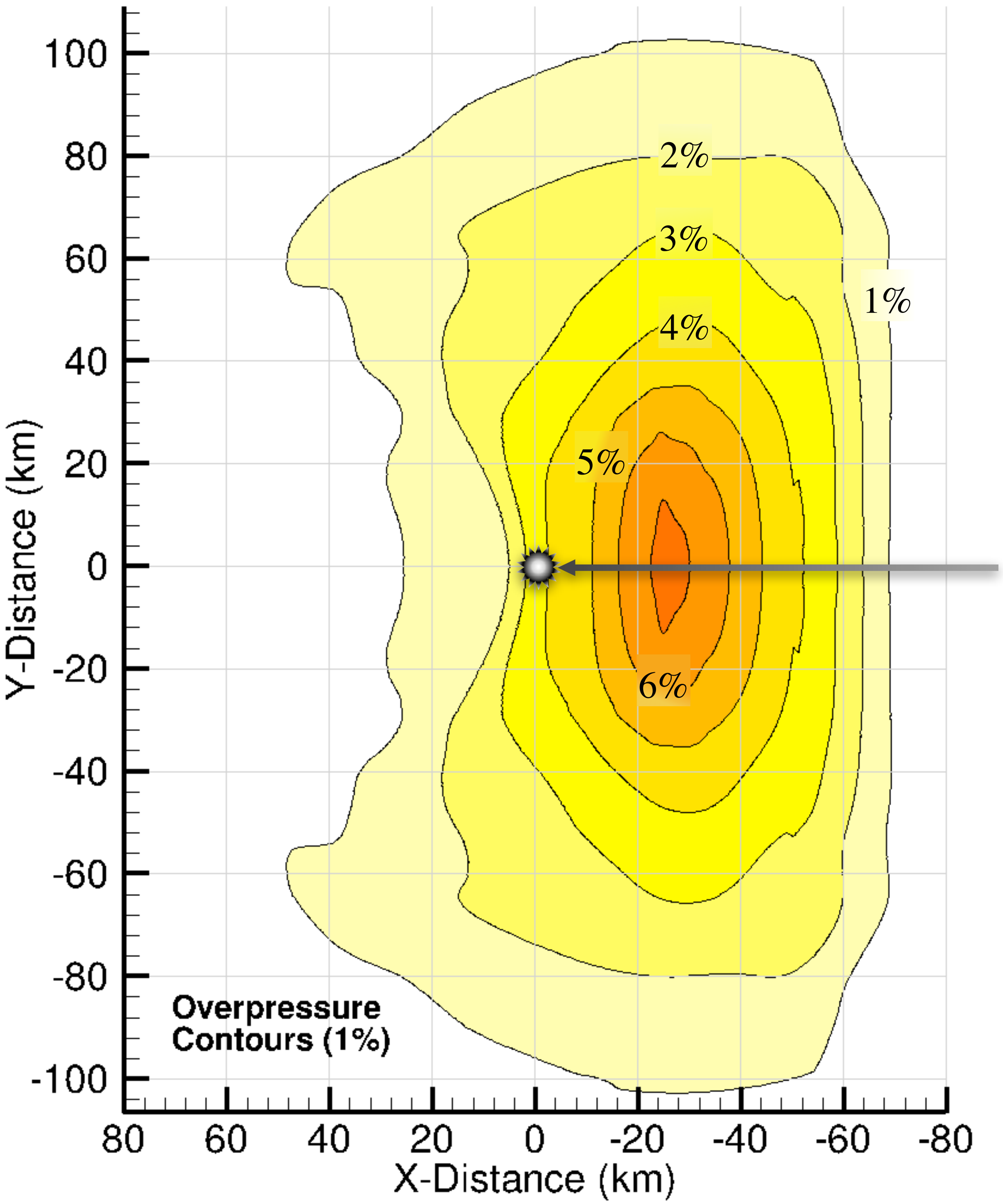

Validation: Chelyabinsk Meteor

Peak Ground Overpressures

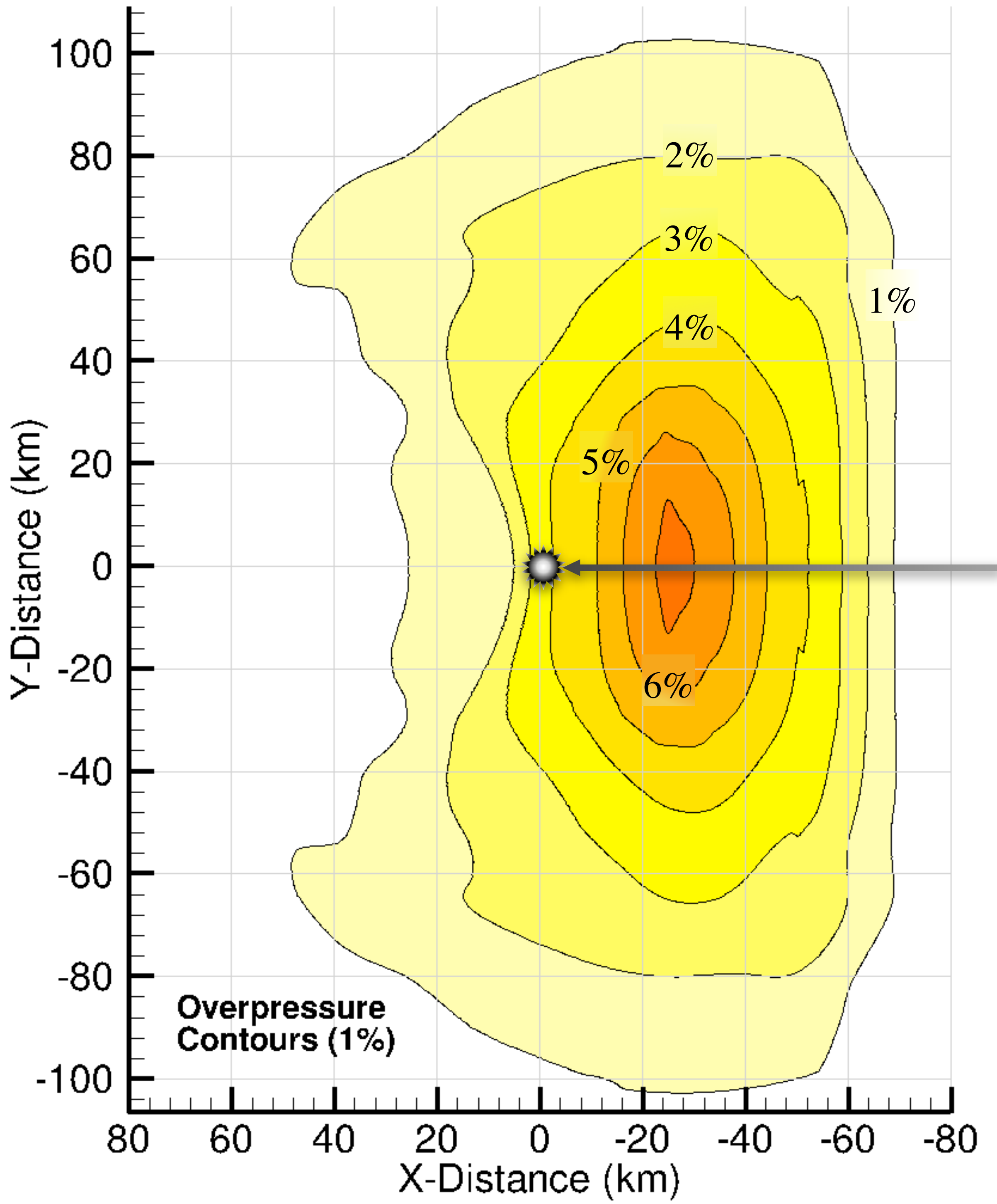

Glass Damage Data Comparison

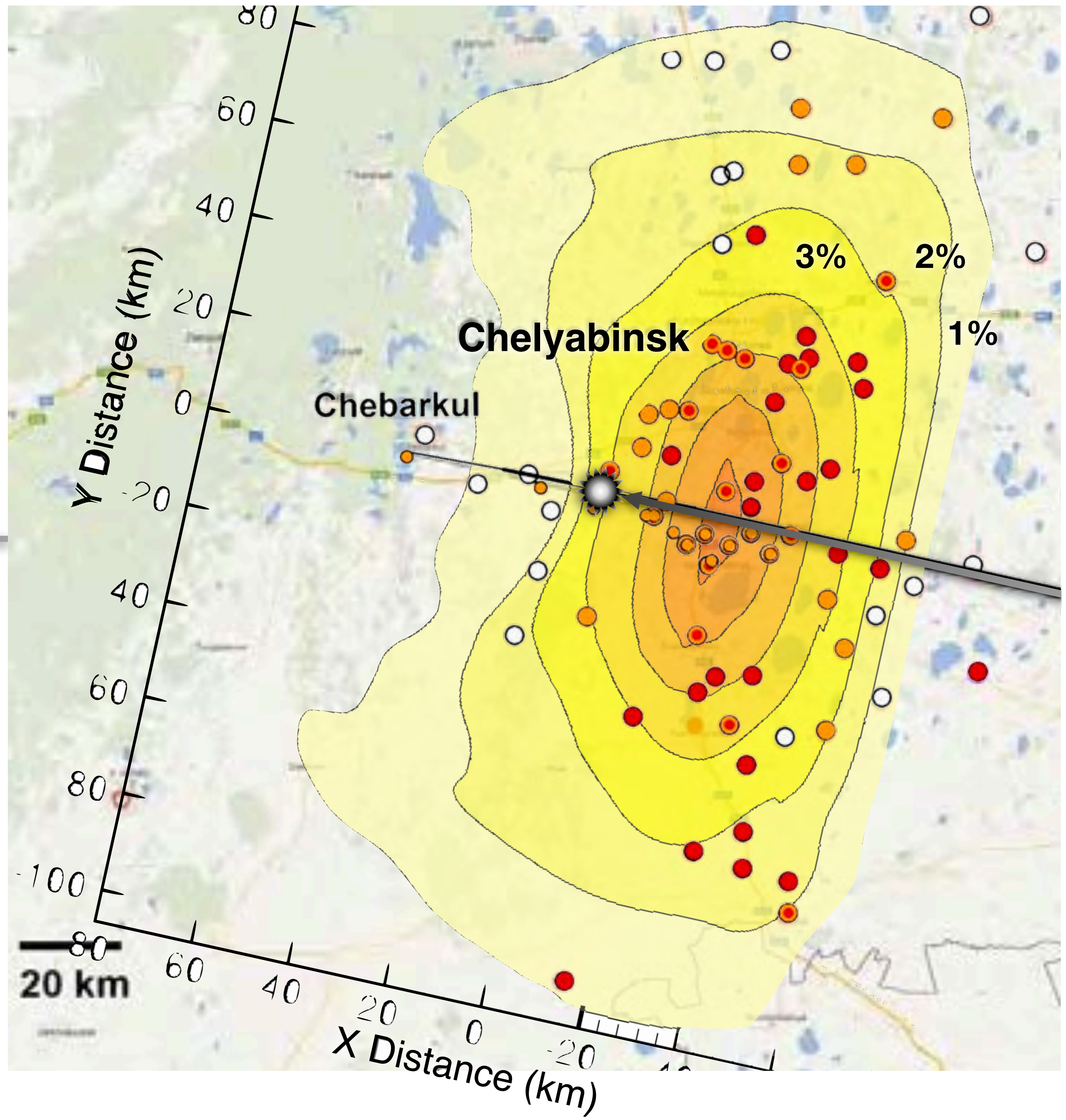

Validation: Chelyabinsk Meteor

Peak Ground Overpressures

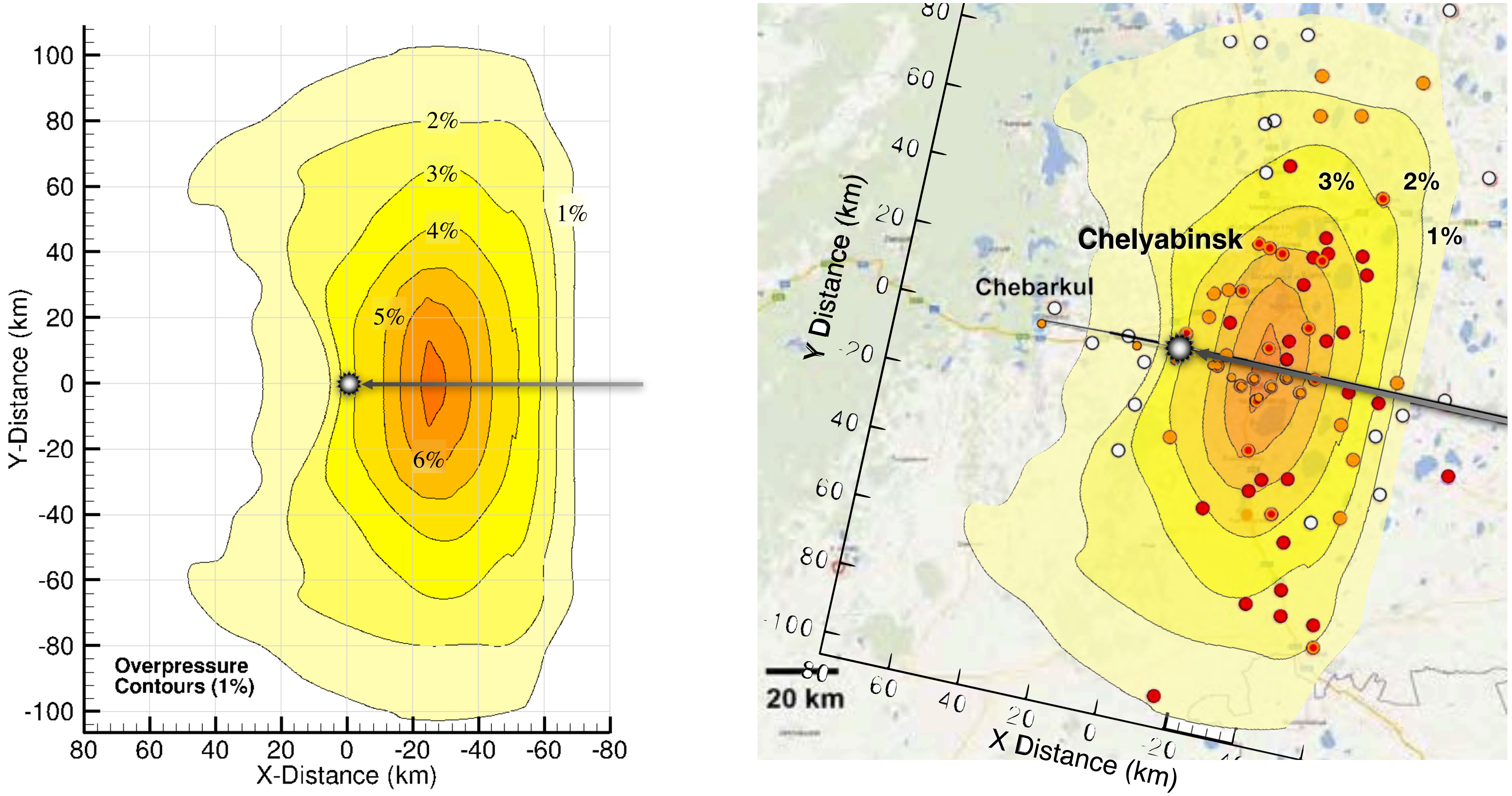

- Glass damage data collected by the Chelyabinsk Airburst Consortium
- Statistical correlation (Mannan & Lees) show 700 Pa (0.69%) shatters ~5% of typical windows, 6% overpressure breaks roughly 90%.
- Footprint similar to those in Popova et al. (ScienceExpress)
- Breakage data estimate overpressure at chelyabinsk ~2-4% (P. Brown)

Validation: Chelyabinsk Meteor

Shock Arrival Time

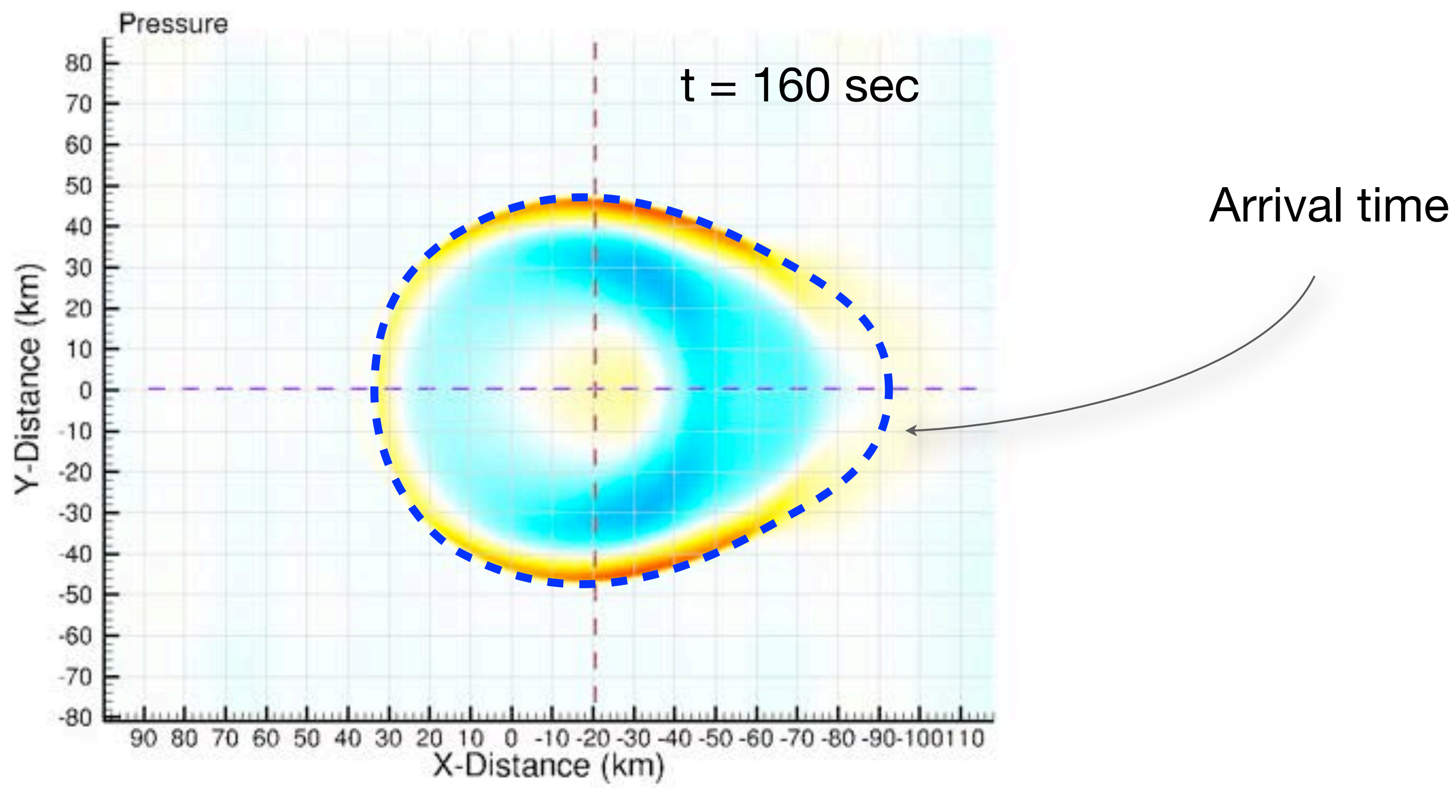

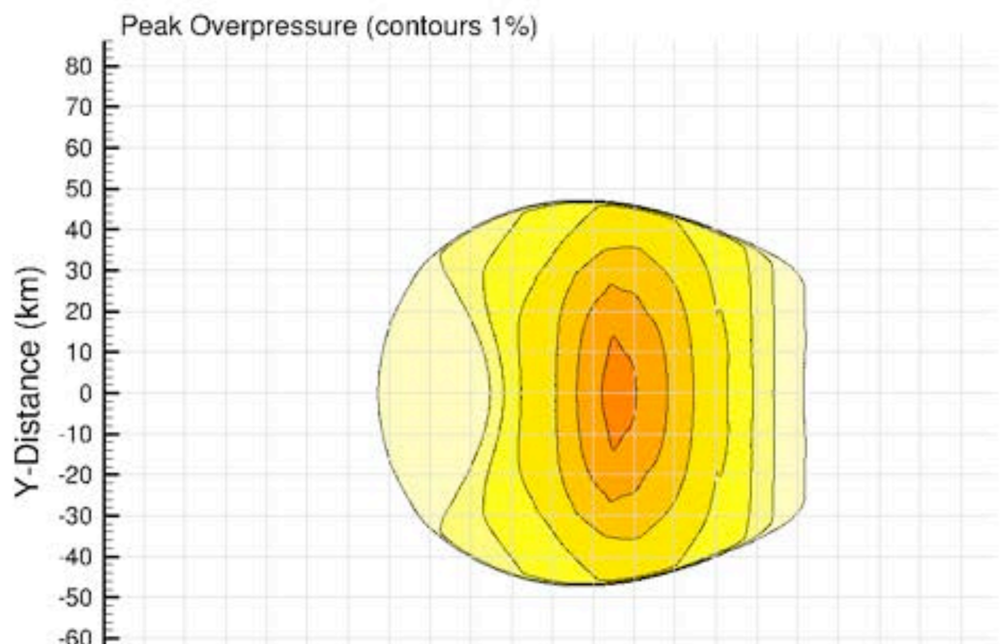

Validation: Chelyabinsk Meteor

Shock Arrival Time

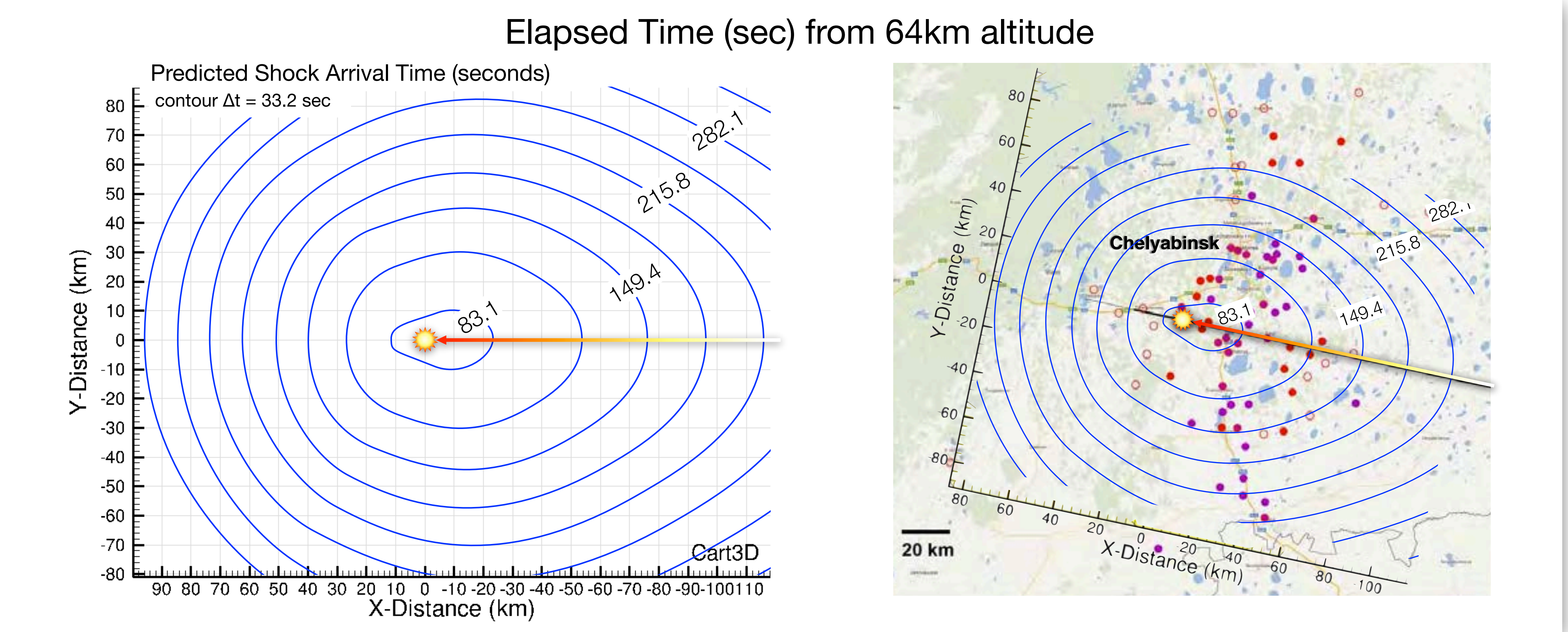

- Peak brightness at ~4 sec. elapsed time
- First arrival at ~78 sec after peak brightness,
- Predict ~90 sec (from peak brightness) at Korkino and Yemanzhelinsk
- Arrival in vicinity of Chelyabinsk at 140 - 145 seconds
- Neglected local wind, temperature and other effects of the real atmosphere
- Overall very good agreement with data & best predictions in literature

Overview

Report current status of effort and connection with PRA and tsunami

- Modeling & Solver
- Verification & Validation
  - Basic
  - Chelyabinsk Case Study
- Investigations of ground-footprint sensitivity
  - Line-source vs time-dependent entry
  - Entry Angle
- Upcoming Efforts

Overview

Report current status of effort and connection with PRA and tsunami

- Modeling & Solver
- Verification & Validation
  - Basic
  - Chelyabinsk Case Study
- Investigations of ground-footprint sensitivity

- Sensitivity to entry modeling
  - Time-dependent compared to simple line source
  - Entry angle / Spherical charge investigation

- U

Sensitivity - Entry Modeling

Time-Dependent modeling vs simple line source

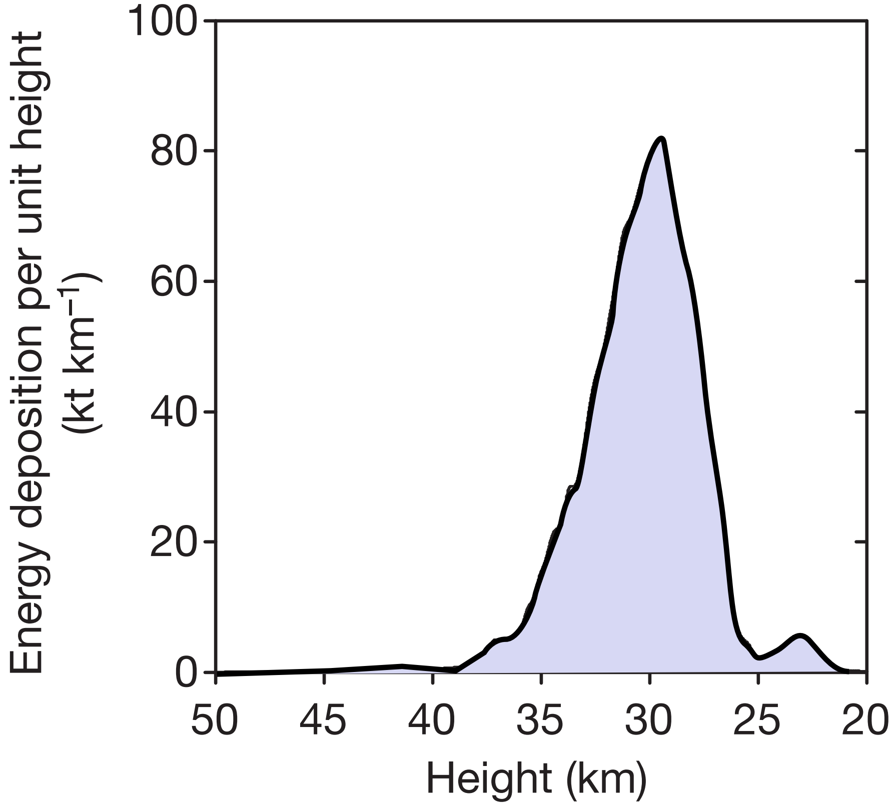

- Entry only lasts for seconds, blast propagates for minutes
  - Detailed entry modeling requires very fine time-scales ($\Delta t \approx$ 1.e-4)
  - Cost: 90M cell simulation: (1000 cores x 8-12 hrs) - Under 1% of NAS Pleiades
  - Line Source for mass, momentum and energy can reduce cost by 50%
- When is line source modeling appropriate?

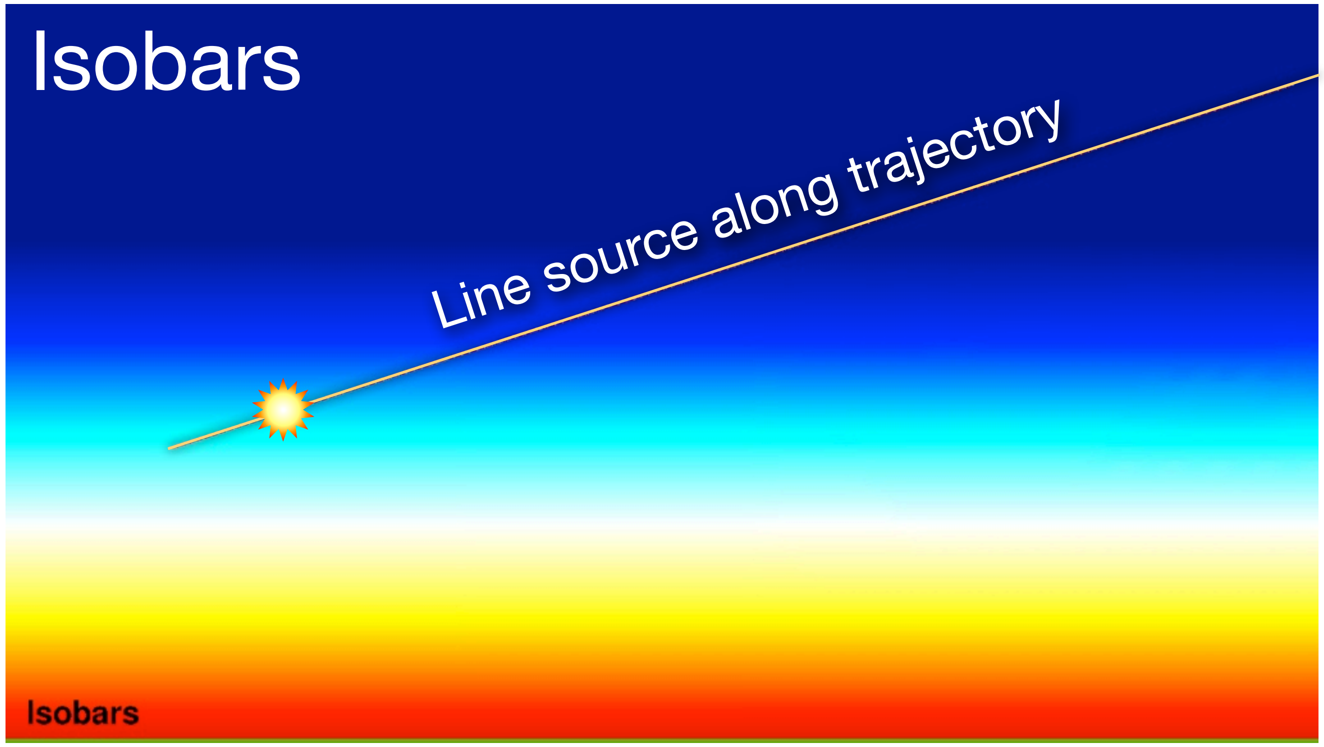

Sensitivity - Entry Modeling

Seconds after entry

Time-Dependent

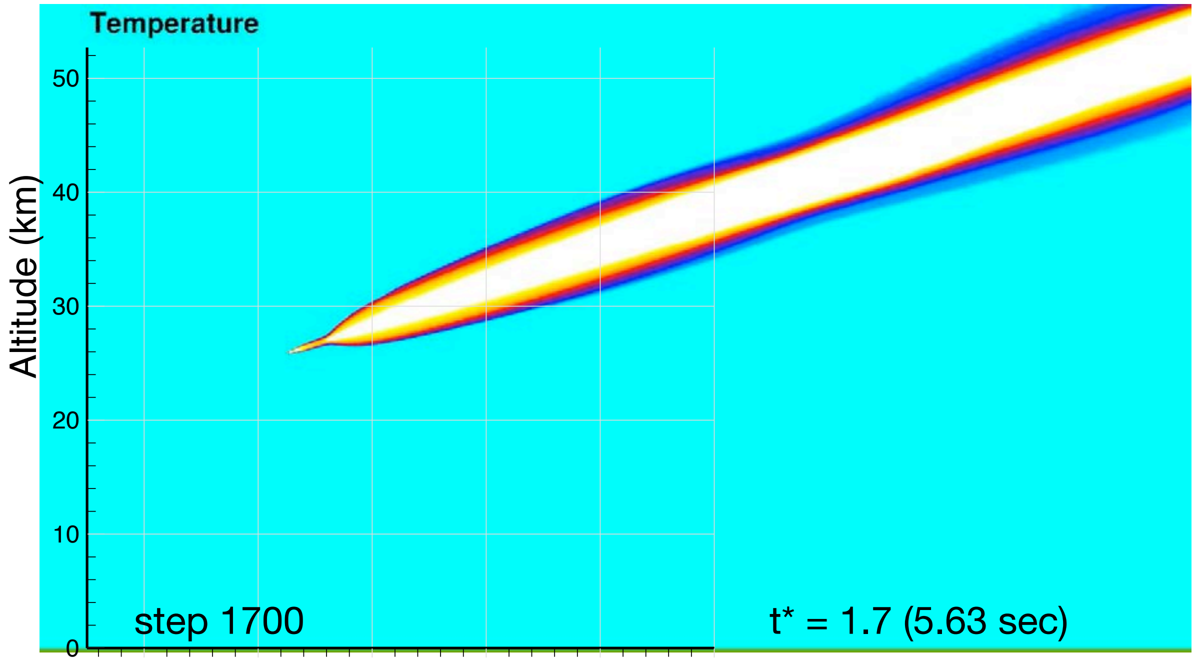

Line Source

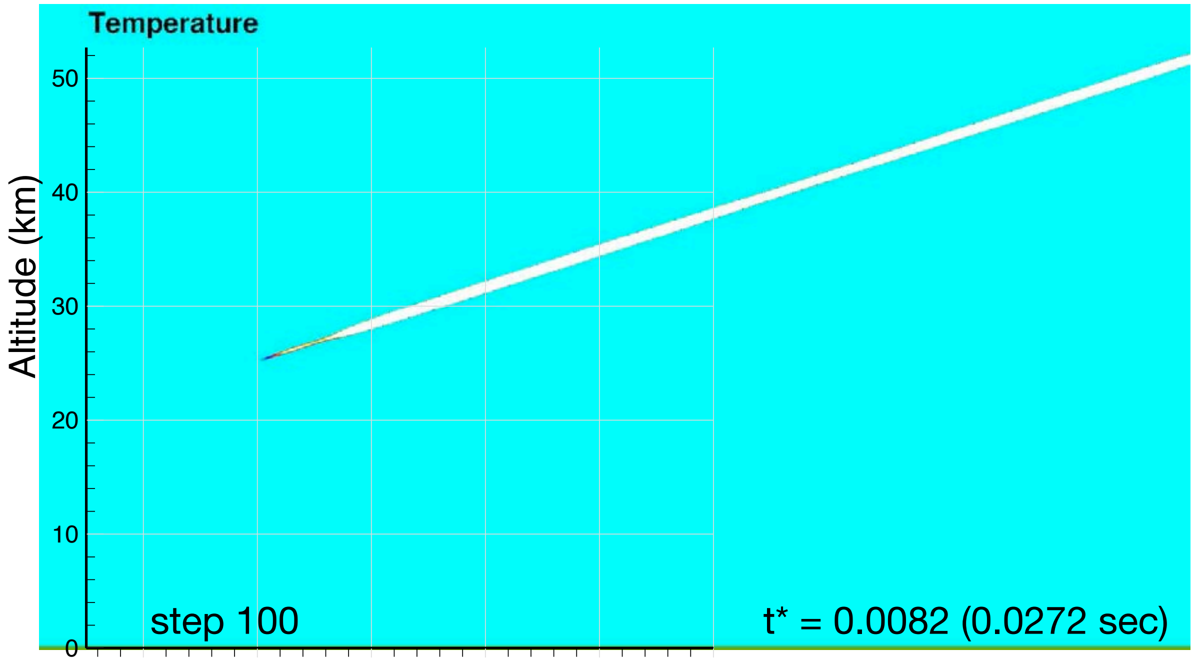

Sensitivity - Entry Modeling

Seconds after entry

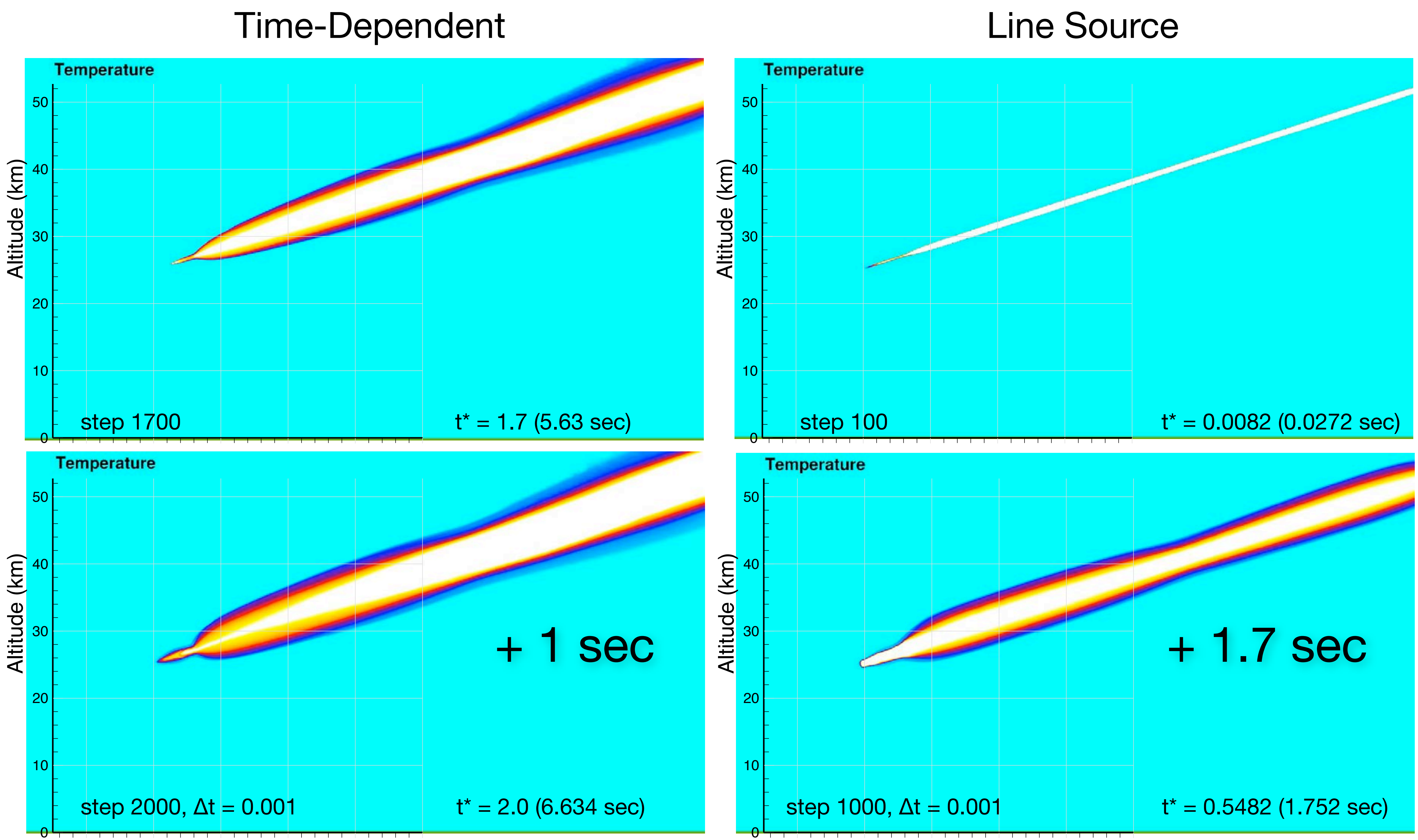

Sensitivity - Entry Modeling

Minutes after entry

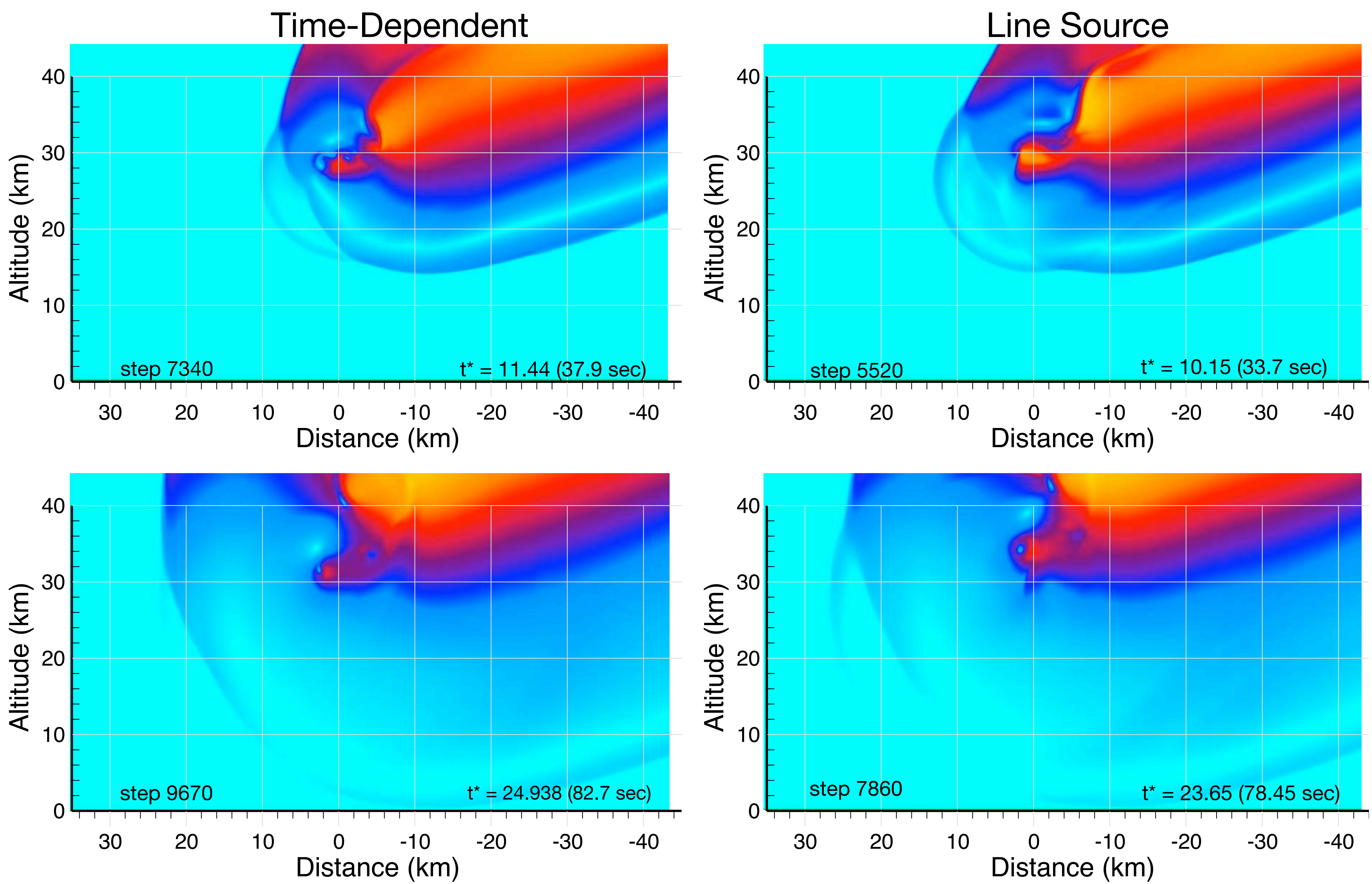

Sensitivity - Entry Modeling

Ground Footprint

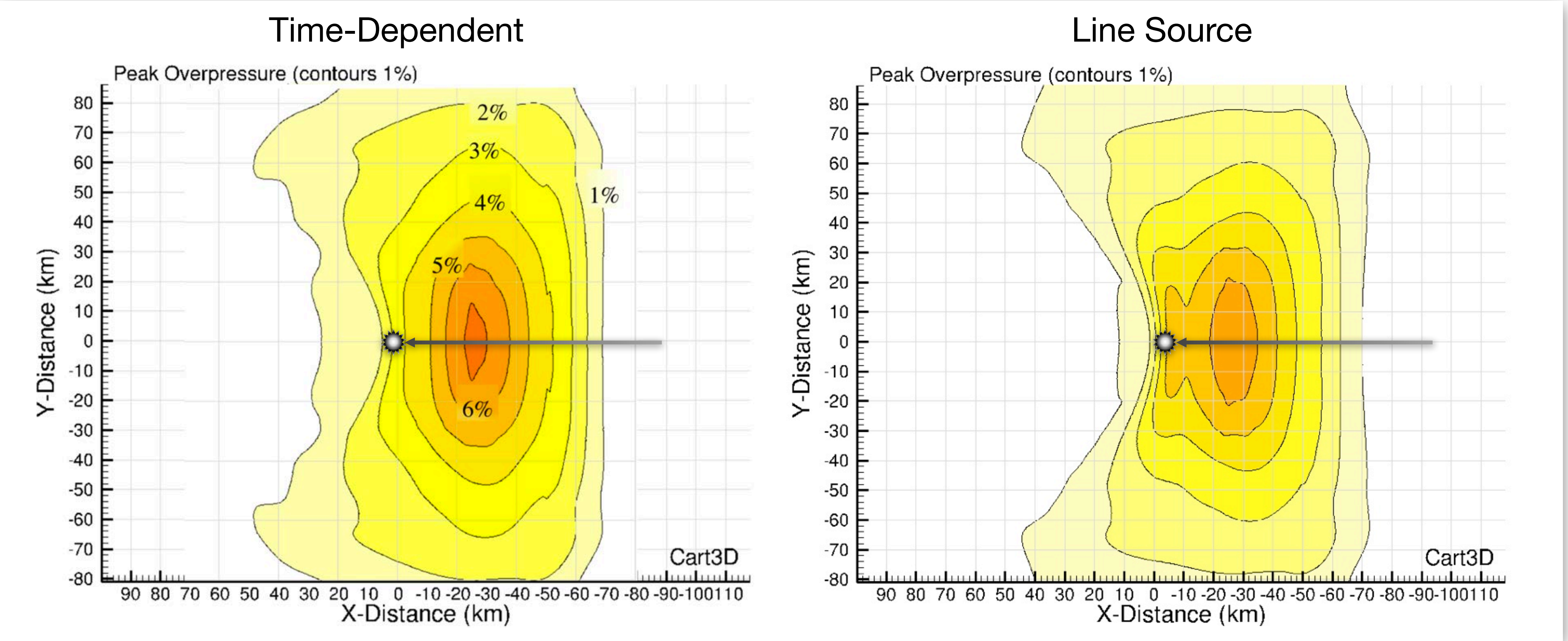

- Some differences in highest overpressures (~1%) at earliest arrival time
- Closer agreements at later time
- Good agreement for location of peak ground pressure
- Good agreement of arrival time from peak brightness
- Geometry dictates that low-entry trajectories will show most discrepancy

Sensitivity - 90° Entry vs Spherical Charge

How good is a static spherical charge model?

- Very cheap spherical charge models exist.
- Various handbook methods for damage estimation use spherical charge data
- Can these be used in risk assessment?
  - Where are these appropriate?
  - Perform quantitative assessment
- Investigate ground footprint
  - Accuracy of overpressure
  - Extent/strength of footprint
  - Details of impulse of blast on ground

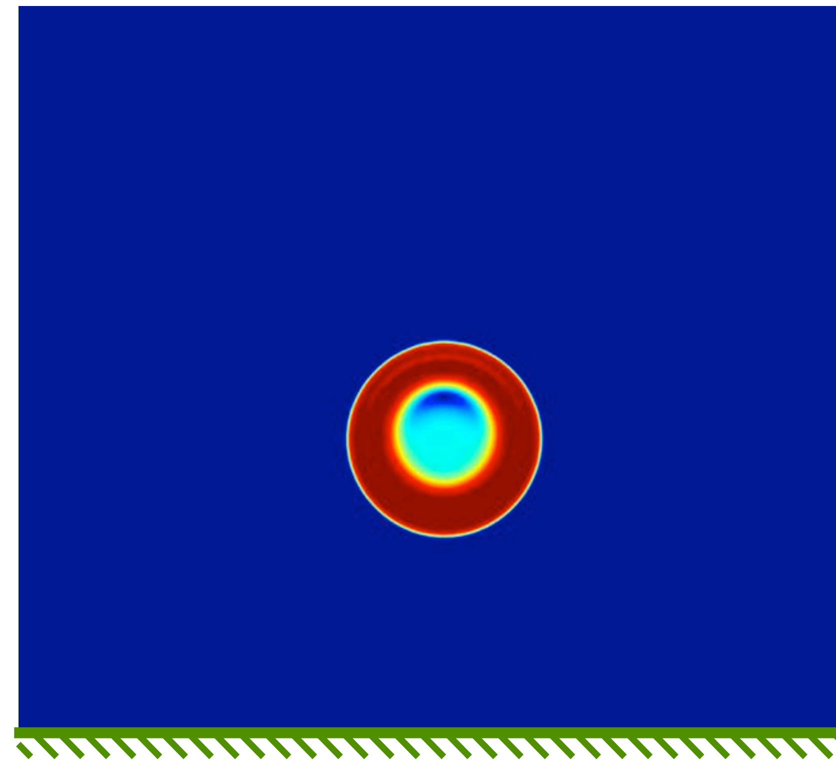

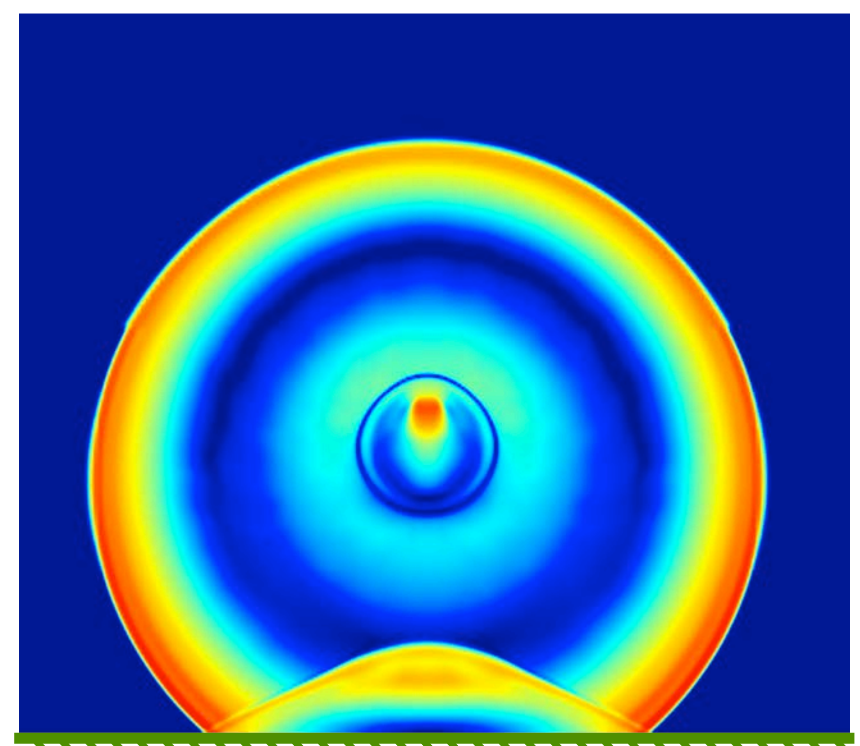

Sensitivity - 90° Entry vs Spherical Charge

How good is a static spherical charge model?

Line-Source at 90°

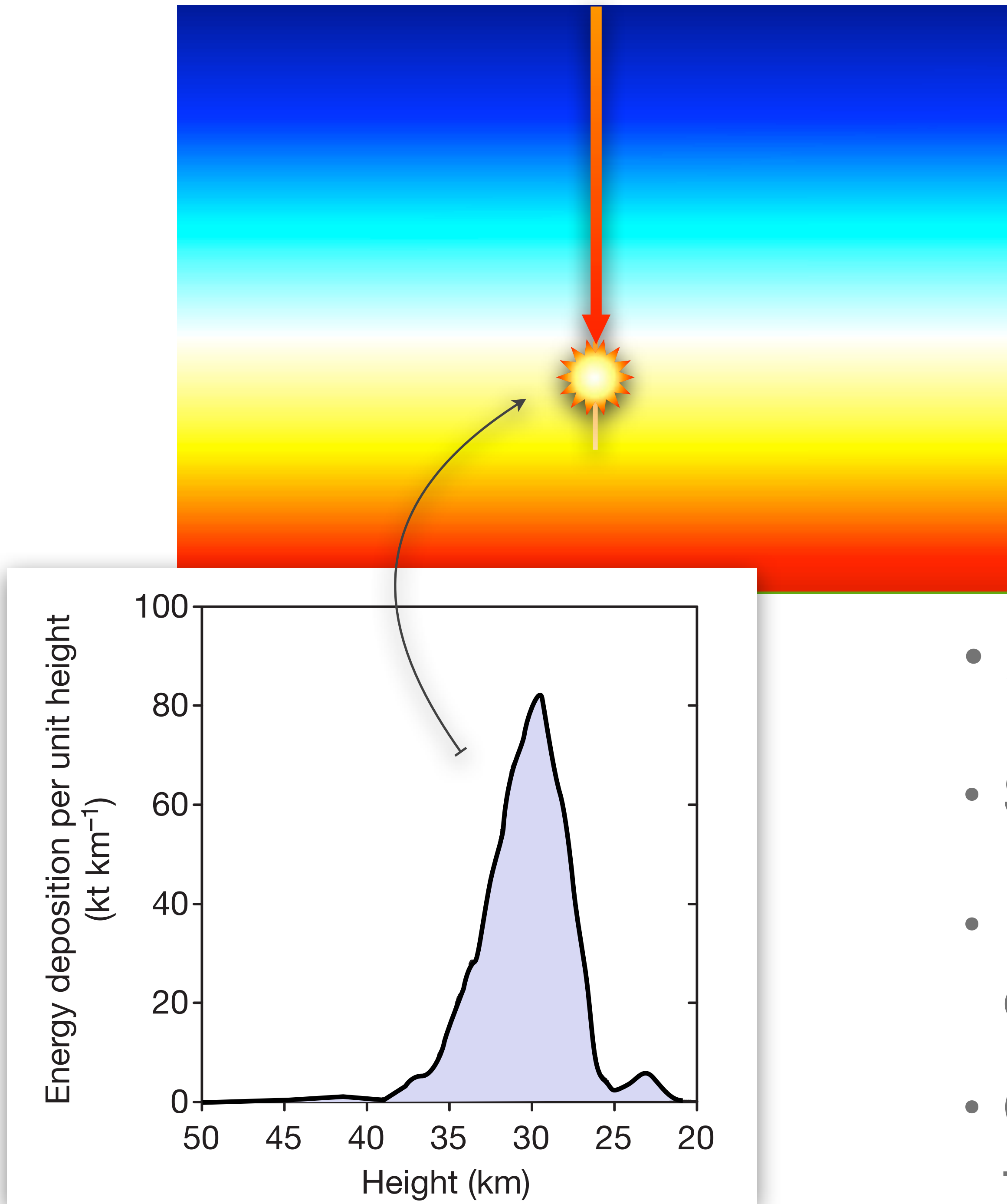

Spherical Charge

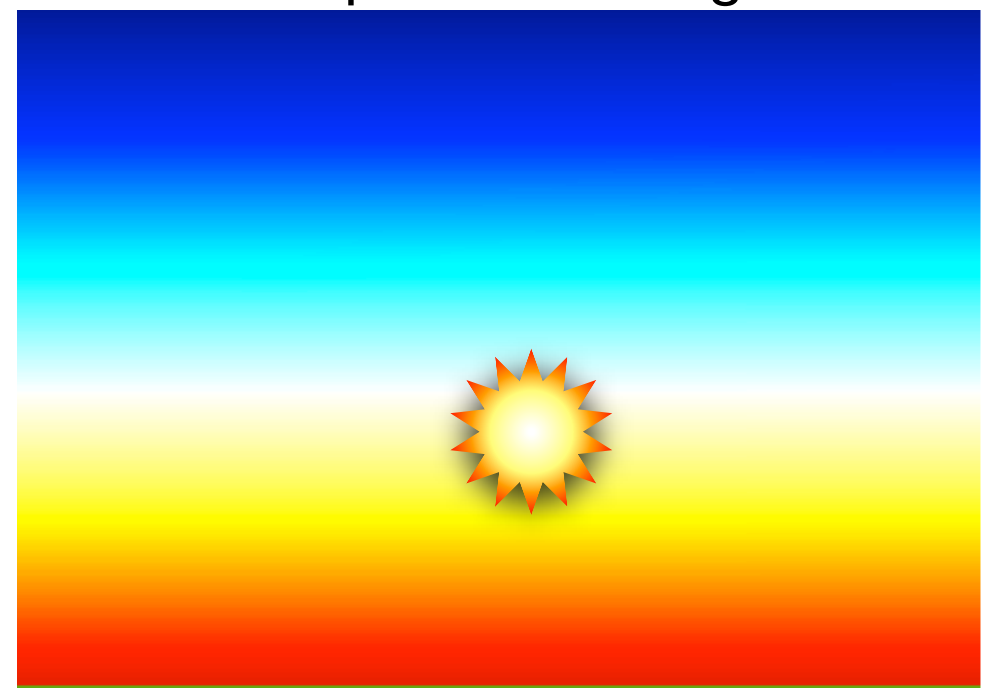

- E_{tot} = 520 kt, m_{tot} = 12.5e6 kg
- Spherical charge @ 29.5km altitude, r_i = 1km
- Line Source, 90° trajectory with same energy deposition as before
- Can also compare line source with 18° case for insight into entry angle sensitivity

Sensitivity - 90° entry vs Spherical Charge

Time evolution

Line Source

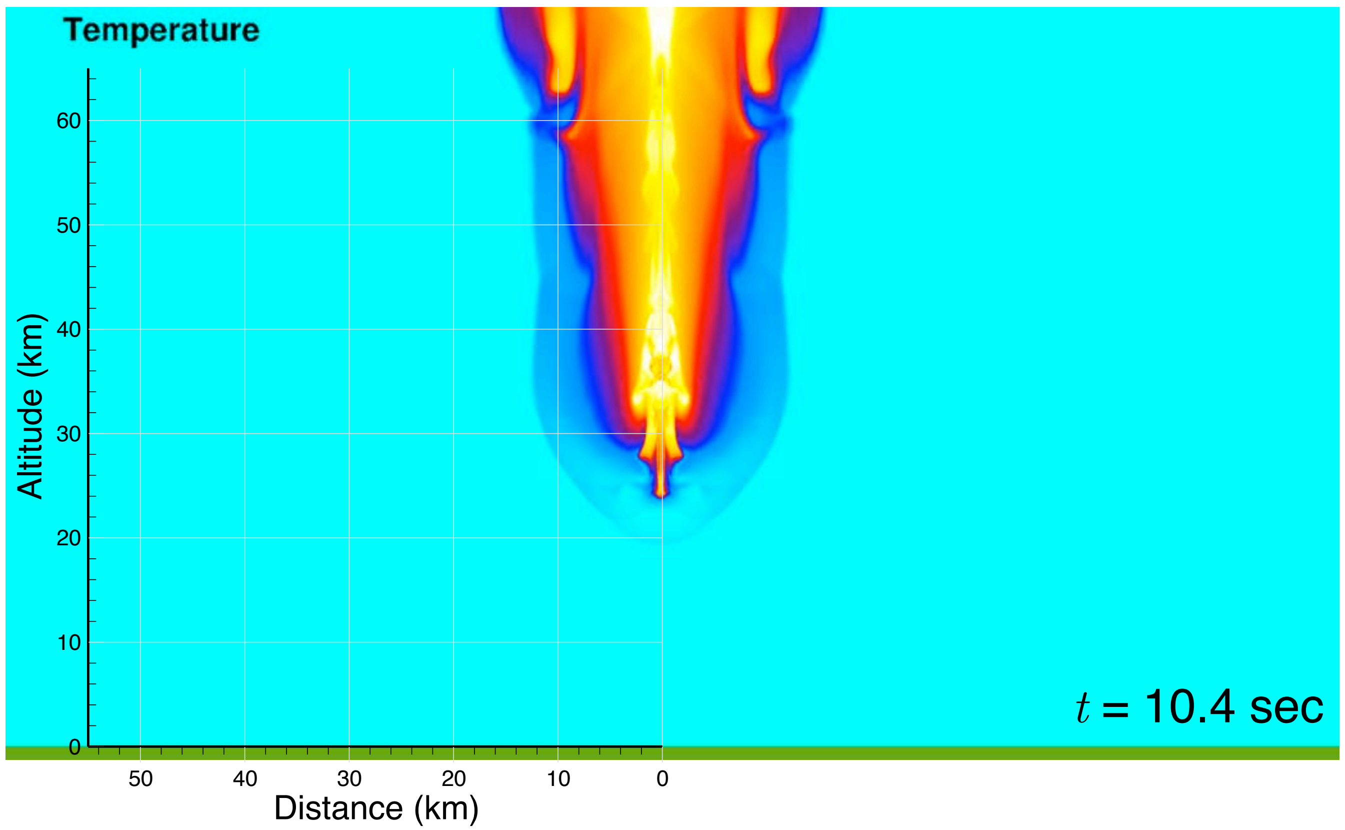

Spherical Charge

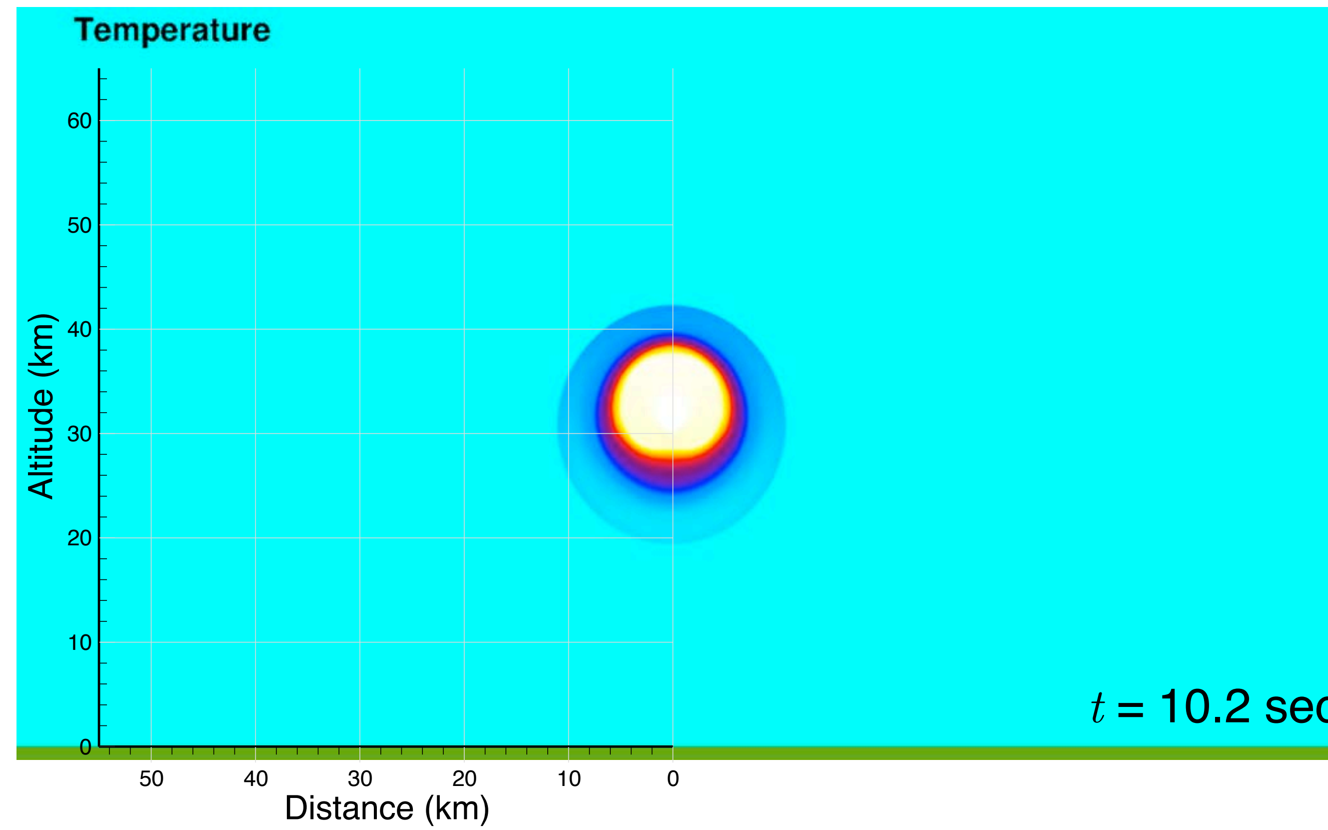

$$t = 10 \text{ sec}$$

Sensitivity - 90° entry vs Spherical Charge

Time evolution

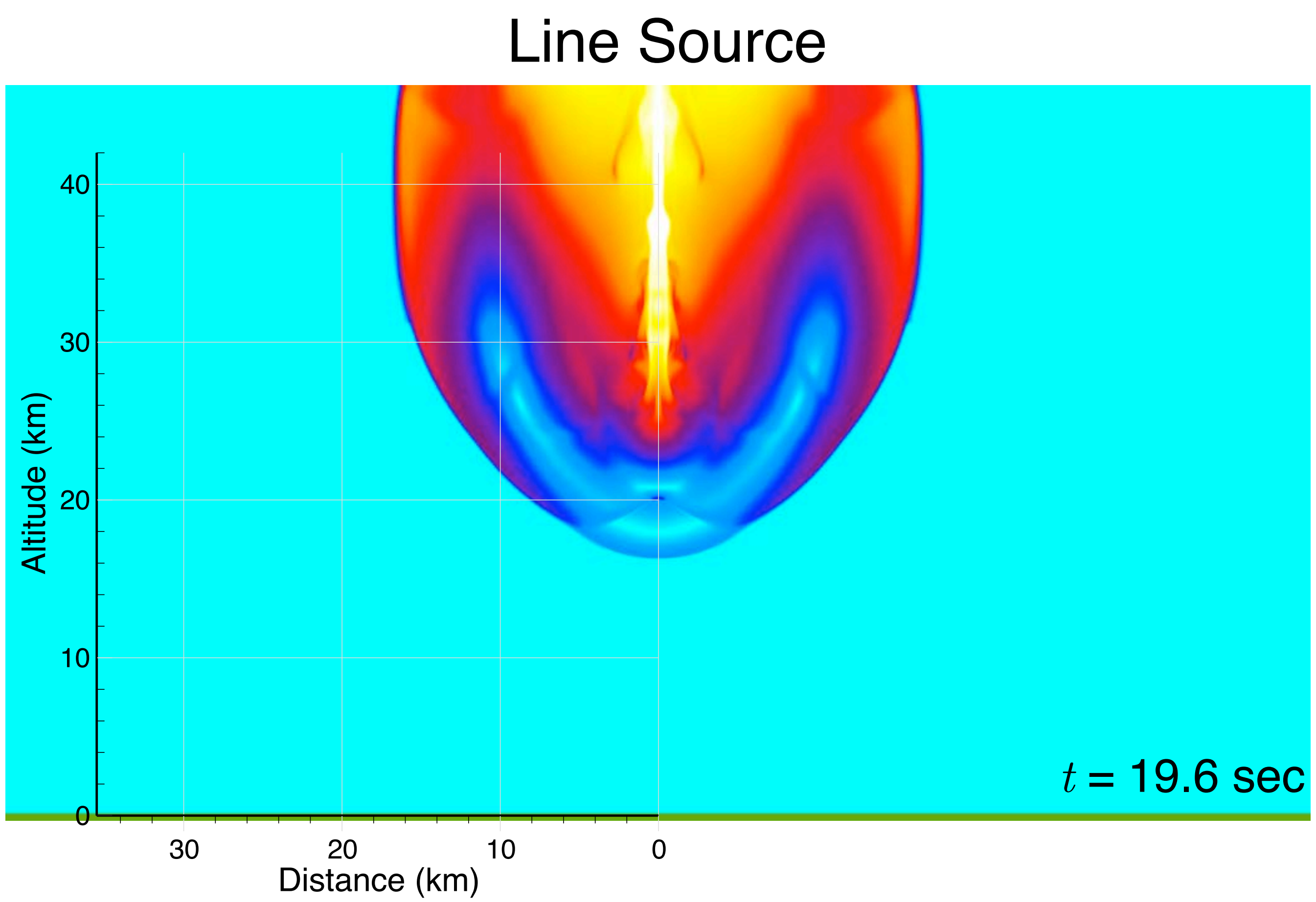

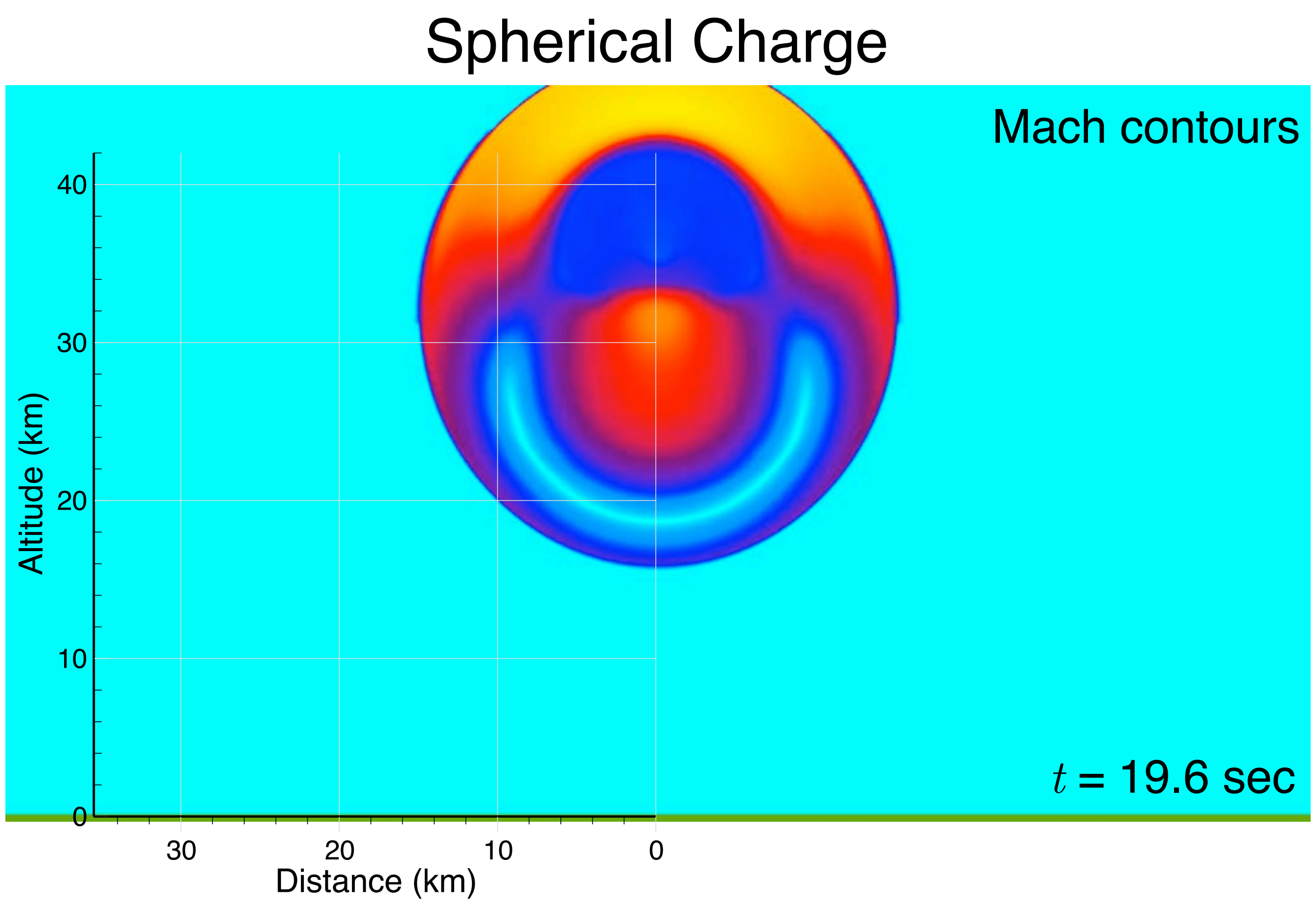

$t = 19.6$ sec

Sensitivity - 90° entry vs Spherical Charge

Time evolution

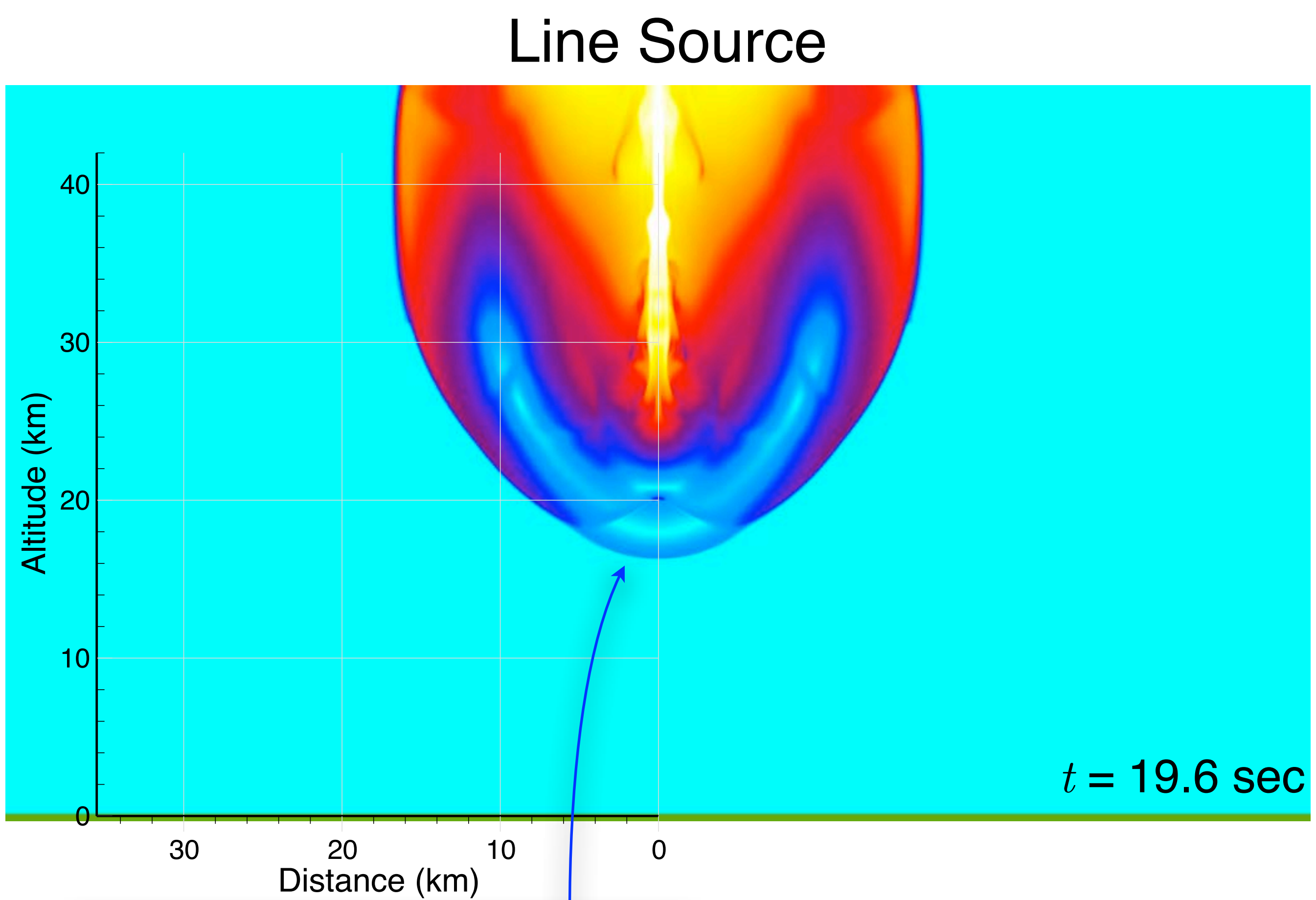

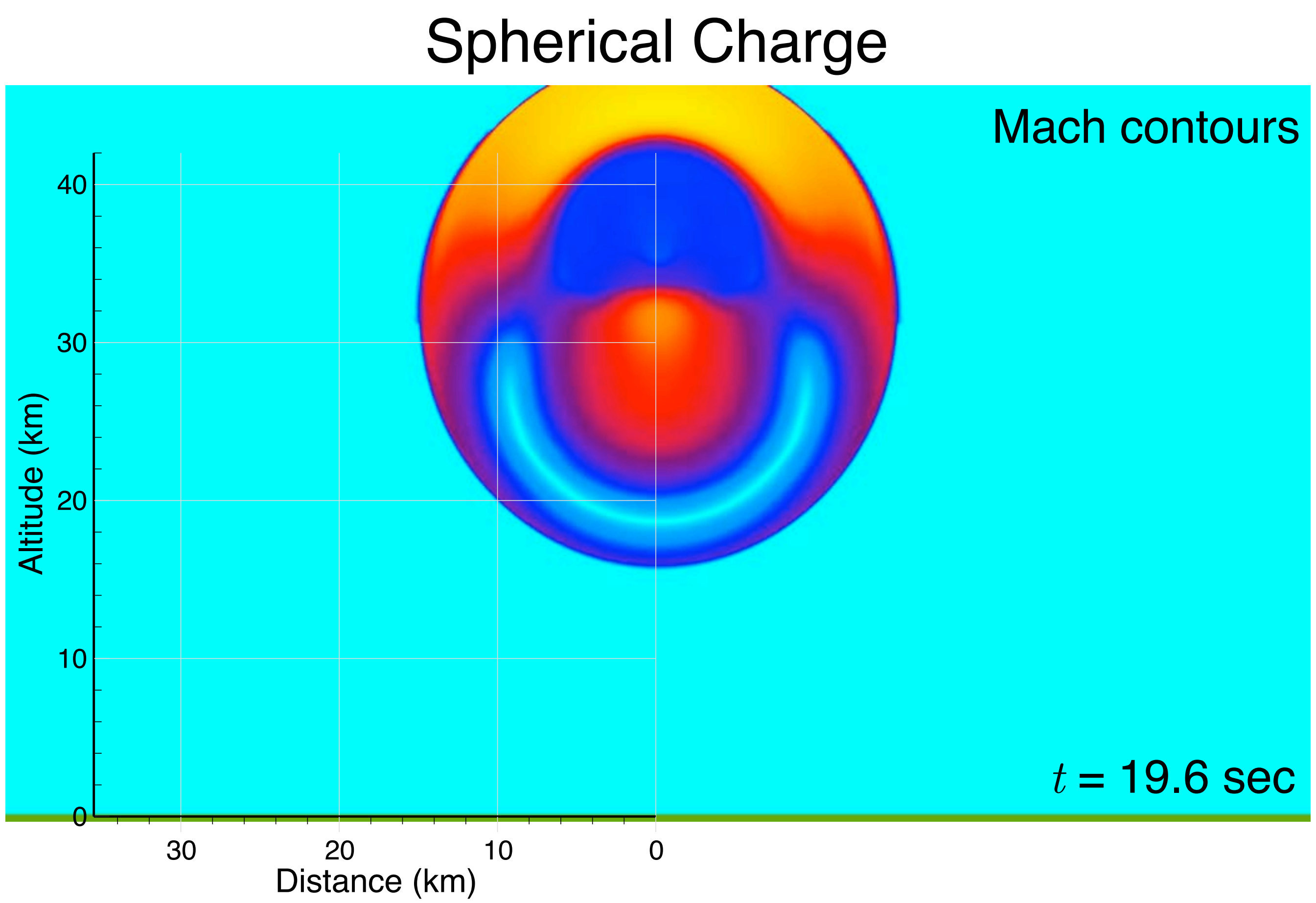

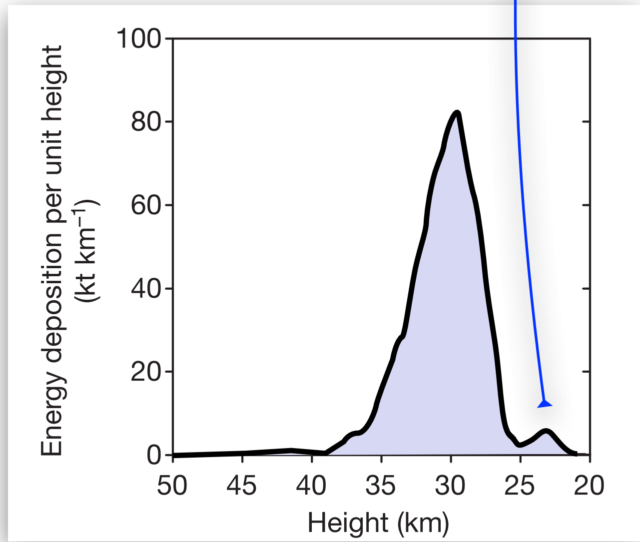

t = 19.6 sec

Sensitivity - 90° entry vs Spherical Charge

Time evolution

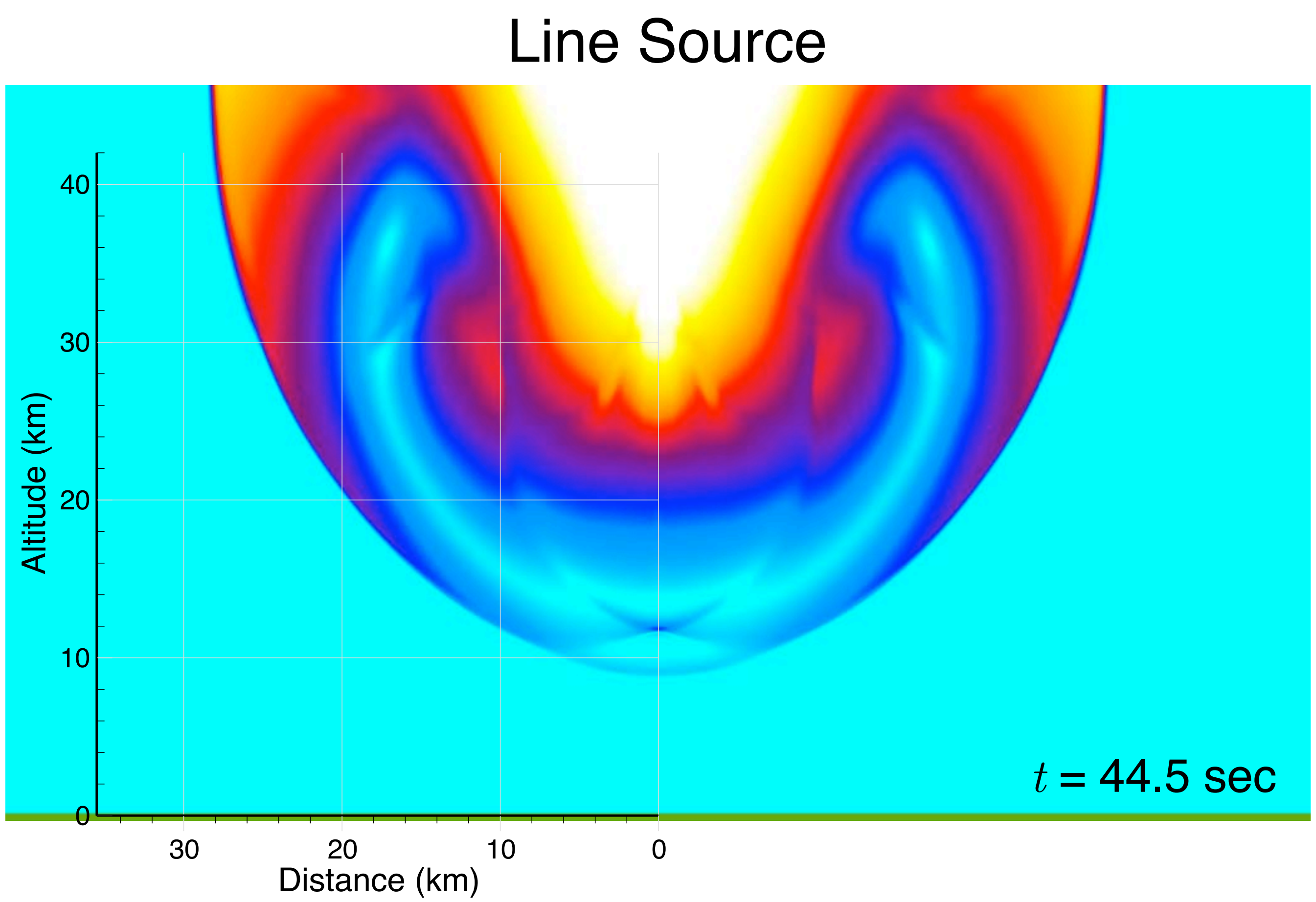

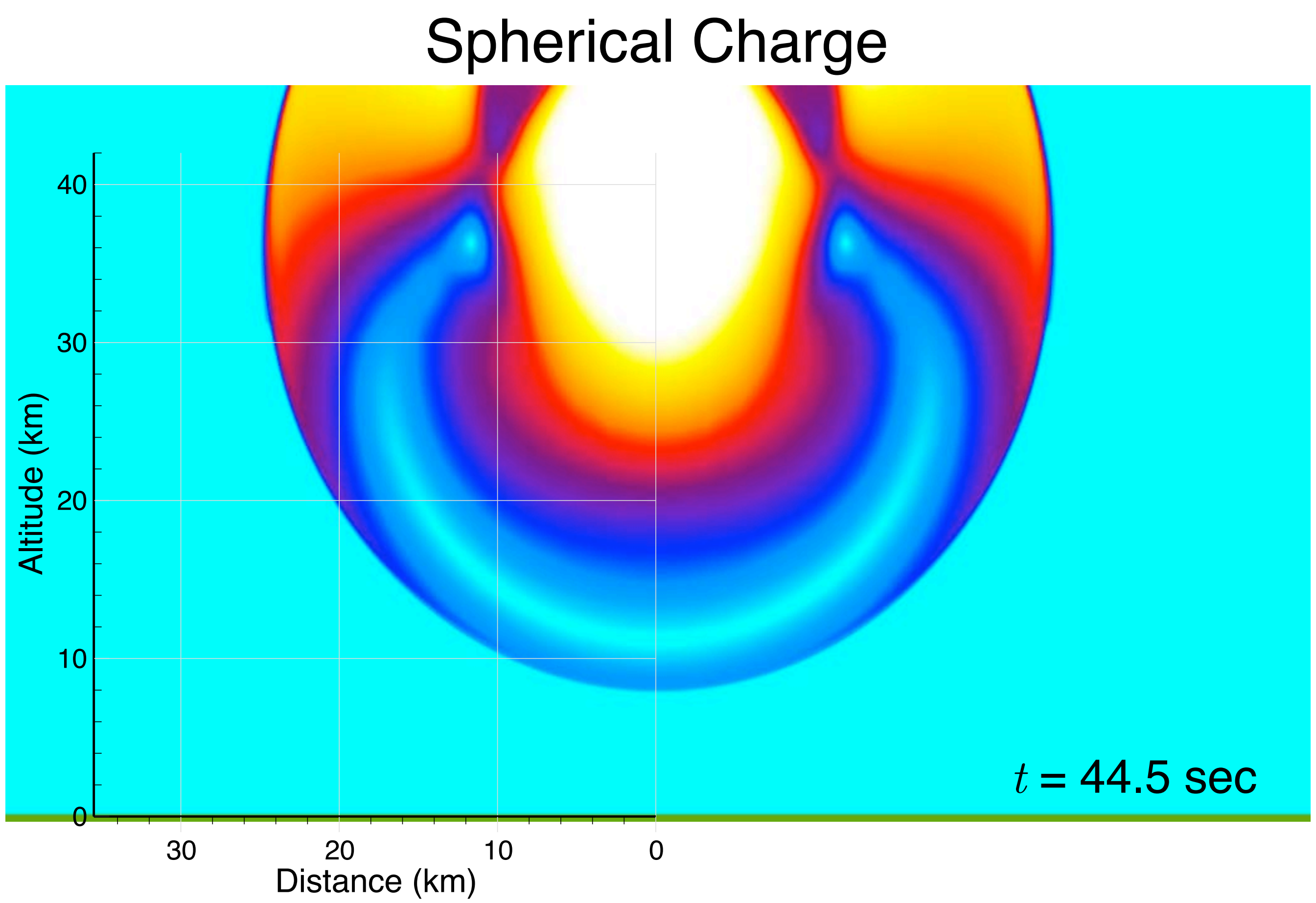

t = 44.5 sec

Sensitivity - 90° entry vs Spherical Charge

Time evolution

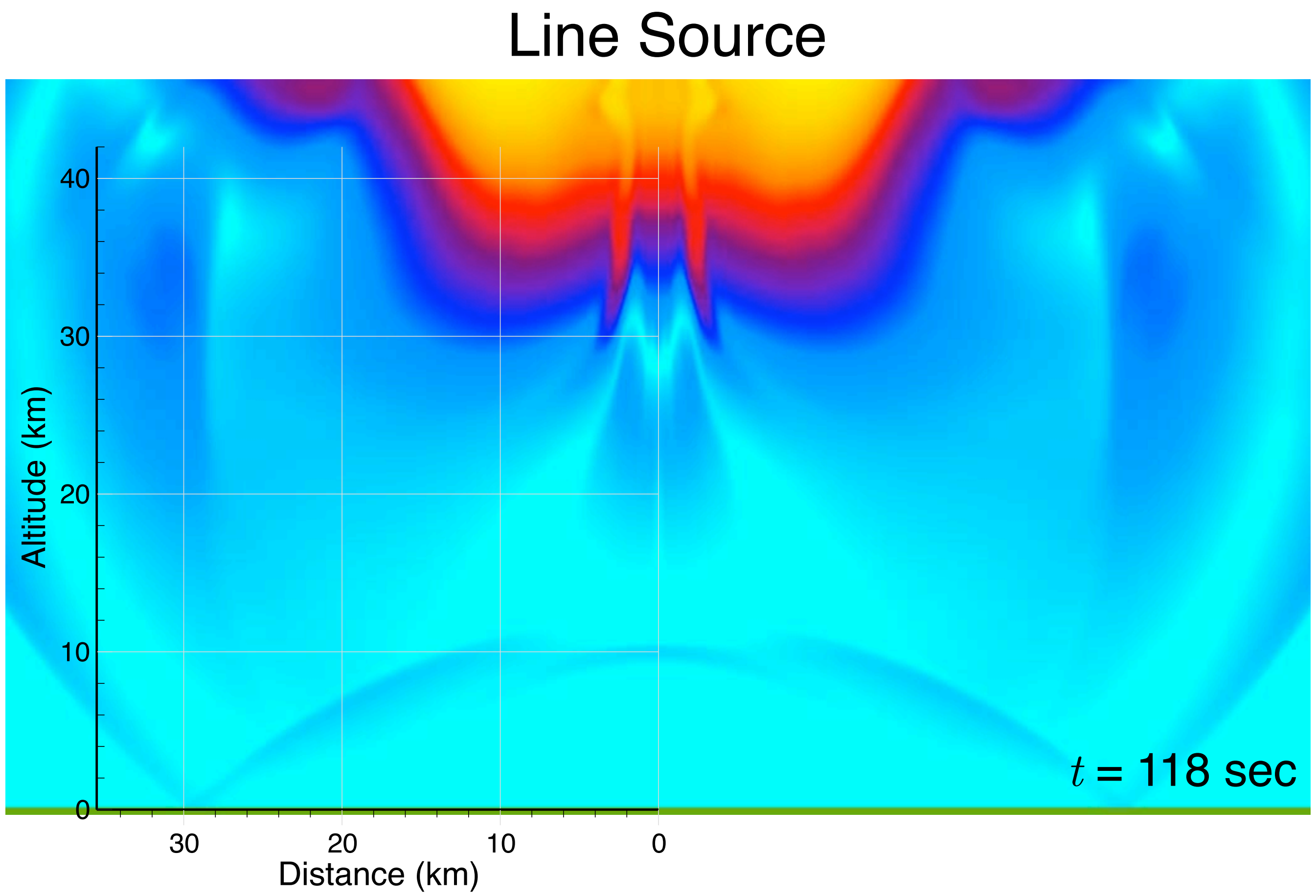

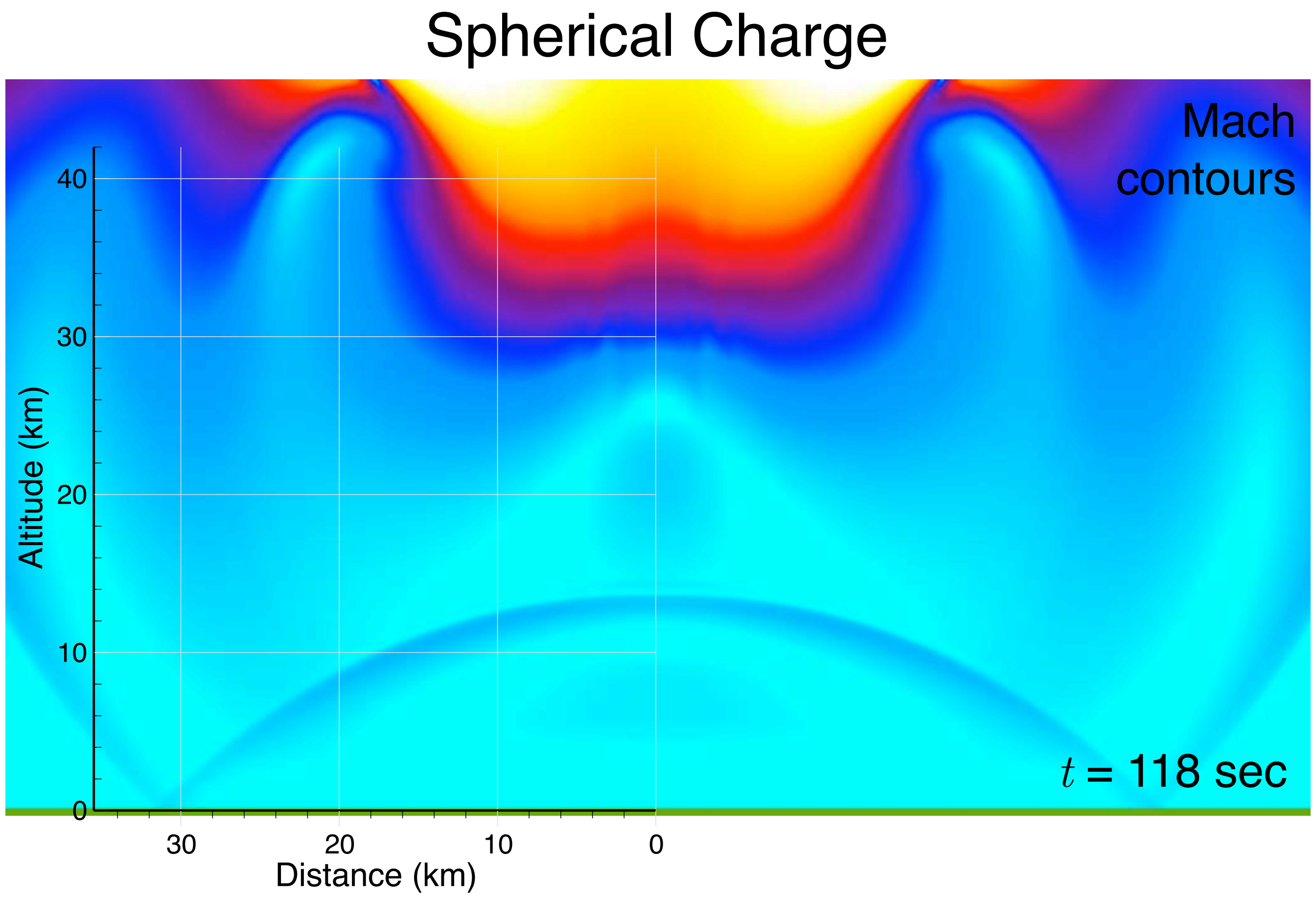

$t = 118$ sec

Sensitivity - 90° entry vs Spherical Charge

Ground footprint comparison

- Very similar envelopes - modulo details of energy deposition profile chosen.
- Both show lower peak overpressure than 18° trajectory

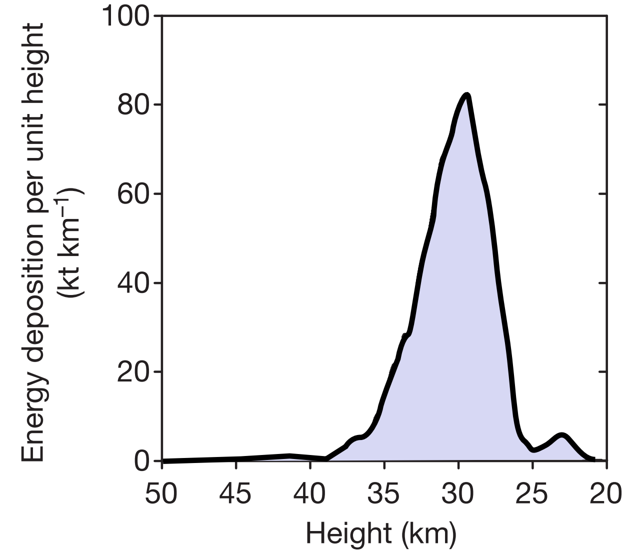

Line Source

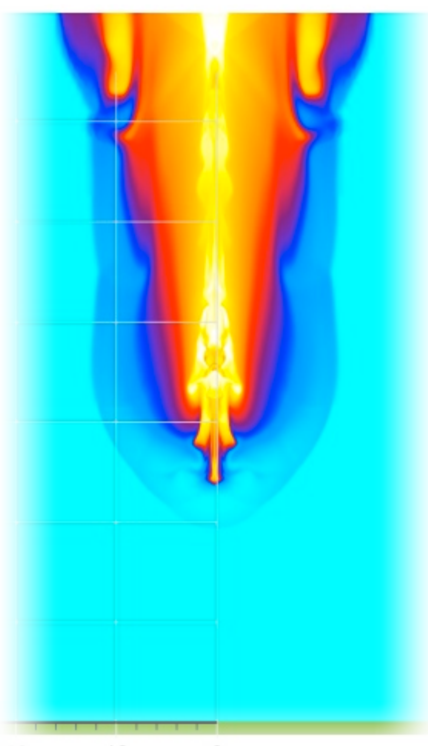

Envelope of Max and Min Ground Pressures

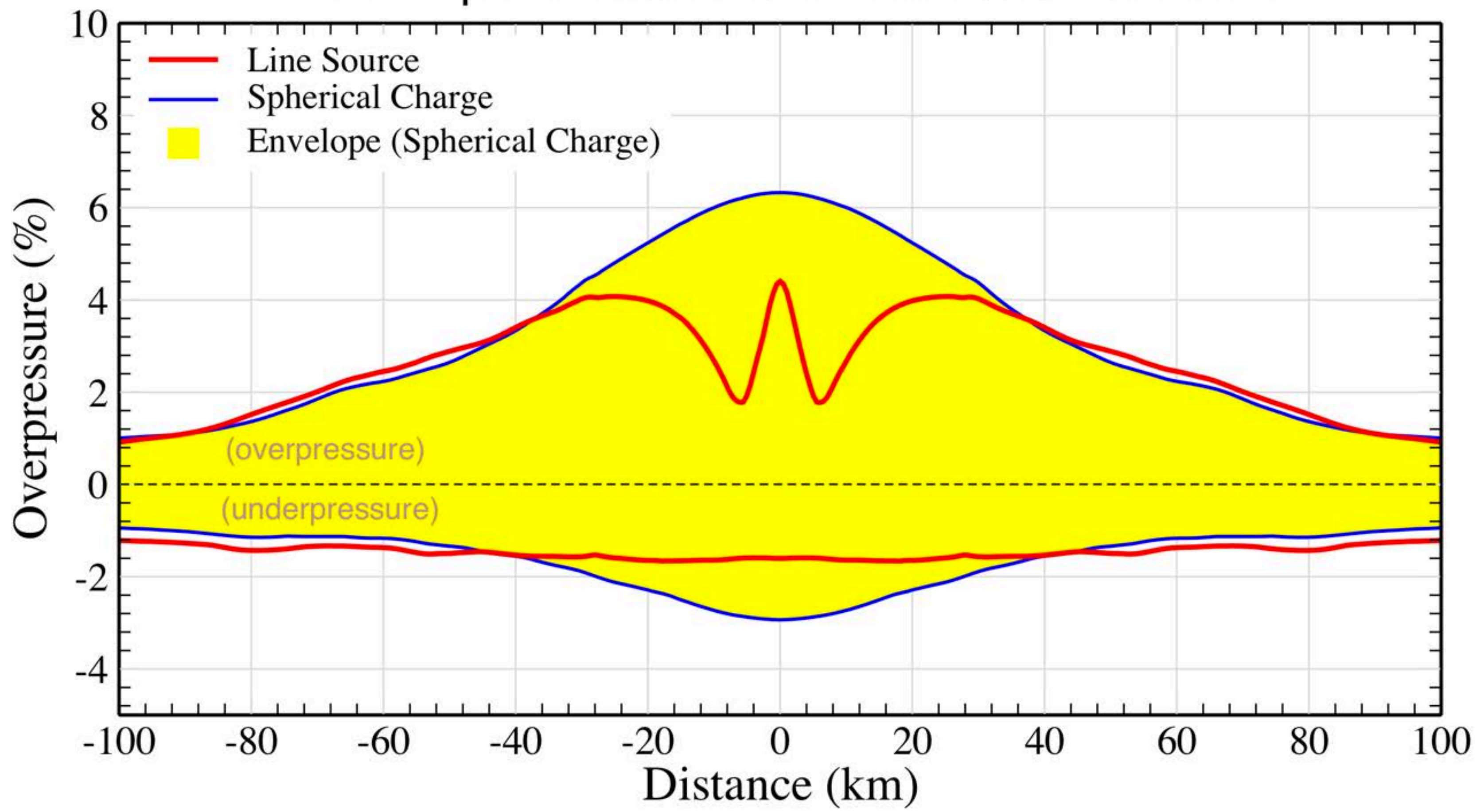

Spherical Charge

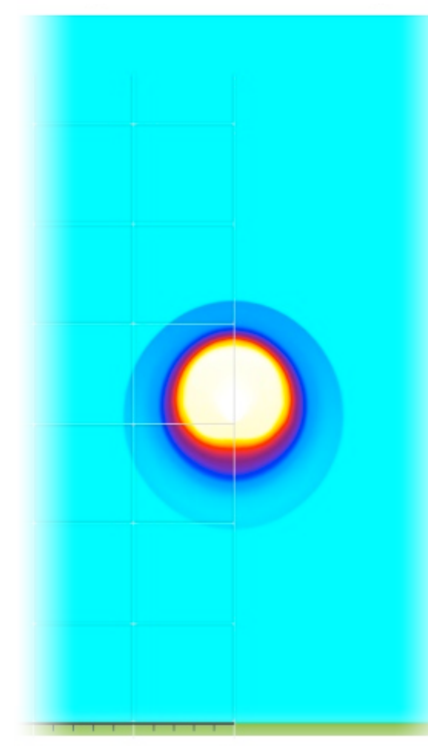

Sensitivity - 90° entry vs Spherical Charge

Ground footprint comparison

- Detailed pressure impulse shows similar instantaneous profiles as blast evolves

- Blast arrival times agree to within 2-3 seconds

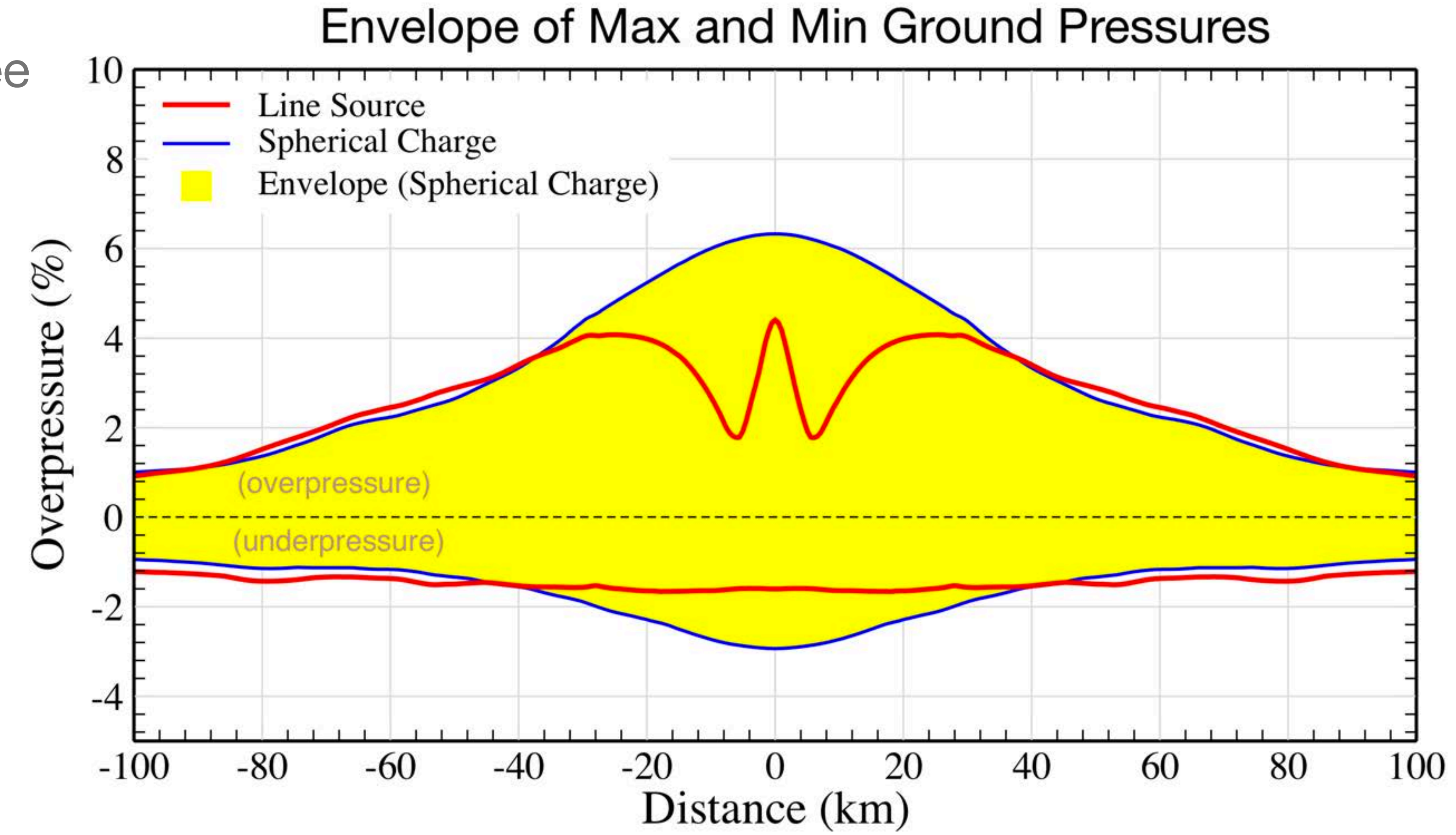

Sensitivity - 90° entry vs Spherical Charge

Ground footprint comparison

- Detailed pressure impulse shows similar instantaneous profiles as blast evolves
- Blast arrival times agree to within 2-3 seconds

Envelope of Max and Min Ground Pressures

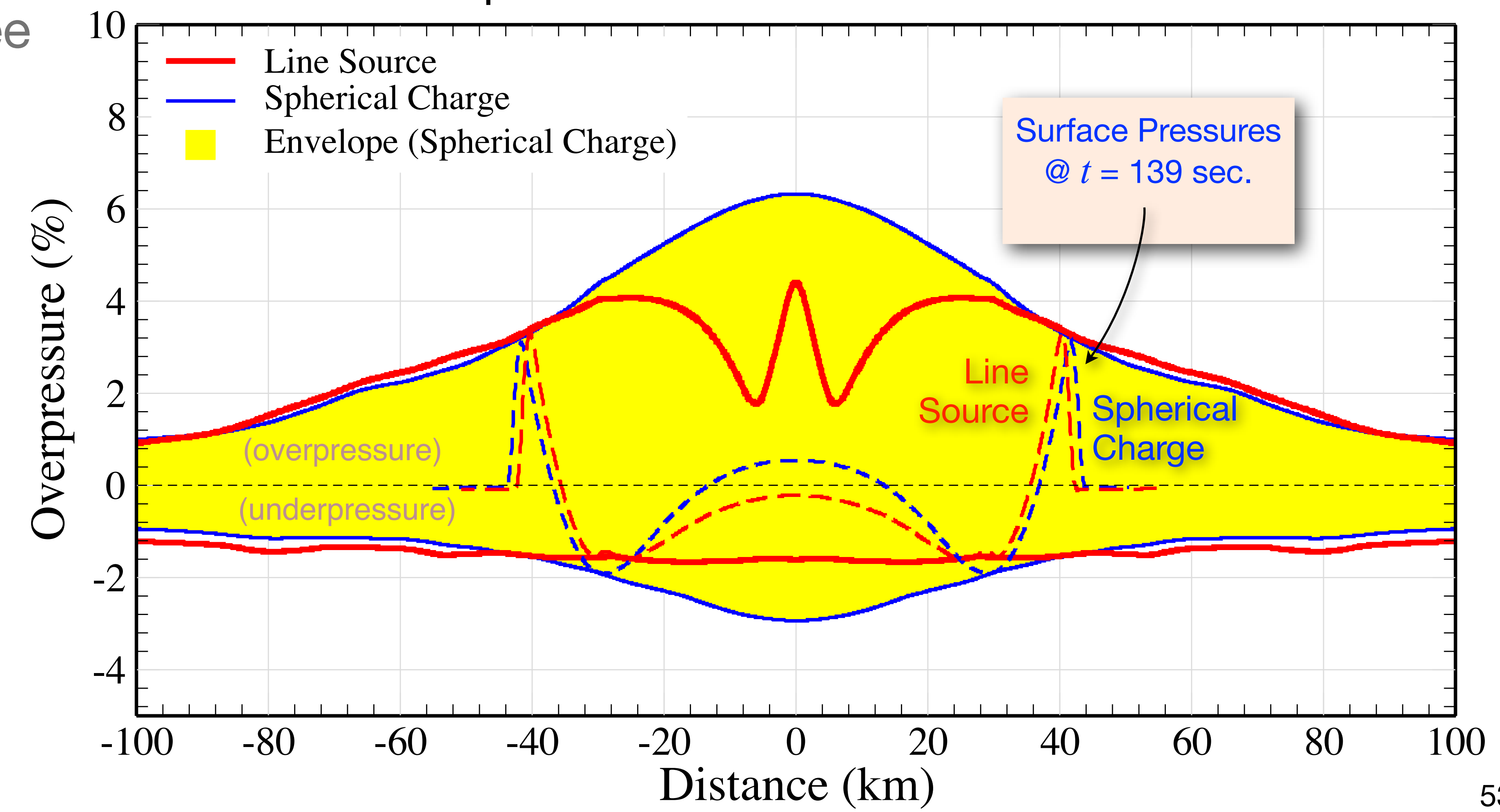

Summary

Atmospheric propagation and ground effects modeling

- Outlined modeling for far-field propagation of airburst events using a Cartesian finite-volume method
- Showed basic verification and validation
  - Good prediction for model problems
  - Good prediction of footprint and arrival time data for Chelyabinsk meteor
- Showed envelopes and time-evolution of ground footprints for damage prediction and atmospheric-driven tsunami simulations
- Preliminary sensitivity investigations
  - Line source vs full time-dependent entry
  - Effects of Entry angle & comparison with specific spherical blast

Full paper for modeling and V&V planned at AIAA SciTech 2016 in San Diego (Jan 2016)

Next Steps...

Atmospheric propagation and ground effects modeling

- Parametric drivers
  - Vary entry angle, size and strength of asteroid
  - Parametric modification of energy deposition curve
  - Precompute parametric studies -- feed results to PRA
- Cratering & splashing
- Terrain and structures
  - Refine particular when scenario arises (e.g. PDC 15)
- Update models being output to Physics-Based Risk Analysis
- Update models being input from entry and breakup modeling

Thank You!

- NASA Advanced Supercomputing Division – Task 3 & 4 teams

Marian Nemec
Jonathan Chiew
Chris Mattenberger
Lorien Wheeler
Donovan Mathias
George Anderson
Darrel Robertson

- Entry Systems Division – Task 2 team

Dinesh Prabhu
Ethiraj Venkatapathy

- New York University

Marsha Berger

- NASA PD IPT

James Arnold
Jessie Dotson
Derek Sears
Craig Burkhard
David Morrison

- IPT Seminar Speakers

Peter Jenniskens
Olga Popova
Paul Chodas
Peter Brown
Jay Melosh

- NASA NEO Office

Lindley Johnson